

8-2006

NANOPARTICLE AGGLOMERATES FOR PULMONARY DRUG DELIVERY

Rohan Bhavane

The University of Texas School of Health Information Sciences at Houston

Follow this and additional works at: https://digitalcommons.library.tmc.edu/uthshis_dissertations



Part of the [Medicine and Health Sciences Commons](#)

Recommended Citation

Bhavane, Rohan, "NANOPARTICLE AGGLOMERATES FOR PULMONARY DRUG DELIVERY" (2006). *UT SBMI Dissertations (Open Access)*. 10.

https://digitalcommons.library.tmc.edu/uthshis_dissertations/10

This is brought to you for free and open access by the School of Biomedical Informatics at DigitalCommons@TMC. It has been accepted for inclusion in UT SBMI Dissertations (Open Access) by an authorized administrator of DigitalCommons@TMC. For more information, please contact digitalcommons@library.tmc.edu.

NANOPARTICLE AGGLOMERATES FOR PULMONARY DRUG DELIVERY

A Dissertation

Presented to the Faculty of
The University of Texas
Health Science Center at Houston
School of Health Information Sciences
in Partial Fulfillment
of the Requirements
for the Degree of

Doctor of Philosophy

By

Rohan Bhavane

Committee Members:

Ananth V. Annapragada, PhD
Kim Dunn, MD, PhD
Elmer Bernstam, MD, MSE, MS
Ramanan Krishnamoorti, PhD

NANOPARTICLE AGGLOMERATES FOR PULMONARY DRUG DELIVERY

By

Rohan Bhavane, MS

August 16th, 2006

APPROVED:

Chairman of the Committee
Ananth V. Annapragada, PhD
Associate Professor,
Health Information Sciences

Kim Dunn, MD, PhD
Asst. Professor & Asc. Dean Acad. Affairs,
Health Information Sciences

Elmer Bernstam, MD, MSE, MS
Assistant Professor
Health Information Sciences

Ramanan Krishnamoorti, PhD
Professor & Asc. Dean of Research
Chemical Engineering, Univ. of Houston

Acknowledgements

This thesis is dedicated to my parents for their unconditional love and support in my endeavors. Their sacrifices will never be forgotten.

I would like to thank my advisor Dr. Annapragada for having given me the opportunity to work with him on this project. His influence as a mentor both on a scientific and a personal level has been phenomenal. I made some of my best friends working in his lab, so much so that I feel they are a part of my extended family. Emmanuel – thanks for all your help. Ashish, Ketan, Stathis, and Natalya, you guys have been a great source of encouragement and entertainment.

I would like to thank my committee members for their helpful discussions. The animal experiments would not have been possible without the help of the Veterinary staff at UTHSC. Dr. Dani Zander's help in performing the histological analysis is greatly appreciated.

I would like to thank Debbie for helping me out with all the administrative work, and of course not losing her patience with me. This work would not have been possible in part if it were not for the timely ordering of material and animals, for which I thank Namiko.

Financial support for this work was provided by the Whitaker Foundation.

NANOPARTICLE AGGLOMERATES FOR PULMONARY DRUG DELIVERY

By

Rohan Bhavane

Academic Advisor: Ananth V. Annapragada, PhD

Abstract

The Pulmonary route has been traditionally used to treat diseases of the respiratory tract. However, important research within the last two decades have shown that in addition to treating local diseases, a wide range of systemic diseases can be treated by delivering drugs to the lungs. The recent FDA approval to market Exubera®, an inhalable form of insulin developed by Pfizer, to treat Diabetes, may just be the stepping stone that the pharmaceutical industry needs to market other drugs to treat systemic diseases via the lungs. However, this technology still needs repeated drug doses to control glucose levels, as the inhaled drug is cleared rapidly.

Technologies have been developed where inhaled particles are capable of controlled release of drug from the lungs. An important feature of these technologies is the large geometric size of the particles that makes it difficult for the lung macrophages to clear these particles, which results in longer residence times for the particles in the lungs. Owing to the porosity, these particles have lower densities making them deliverable to the deep lungs. However, no modulation of drug release can be achieved with these technologies when more drug release may be required. This additional requirement can only be assuaged by additional dosing of the drug formulation, which can have undesirable effects due to excess loading of excipients in the lungs.

In an attempt to bring about modulation of release from long residence time particles, a novel concept was developed in our laboratory that has been termed as

the Agglomerated Vesicle Technology (AVT). Liposomes with encapsulated drug were agglomerated using well known cross linking chemistries to form agglomerates in the micron sized range. The large particles exhibited aerodynamic sizes in the respirable size range with minimal damage to the particles upon nebulization. By breaking the cross links between the liposomes with a cleaving agent, it was anticipated that triggered release of drug from the AVT particles could be achieved. In vivo studies done in healthy rabbits showed that post-administration modulation of drug release is possible from the AVT particles after the introduction of the cleaving agent.

This study has important implications for the future development of this technology, where the AVT particles can be made “sensitive” to the product of disease. It is envisaged that a single dose of AVT containing the appropriate drug when administered to the lungs would maintain drug levels at a controlled rate over an extended period of time. When the need for more drug arises, the product of the disease would trigger the AVT particles to release more drug as needed to control the condition, thus eliminating the need for repeated drug doses and improved compliance amongst patients.

Table of Contents

Table of Contents	iv
List of Figures	vii
List of Tables	xii
Nomenclature	xiii
Chapter 1	1
Introduction	1
1.1. Pulmonary route of drug delivery	1
1.2. Proposed research aims	3
Chapter 2	6
Background and Significance	6
2.1. Respiratory tract physiology	6
2.1.1. Deposition and clearance of inhaled particles	10
2.2. Agglomerated Vesicle Technology (AVT)	13
2.2.1. Agglomeration methodology of liposomes	16
2.2.1.1. Preparation of liposomes	19
2.2.1.2. Encapsulating drugs within liposomes	21
2.2.1.3. Tether selection for agglomeration	24
2.2.1.4. Agglomeration chemistries	24
2.2.2. Triggered release of drug	27
2.2.2.1. Using cysteine as a trigger	27
Chapter 3	28
Methods and Experimental Procedures	28
3.1. Analytical Methods	28
3.1.1. Dynamic Light Scattering	28
3.1.2. Fraunhofer Diffraction Pattern Analysis	31
3.1.3. Cascade impaction for aerodynamic characterization of aerosols	34
3.1.4. Microscopy	36
3.1.4.1. Confocal Laser Scanning Microscopy	36
3.1.4.2. Negative Staining Electron Microscopy	38
3.1.5. HPLC assay	39
3.2. Experimental procedures of the 1 st generation of AVT (in vivo non-cleavable)	41
3.2.1. In vitro experiments with blank liposomes	42
3.2.1.1. Materials	42
3.2.1.2. Fabrication and characterization of liposomes	42
3.2.1.3. Fabrication and characterization of agglomerates	43
3.2.2. In vitro studies with Ciprofloxacin loaded liposomes	44
3.2.2.1. Materials	44
3.2.2.2. Fabrication and characterization of liposomes	45
3.2.2.3. Loading of liposomes with ciprofloxacin	45
3.2.2.4. Agglomeration and characterization of Ciprofloxacin-loaded liposomes	47
3.2.2.5. Aerodynamic properties of agglomerates	47
3.2.2.6. Stability upon nebulization	49
3.2.2.7. In vitro release studies	50

3.2.3. <i>In vivo studies of Ciprofloxacin loaded liposomes</i>	50
3.2.3.1. Materials	51
3.2.3.2. Animals.....	51
3.2.3.3. Fabrication and characterization of liposomes	52
3.2.3.4. Loading of liposomes with Ciprofloxacin	52
3.2.3.5. Agglomeration and characterization of Ciprofloxacin-loaded liposomes.....	53
3.2.3.6. Pharmacokinetic study in rabbits	54
3.2.4. <i>In silico study of Ciprofloxacin pharmacokinetics of the 1st generation AVT</i>	56
3.3. Experimental procedures of the 2 nd generation of AVT (in vivo cleavable)	62
3.3.1. <i>In vitro studies with blank liposomes</i>	62
3.3.1.1. Materials	62
3.3.1.2. Fabrication and characterization of liposomes	62
3.3.1.3. Agglomeration and characterization of blank agglomerates.....	63
3.3.2. <i>In vitro studies with carboxyfluorescein loaded liposomes</i>	64
3.3.2.1. Materials	64
3.3.2.2. Fabrication and characterization of liposomes	64
3.3.2.3. Agglomeration and characterization of carboxyfluorescein agglomerates	65
3.3.2.4. Visual analysis of agglomerates by Confocal microscopy	65
3.3.3. <i>In vitro studies with Ciprofloxacin loaded liposomes</i>	66
3.3.3.1. Materials	66
3.3.3.2. Fabrication and characterization of liposomes	67
3.3.3.3. Loading of liposomes with Ciprofloxacin	67
3.3.3.4. Agglomeration and characterization of Ciprofloxacin loaded liposomes	68
3.3.3.5. Visual analysis of agglomerates by negative stain electron microscopy	68
3.3.3.6. Release studies	69
3.3.4. <i>In vivo cysteine triggered release studies</i>	70
3.3.4.1. Materials	70
3.3.4.2. Animals.....	70
3.3.4.3. Fabrication and characterization of liposomes	71
3.3.4.4. Preparation and characterization of agglomerated liposomes.....	71
3.3.4.5. Pharmacokinetic study in rabbits	72
3.3.4.6. Lipid assay of instilled formulations in rat lungs.....	74
3.3.4.7. Histology of rat lungs to assess inflammation	75
3.3.4.8. Cytokine assay from rat lungs as a measure of inflammation.....	76
3.3.5. <i>In silico study of Ciprofloxacin pharmacokinetics of the 2nd generation AVT</i>	78
Chapter 4	79
Results and Discussions	79
4.1. The 1 st Generation of AVT (in vivo non-cleavable)	79
4.1.1. <i>In vitro experiments with blank liposomes</i>	79
4.1.1.1. Characterization of liposomes	79
4.1.1.2. Agglomeration of liposomes with DTBP	80
4.1.2. <i>In vitro studies with Ciprofloxacin loaded liposomes</i>	87
4.1.2.1. Characterization of Ciprofloxacin loaded liposomes.....	87
4.1.2.2. Agglomeration of Ciprofloxacin loaded liposomes with DTBP.....	88
4.1.2.3. Aerodynamic characterization of agglomerates.....	91
4.1.2.4. Stability upon nebulization studies	92
4.1.2.5. Release studies	95

4.1.3. <i>In vivo studies with Ciprofloxacin loaded liposomes</i>	97
4.1.3.1. Characterization of Ciprofloxacin loaded liposomes.....	97
4.1.3.2. Agglomeration of liposomes with DTBP	98
4.1.3.3. Pharmacokinetic studies in rabbits.....	99
4.1.4. <i>In silico study of pharmacokinetics of 1st generation AVT</i>	102
4.2. The 2 nd generation of AVT (in vivo cleavable).....	106
4.2.1. <i>In vitro studies with blank liposomes</i>	106
4.2.1.1. Characterization of liposomes.....	106
4.2.1.2. Agglomeration of liposomes with DTSSP	106
4.2.2. <i>In vitro studies with carboxyfluorescein (CF) loaded liposomes</i>	108
4.2.2.1. Characterization of liposomes.....	108
4.2.2.2. Agglomeration of liposomes with DTSSP	108
4.2.2.3. Visual analysis of agglomerates by Confocal microscopy	109
4.2.3. <i>In vitro studies with Ciprofloxacin loaded liposomes</i>	111
4.2.3.1. Characterization of Ciprofloxacin loaded liposomes.....	111
4.2.3.2. Agglomeration of Ciprofloxacin loaded liposomes with DTSSP	112
4.2.3.3. Visual analysis of agglomerates by negative stain electron microscopy	112
4.2.3.4. Release studies.....	114
4.2.4. <i>In vivo cysteine triggered release studies</i>	116
4.2.4.1. Characterization of liposomes.....	116
4.2.4.2. Agglomeration of liposomes with DTSSP	116
4.2.4.3. Pharmacokinetic studies in rabbits.....	117
4.2.4.4. Lipid assay of instilled formulations in rat lungs.....	121
4.2.4.5. Histology of rat lungs to assess inflammation.....	122
4.2.4.6. Cytokine assay from rat lungs as a measure of inflammation.....	124
4.2.5. <i>In silico study of Ciprofloxacin pharmacokinetics</i>	125
Chapter 5	128
Conclusions and Future work.....	128
5.1. Conclusions.....	128
5.2. Future work.....	132
5.3. Clinical perspectives of the work.....	133
Bibliography	136

List of Figures

	Page
Figure 1. (a) The wall of the trachea and (b) the upper respiratory tract consisting of the trachea, the bronchi and the bronchioles.	7
Figure 2. (a) Characteristic dimensions of the airway tree and (b) Epithelial cell size and surface fluid thickness in different regions.	9
Figure 3. Deposition/clearance fate of inhaled particles in/from the deep lung.	11
Figure 4. Schematic of core particles bearing ligands (a); agglomeration of core particles by linkers to form agglomerates (b); based on the linker chemistry some can be cleaved in-vivo by components of lung fluid or addition of a second agent (c).	13
Figure 5. a) A unilamellar liposome; and b) details of the lipid bilayer.	17
Figure 6. Dependence of the amount of encapsulated insulin to size of liposomes passively encapsulating insulin from a pool concentration of 30 mg/mL.	21
Figure 7. Schematic representation of the active loading technique.	23
Figure 8. Reaction scheme for DTBP agglomeration followed by cleavage with DTT.	25
Figure 9. Agglomeration scheme for DTSSP agglomeration.	26
Figure 10. Fraunhofer Diffraction Pattern Analysis system.	31

Figure 11. Working principle of confocal microscopy.	37
Figure 12. Schematic for collecting nebulized formulations of liposomes and agglomerates for evaluating effects upon nebulization.	49
Figure 13. Sketch of the compartmental model.	56
Figure 14. DLS results of blank liposomes with 2% PEG-NH ₂ and 3% PEG-NH ₂ used for making agglomerates of DTBP.	80
Figure 15. Time progression of agglomeration reaction of liposomes (50 mM lipid) carrying (a) 2% PEG-NH ₂ with 50 times DTBP, and (b) 3% PEG-NH ₂ with 25 times DTBP. The reactions were stopped with Tris and evaluated by Fraunhofer diffraction.	82
Figure 16. Size distributions of agglomerates obtained by Fraunhofer diffraction after using different molar excess of DTBP linker over 3% PEG-NH ₂ . Liposomes used were (a) 20 mM lipid, and (b) 50 mM lipid. The agglomerates were measured after 3 days from the start of the reaction.	83
Figure 17. Size distributions of agglomerates obtained by Fraunhofer diffraction after using liposomes with different lipid molarities with 100 molar excess of DTBP over (a) 2% PEG-NH ₂ , and (b) 3% PEG-NH ₂ on liposomes. The agglomerates were measured after 3 days from the start of the reaction.	85
Figure 18. Fraunhofer diffraction results showing the effect of pH on the agglomeration of the liposomes.	86
Figure 19. Size distribution of Ciprofloxacin loaded liposomes.	88
Figure 20. Fraunhofer diffraction results of agglomerates of Ciprofloxacin loaded liposomes made at pH 5.2 and 8.5.	89

Figure 21. Size analysis of agglomerates of Ciprofloxacin loaded liposomes before and after cleavage with 30 and 60 mg/ml of DTT at 37 °C.	90
Figure 22. Aerodynamic diameters of DTBP agglomerates (Prep I) determined by cascade impaction.	91
Figure 23. Effect of nebulization on the size of liposomes	93
Figure 24. Effect of nebulization on the size of agglomerated liposomes.	94
Figure 25. Loss of encapsulated Ciprofloxacin from liposomes and agglomerates after nebulization.	94
Figure 26. In vitro release of Ciprofloxacin from liposomes, and agglomerates (Prep I) with and without cleavage with DTT. Arrows indicate time points at which agglomerates were cleaved with DTT.	96
Figure 27. Size distribution of agglomerates (AVT1) used in animal studies.	98
Figure 28. Pharmacokinetic data for the different formulation tested in rabbits. (n=1 for the free Ciprofloxacin study, and n=3 for the other studies. Study with liposomes and free Ciprofloxacin was done over 2 days. The AVT studies were done over 1 day).	100
Figure 29. Model fit to data for pharmacokinetic studies done with liposomes.	103
Figure 30. Model fit to data for pharmacokinetic studies done with AVT1.	104
Figure 31. Fraunhofer diffraction analysis of liposomes agglomerated with DTSSP, and subsequent cleavage with cysteine at 37 °C. Agglomerates with (a) 20 mM lipid, and (b) 1.25 mM lipid.	107
Figure 32. Fraunhofer analysis of agglomerates of liposomes encapsulating CF.	109

Figure 33. Slices of confocal image of an agglomerate encapsulating carboxyfluorescein. Data at top right corner of each image is the Z-stack height, with Z-stack slices taken every 0.5 μm . 110

Figure 34. Size distribution of agglomerates of liposomes encapsulating Ciprofloxacin. 112

Figure 35. Negative stain electron microscope images (1% uranyl acetate) taken on a JEOL JEM 1230. (a) liposomes at 10 K magnification, scale bar 0.2 μm ; (b) agglomerate at 10 K magnification, scale bar 0.2 μm ; (c) agglomerate at 2 K magnification, scale bar 2 μm ; (d) agglomerate at 4 K magnification, scale bar 1 μm . 113

Figure 36. In vitro release profiles from uncleaved agglomerates, agglomerates that were repeatedly cleaved with cysteine, and agglomerates treated with plain buffer. (Arrows indicate time points at which 50 μl of either buffer or cysteine containing buffer is introduced.) 115

Figure 37. Particle size distribution, by Fraunhofer Diffraction, of the agglomerates used in the pharmacokinetic and lipid assay studies. 116

Figure 38. Pharmacokinetic data of AVT2 particles, with and without cysteine treatment. Arrows indicate time points when 1 ml cysteine (60 mg/ml) was instilled. $n=3$ animals. 117

Figure 39. Comparison of the pharmacokinetics of liposomes, AVT1, AVT2, and AVT2 followed by cysteine. Study with liposomes was done over 2 days. The AVT studies were done over 1 day. $n=3$ animals. 119

Figure 40. Percentage of original dosed lipid remaining in the lungs on the basis of fluorescence assay of the tagged lipid. $n = 3$ animals. 121

Figure 41. Histological analysis of hematoxylin-eosin stained lung tissue 24 hrs after treatment (original magnification 100X); (A) saline-treated animals; 122

(B) ConA-treated rats; (C) liposome-treated animals; (D) AVT-treated animals.
 $n = 2$ animals

Figure 42. Levels of cytokines detected 48 hours after the different treatments 124
($n = 3$ animals)

Figure 43. Model fit to experimental data for (a) AVT2, and (b) AVT2 + 125
Cysteine.

List of Tables

	Page
Table 1. <i>Pharmacokinetic Parameters fixed from literature</i>	59
Table 2. <i>Reaction conditions that were used for making the agglomerates of blank liposomes with DTBP cross-linker.</i>	81
Table 3. <i>Formulation of Ciprofloxacin instilled in the lungs of rabbits.</i>	99
Table 4. <i>AUC₀₋₂₄ for pharmacokinetic data of figure 28.</i>	102
Table 5. <i>Values of input dose used in the model.</i>	102
Table 6. <i>Unknown parameters estimated for pharmacokinetic study with liposomes</i>	103
Table 7. <i>Unknown parameters estimated for pharmacokinetic study with AVT1.</i>	105
Table 8. <i>Dose of AVT2 instilled in the lungs of rabbits.</i>	118
Table 9. <i>AUC₀₋₂₄ for each of the formulations tested.</i>	120
Table 10. <i>Unknown parameters estimated for pharmacokinetic study with AVT2.</i>	126
Table 11. <i>Unknown parameters estimated for pharmacokinetic study with AVT2 + cysteine.</i>	127

Nomenclature

AUC	area under the curve
AVT	agglomerated vesicle technology
BAL	bronchoalveolar lavage
CLSM	Confocal laser scanning microscopy
ConA	Concanavalin A
D_{aer}	aerodynamic diameter
D_{geo}	geometrical diameter
DI water	deionized water
DLS	dynamic light scattering
DPI	dry powder inhaler
DPPC	1,2-Dipalmitoyl-sn-Glycero-3-Phosphatidylcholine
DSPE	1,2-Distearoyl-sn-Glycero-3-Phosphatidylethanolamine
DSPE-PEG-NH₂	Distearoylphosphoethanolamine[Amino(polyethylene glycol)]
DTB	dithiobenzyl
DTBP	dimethyl 3,3'-dithiobispropionimidate•2HCl
DTSSP	Dithiobis[succinimidylpropionate]
DTT	dithiothreitol
EGS	ethylene glycolbis(succinimidylsuccinate)
FDPA	Fraunhofer diffraction pattern analysis

HE	Hematoxylin-eosin
HPLC	high performance liquid chromatography
i.v.	intravenous
i.p.	intraperitoneal
MDI	metered-dose inhaler
MLVs	multi-lamellar vesicles
MMAD	mass mean aerodynamic diameter
MWCO	molecular weight cut-off
NHS	N-hydroxysuccinimide
PBS	phosphate buffered saline
PEG	polyethylene glycol
PK	pharmacokinetic
RES	reticuloendothelial system
rpm	revolutions per minute

Chapter 1

Introduction

1.1. Pulmonary route of drug delivery

Inhalation therapy has been used for more than 4000 years primarily for the treatment of respiratory diseases. Ancient therapies have included inhaling smoke emanating from lit medicinal concoctions to inhaling vapors released from aromatic plants [1]. Aerosolized delivery of drugs to the lungs has greatly improved the treatment of various respiratory diseases. As examples, anti-inflammatory and bronchodilator aerosol medications have been the cornerstone of asthma treatment; and antibiotics have been used for treating cystic fibrosis and lung infections.

The pulmonary drug delivery area has grown tremendously since the mid 20th century into a multi-billion dollar industry. During the past two decades, the lungs have been considered a promising route for the administration of therapeutics not only for the treatment of local pulmonary diseases (e.g. asthma) but also for the treatment of systemic conditions (e.g. diabetes). This increased interest in pulmonary drug delivery is based on (1) the high bioavailability of protein and peptide drugs when delivered to the respiratory system, (2) the large surface area (140 m²) of the adult lung, in intimate contact with the circulatory system via the alveoli, (3) the equivalence of inhalation to arterial injection, and (4) the consequent avoidance of first pass

hepatic and renal effects. Compounds with high potential for delivery by the respiratory route include insulin, cyclosporine, interferon, antitrypsin, protease inhibitors, deoxyribonucleases, recombinant adenoviruses and many more [2]. Further, in the wake of recent terrorist attacks on the United States, there has been a renewed interest in protection against biological agents, many of which infect via the respiratory route, and are therefore best protected against by the respiratory delivery of anti-infectives and antibiotics [3].

It has long been recognized that the lung allows high systemic bioavailability of proteins like insulin [4]. This has driven the development of a number of inhaled insulin projects [5]. The goal for a systemically active, inhaled drug is to reach the deep lung region in order to be transported into the blood stream. In order to reach the deep lung, particles must have an aerodynamic diameter (D_{aer}) in the 1 – 5 μm range. The aerodynamic diameter is related to the geometric diameter (D_{geo}) as $D_{\text{aer}} = D_{\text{geo}} \cdot q^{0.5}$, where q is the specific gravity of the particle. For particles with specific gravity = 1 (the case for most solid pharmaceutical powders), the geometric diameter and the aerodynamic diameter are identical. Therefore, particles that are optimal for deep lung delivery will often also have a geometric diameters in the 1 – 5 μm range, putting them in the size range where pulmonary macrophage activity is the highest (this is not surprising, since the macrophage system was probably optimized by evolutionary processes to eliminate inhaled particles that reach the deep lung). Solid drug particles optimized for drug delivery to the deep lung would

therefore meet the same fate, and be cleared by macrophage uptake and likely pass via the pores of Kohn into the circulatory system and thence to the reticuloendothelial system (RES). Only the portion of the particles that were not thus affected would contribute to drug delivery. A secondary consequence of this rapid macrophage uptake and clearance is the short duration of delivery for an inhaled drug, since the delivery must take place before macrophage mediated clearance of the particles takes place. Typically, this time frame is around an hour.

However, a breakthrough discovery was made around 1997, when Edwards et al. [6] recognized that the macrophage uptake system relies on the geometric diameter of particles to recognize and clear them, while the deposition of the particles in the lung depends on the aerodynamic diameter of the particles. They fabricated light, porous particles that were physically quite large (10's of microns) but had the aerodynamic behavior of smaller (1-3 microns) particles. These porous particles, originally fabricated from PLA/PLGA polymers loaded with insulin were shown to reside in the rat lung for extended periods of time, and provide extended release of insulin for up to 72 hours.

1.2. Proposed research aims

While these advances permit controlled release of the drug at some pre-programmed rate, they do not permit modulation of this rate on demand. To

address this need, our group has advanced a new technology [7] based on chemically agglomerated vesicles (the AVT technology) that allows the modulation of the release rate from long-residence time particles deposited in the lung. The AVT particles exhibited controlled release patterns of the antibiotic Ciprofloxacin in vitro. The modulation was accomplished by cleavage of the linkages agglomerating the vesicles, both disrupting the vesicular structure and releasing internal surface area for transport of the drug across the vesicle wall. However, the cleaving agents used to trigger the release from the first generation of AVT particles are not acceptable for in vivo applications. Therefore, a new generation of in vivo compatible agglomerated liposomes was recently developed based on PEG conjugate containing a dithiobenzyl (DTB) urethane linkage cleavable by cysteine. It has been shown in vitro that the release rate of encapsulated compounds from these carriers can be modulated by the addition of mild thiolytic agents such as cysteine [8]. While there are low levels of cysteine and glutathione in the lung, capable of causing some cleavage of disulfide links between nanoparticles, the further addition of a free thiol as a “cleaver” dose would trigger the accelerated release of drug by cleavage of the inter-particle links and liberation of free nanoparticles. When administered in vivo, these particles facilitated post-administration-modulation of drug release. Thus, insulin release with the possibility of controlled post-administration changes in the release rate was demonstrated for the first time [9]. However, continuing concerns about the cleavage of this linkage by endogenous cysteine remained.

This therefore led us to seek alternative linkages that would not cleave in the presence of endogenous thiols, but would cleave upon the administration of exogenous cysteine, at levels higher than that present normally in the body. The availability of such a linkage would facilitate more complete control over the release of drug from the nanostructured AVT particles.

In this study, it is sought to extend the application of the AVT platform and demonstrate in a healthy animal model the controlled and cysteine-mediated modulation of drug release from agglomerates in the lungs. As a test drug, Ciprofloxacin has been used in this study.

The following specific aims were addressed to test the controlled and modulated drug release features of the Agglomerated Vesicle Technology (AVT):

- 1) In vitro characterization of the agglomerates based on size/structure (utilizing light scattering and microscopy techniques), and release characteristics to select the optimal conditions for making the AVT to be tested in vivo.
- 2) To test in a rabbit model the controlled and modulated release characteristics of different AVT and liposomal formulations of Ciprofloxacin after instillation in the lungs.
- 3) To evaluate acute toxicity issues of the AVT by instilling Ciprofloxacin formulation of AVT and liposomes in the lungs of rats and evaluate inflammation by histology and assay of cytokines.

Chapter 2

Background and Significance

2.1. Respiratory tract physiology

The success of a therapy using aerosolized medications depends on its ability to deliver sufficient drug to appropriate sites in the lungs with minimal side effects. This in turn depends on aspects of airway anatomy and physiology, which change with disease and age [10, 11].

The respiratory tree includes (1) the conducting airways with thick walls consisting of the trachea, the 2 bronchi and the bronchioles, and (2) the alveoli (where gas exchange occurs) across thin walls. The trachea is a flexible tube extending from the larynx. It is composed of 3 layers as shown in figure 1a: 1) the mucosa made up of goblet cells and ciliated epithelium, 2) the submucosa which is a connective tissue, and 3) the adventitia, which is the outermost layer made of C-shaped rings of hyaline cartilage. The trachea bifurcates into the left and right bronchi which continue subdividing into the bronchioles (figure 1b). The tissue walls of the bronchi and the bronchioles mimic that of the trachea. However, as the conducting airways become smaller, structural changes occur. There is a lack of cartilage support and increased amount of smooth muscle. Additionally, the epithelium is cuboidal without mucus-producing cells. The respiratory zone is defined by the presence of alveoli. The terminal bronchioles feed into the

respiratory bronchioles which lead in to alveolar ducts, then to terminal clusters or alveolar sacs composed of alveoli. The respiratory zone accounts for most of the lung's volume since it consists of 300 million alveoli providing a tremendous surface area for gas exchange.

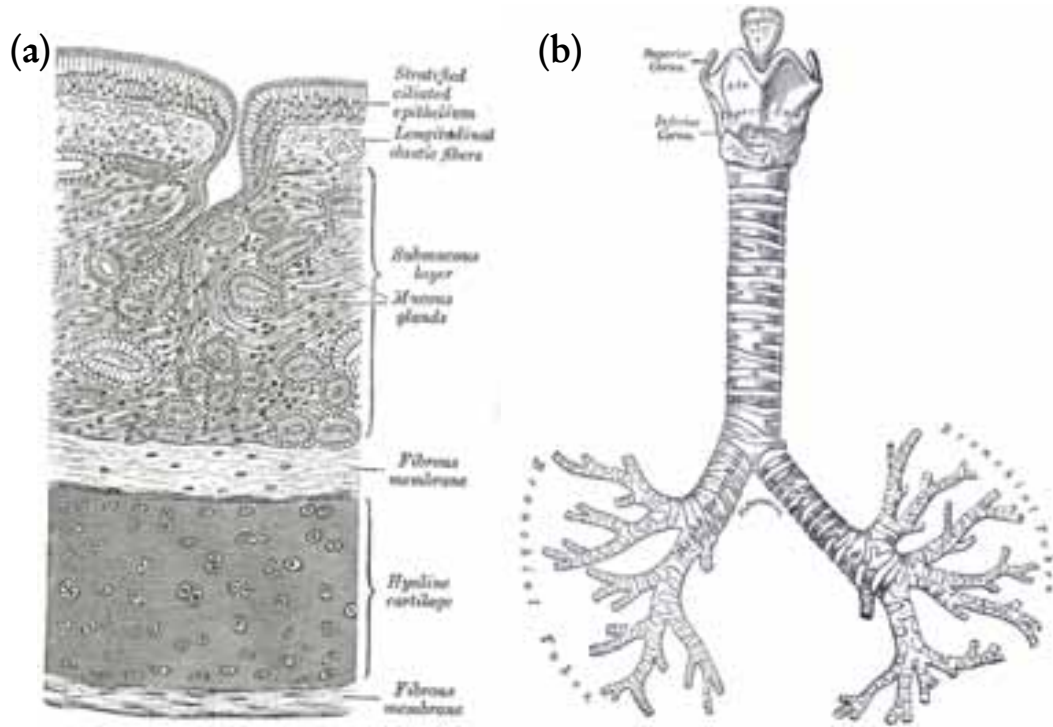


Figure 1. (a) The wall of the trachea and (b) the upper respiratory tract consisting of the trachea, the bronchi and the bronchioles [12]




The airways bifurcate more than 17 times resulting in an enormous surface area of the alveolar region. A laborious study conducted by Weibel [13] extracted the dimensions in different regions of the lungs summarized in figure 2a. In many recent studies, the alveolar surface area of human adults was estimated to be $\sim 100 \text{ m}^2$ [14, 15], which represents half a tennis court. The total lung capacity averages 6.7 and 4.9 liters in men and women, respectively [15]. It

should be noted that under normal (tidal) breathing conditions the lungs are half empty. The conducting zone contains 4% of the inhaled air, and the alveoli the rest.

A drug molecule administered to the lungs must overcome 5 barriers in order to reach blood circulation [16]:

1. *Surfactant*: The lung surfactant spreads at the air/water interface. It is a single molecule thick in most places with the fatty acid tails facing the air side but it may cause large molecules to aggregate which could enhance engulfment and digestion by airspace macrophages. The surfactant's role is to reduce the surface tension of the alveolar walls in order to prevent the complete collapse of the airways during exhalation.
2. *Surface lining fluid*: It is the reservoir for lung surfactant. It has similar composition as plasma. In the airways the thickness of the lining fluid is between 5-10 μm , and in the alveoli 0.05-0.2 μm . The fluid in the conductive airways contains mucus which flows toward the trachea by the action of cilia. Mucus is absent in the alveolar fluid.
3. *Epithelium*: This is the most important barrier. It consists of a single-cell layer of thick columnar cells in the airways, and thin and broad cells in the alveoli.

(a)

	Generation		Diameter (cm)	Length (cm)	Number	Total cross-sectional area, cm ²	
Conducting zone	Trachea		0	1.80	12.0	1	2.54
	Bronchi		1	1.22	4.8	2	2.33
			2	0.83	1.9	4	2.13
			3	0.56	0.8	8	2.00
			4	0.45	1.3	16	2.48
	Terminal bronchioles		5	0.35	1.07	32	2.11
			16	0.06	3.17	8×10^4	180.0
			17				
			18				
			19	0.05	0.10	5×10^5	10^3
Transitional and respiratory zones	Respiratory bronchioles		20				
			21				
			22				
			23	0.04	0.05	8×10^6	10^4
			24				

(b)

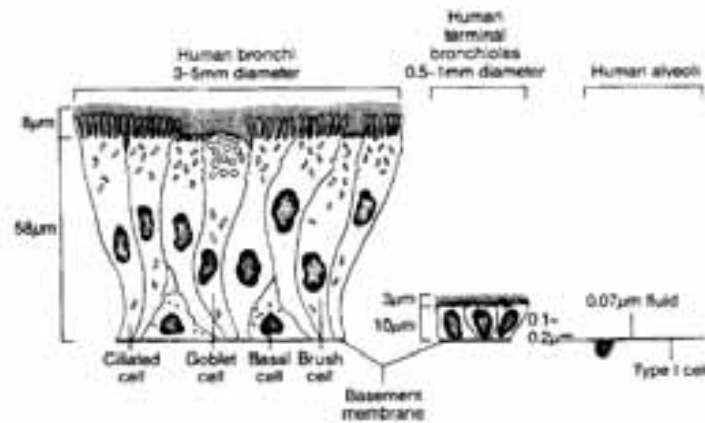


Figure 2. (a) Characteristic dimensions of the airway tree [13] and (b) Epithelial cell size and surface fluid thickness in different regions [16].

4. *Interstitium and basement membrane:* The interstitium is the extracellular space inside tissues. The epithelial and endothelial cells are attached to a tough but thin layer of fibrous material known as the basement membrane. Its role in macromolecule absorption is not known exactly.
5. *Vascular endothelium:* The final barrier to systemic absorption is a monolayer of cells that construct the walls of small blood vessels and

lymphatics. Even at the tightest junctions, the vascular endothelium exhibits higher permeability to macromolecules than the epithelium.

2.1.1. *Deposition and clearance of inhaled particles*

For efficient pulmonary drug delivery, the aerosol must deposit in the lower airways. Since the lungs are in direct contact with the atmosphere, different defense lines protect the deep lungs from exposure to particles present in the inhaled air. There are several mechanisms in the upper respiratory tract that remove particles and reduce deposition in the lower airways. These mechanisms include impaction, sedimentation and diffusion (related to Brownian motion) [17, 18]. Small particles of diameters below 1 μm remain suspended in the air and are exhaled. A small fraction of them reaches the deep lungs and deposit due to Brownian motion. Particles with diameters larger than 5 μm deposit in the upper respiratory system (mouth, throat and tracheobronchial airways) due to inertial impaction. Insoluble particles are cleared rapidly by cilia within the mucus layer lining the epithelium, which carry particles to the pharynx where they are swallowed, whereas soluble particles are removed via the lymphatic system. Particles with diameters of 1-5 μm deposit in the deep lungs due to a combination of inertial impaction and sedimentation. Scavenging cells (primarily macrophages) engulf and clear these particles either by the mucociliary elevator or the lymphatic system.

Deposition in the respiratory tract is affected by the aerosol's particle size, the patient's inhalation technique and health, and the aerosol delivery system [19]. The most important formulation variable for respiratory drug delivery is the aerodynamic diameter (D_{aer}) of the particles. The mass mean aerodynamic diameter (MMAD) for non-porous particles is defined by:

$$MMAD = \sqrt{\frac{\rho}{\rho_1}} \cdot D$$

where, D is the mass mean geometrical diameter of the particle, ρ is the mean particle mass density, and $\rho_1 = 1 \text{ g/cm}^3$ (density of water). The MMAD of the particle corresponds to the diameter of a sphere of $\rho = 1 \text{ g/cm}^3$ were it to fall under gravity with the same velocity as the particle in question. It is possible to

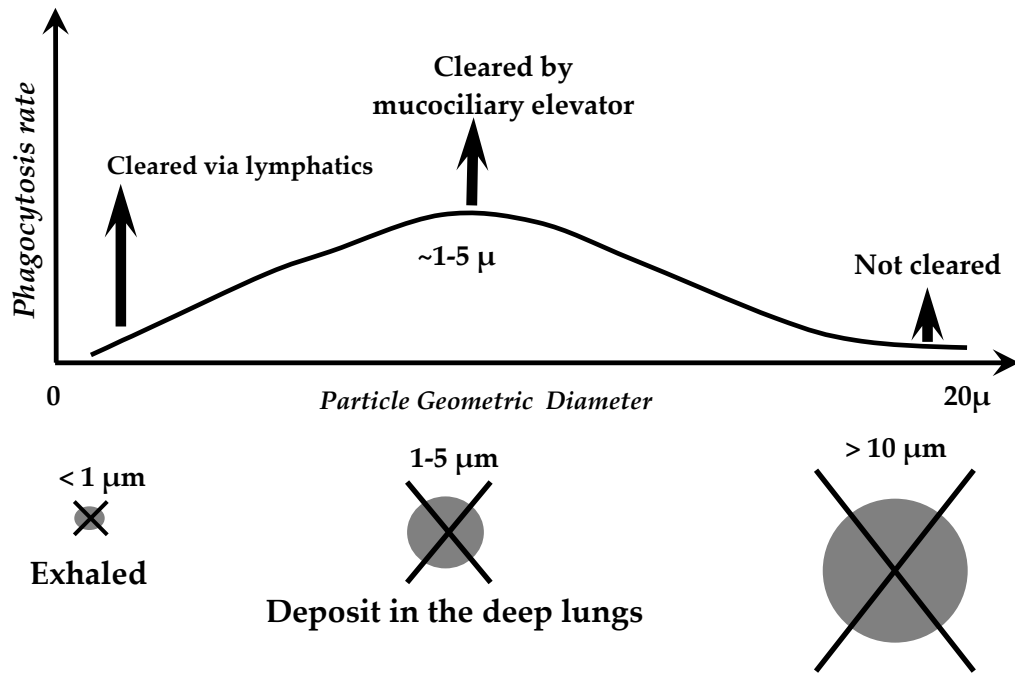


Figure 3. Deposition/clearance fate of inhaled particles in/from the deep lung

generalize the above equation for highly porous particles. Experiments show this optimal aerodynamic diameter to be in the range of 1-5 μm [17]. However, the highly active pulmonary macrophage system is optimized to clear these particles arriving at the deep lung. The majority of crystallized pharmaceutical powders with specific gravity close to 1 and aerodynamic diameters in the respirable range are subject to rapid macrophage uptake, clearance, and removal. The expected lifetime of particles in the 1-5 μm range in the lung is therefore less than 1 hr. Figure 3 summarizes the defense mechanisms of the lungs in order to quickly and effectively remove inhaled particles.

A breakthrough discovery came in the mid 1990s, when Edwards et al. [6] recognized that the macrophage uptake system relied on the geometric diameter of particles to recognize and clear them, while the deposition of the particles in the lung depended on the aerodynamic diameter. They demonstrated that by preparing particles with very low specific gravity (<0.1), aerodynamic diameters in the respirable range (1-5 μm) could be achieved with geometric diameters in the 30 μm range. These geometrically large particles were too large for macrophage uptake and therefore provided long residence time in the lung. Controlled release of insulin over several days was demonstrated by this technique. This technology (called AIR[®]) has led to clinical development of an inhaled insulin formulation by Alkermes and Eli Lilly Company.

2.2. Agglomerated Vesicle Technology (AVT)

In an attempt to bring post-inhalation modulation of drug release rate, our group has recently proposed a microparticle agglomerate of nano-sized liposomal particles, with the agglomeration process consisting of chemical cross-links that are capable of cleavage. This approach has been named as – the

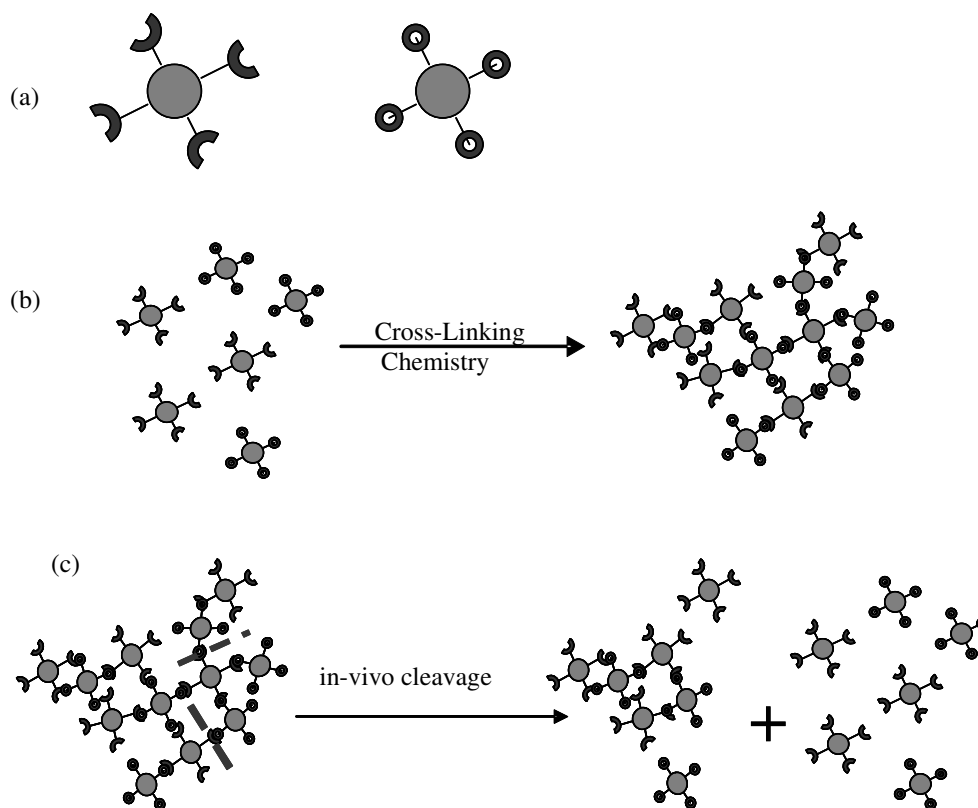


Figure 4. Schematic of core particles bearing ligands (a); agglomeration of core particles by linkers to form agglomerates (b); based on the linker chemistry some can be cleaved in-vivo by components of lung fluid or addition of a second agent (c).

Agglomerated Vesicle Technology (AVT) since it is based on the controlled agglomeration of particles. The cleavage of the cross links releases internal

surface area, as well as possibly results in the disruption of the bilayer. The result is a rapid release of encapsulated drug upon contact of the agglomerates with the cleaving agent. The approach is illustrated in Figure 4. In this figure, core particles with spacer arms, bearing ligands on their ends are shown as the starting point. The core particles could be polymeric nanoparticles with drug incorporated into them, or even drug nanoparticles to which the spacer arms have been conjugated. A particularly versatile choice for core nanoparticles are liposomes, that can conveniently be fabricated to present a variety of ligands at the distal ends of spacer PEG chains [20]. The ligands at the distal ends of the spacer arms are then used to cross-link the nanoparticles into larger clusters or agglomerates, by using a suitable chemical reaction. For example, by choosing nanoparticles with -COOH and -NH_2 ligands, one could cross-link them using the carbodiimide reaction [21]. Depending on the conditions of the reaction mixture, one would expect the resultant agglomerates to have different densities. For example, under diffusion-limited conditions, where the overall concentration of the core nanoparticles and linker are low, the so-called diffusion-limited-aggregation condition would apply, resulting in a limiting fractal dimension of 1.5-2.5 [22 - 25]. Depending on the particular conditions of the chosen reaction scheme, other fractal dimensions could be achieved. Most chemical reactions are expected to be rapid compared to the diffusion of relatively large (100 – 400 nm) liposomes, resulting in DLA (diffusion limited agglomerate) clusters being formed.

Zasadzinski has shown that colloidal aggregation can be made self-limiting by controlling the ratio of the reactive groups on the colloidal surface to cross-linking agents [26]. According to that study, unilamellar vesicles (0.1 μm) incorporating a small fraction of receptors formed aggregates via ligand-receptor interactions. The aggregates had dramatically different sizes depending on the ratio of receptors to cross-linking agents. However, the streptavidin-biotin based linkage is likely to be immunogenic and therefore is not acceptable for clinical use.

The choice of the linker can impart other interesting properties to the agglomerates. For example, EGS [ethylene glycobis(succinimidylsuccinate)] links amino groups with each other, via an ester linkage [21]. The ester bond can be readily hydrolyzed with hydroxylamine, resulting in breakage of a link between the core nanoparticles. If an aggregate were built using the EGS linker, one would expect cleavage of the links to slowly result in release of the core nanoparticles. Assuming that the nanoparticles release drug much faster than the agglomerates, one would therefore expect a progressive increase in drug release rate as the hydrolysis of linkers proceeded. Similarly, if one were to cross-link particles using a dithiobenzyl (DTB) urethane linkage [27], the linker would carry a disulfide bond that would be cleaved by the addition of free thiols. While there are low levels of cysteine and glutathione in the lung, capable of causing some cleavage of disulfide links between nanoparticles, the further addition of a free thiol as a “cleaver” dose would trigger the accelerated release of drug by

cleavage of the inter-particle links and liberation of the free nanoparticles. A non-biocompatible cleaver can be used as an in-vitro tool to investigate the release profile.

Other very interesting structures are also conceivable, for example initial agglomeration by a non-cleavable linker, followed by agglomeration with a cleavable linker, or initial agglomeration by a cleavable linker followed by additional agglomeration by a non-cleavable linker. Inducing cleavage in such a structure would result in other triggered release patterns that could potentially be therapeutically useful.

2.2.1. *Agglomeration methodology of liposomes*

While one could conceive of any nanoparticle presenting an appropriate ligand on the external surface as a candidate for this technology, we have focused on the use of liposomes. Liposomes have several advantages for use as the core nanoparticles: (1) they can easily be produced in a range of sizes, (2) they can efficiently be loaded with a variety of drugs, (3) they can easily incorporate polymer spacers on their exterior surfaces by anchoring the spacer to a lipid molecule that in turn resides in the bilayer wall, (4) the bilayer wall composition can be manipulated to achieve a range of drug release properties, and (5) many lipids, including the ones chosen for liposome preparation are already abundantly present in lung surfactant and lung fluids, and would therefore be

well tolerated by the lung, making high excipient loads quite acceptable. One would have to consider the toxicity of the lipid-polymer conjugate used to provide the inter-particle spacers, but that problem appears small compared to a situation where the entire particle is composed of a polymer that has toxicity issues. In this work therefore, liposomes were chosen that consisted of 55-58% DPPC bilayer, with 40% Cholesterol and 2-5% DSPE-PEG-NH₂.

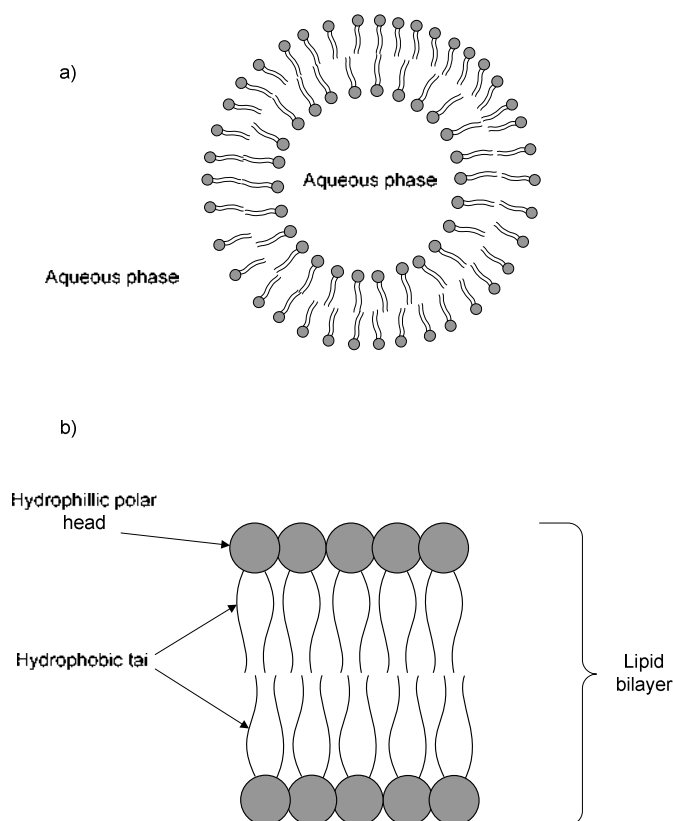


Figure 5. a) A unilamellar liposome; and b) details of the lipid bilayer.

Liposomes, or lipid vesicles, are self-assembled colloidal particles (figure 5) that occur naturally and can be prepared artificially, as shown by Bangham in the mid-1960s [28, 29, 30]. Initially, liposomes served as a case to study biological membranes and later in the 1970s they were considered candidates for drug

delivery. Presently, liposomes are the leading nanoparticles used in drug delivery with several products based on them. These products range from drug-dosage forms (antifungals, anticancer agents, vaccines) and cosmetic formulations (skin-care products, shampoos) to diagnostics and various uses in the food industry.

The benefits associated with the encapsulation of drugs in these carriers were mainly two-fold: (1) protection of the drug from chemical or metabolic degradation after administration, and (2) reduced toxicity through decreased exposure of the drug to healthy tissues. In general, these preparations exhibited significant reduced toxicity in comparison to the same drug administered by the conventional, unencapsulated form. A classic example is that of the antifungal drug, Amphotericin B, which reacts with all cells resulting in high toxicity. Also the peculiar solubility issues of the drug make it an ideal candidate for liposome encapsulation. Early studies in laboratory animals using liposomes containing Amphotericin B showed an increased therapeutic index [30].

A further reason for selecting liposomes as the parent nanoparticles in the agglomerated particle technology is the wealth of literature on the use of liposomes for respiratory drug delivery. Liposomes have long been considered as respiratory drug carriers in aqueous nebulizer-based formulations. A concern with such use, of course, is the disruption of liposomes by the high shear forces experienced by the fluid in the nebulization process. However, there have been studies [31] examining the effects of nebulization by different nebulizers on the

encapsulation of drugs by liposomes. Based on this, one would then be able to select a nebulizer that minimizes the disruption of liposomes, and the resultant loss of encapsulation. Liposomes have also been considered as candidates for dry powder inhalation. While liposomes are in general not stable upon drying (the existence of the bilayer depends on the free energy reduction achieved by the assembly of the amphipathic molecules in aqueous medium) there have been numerous examples of the drying of liposomes after protecting the bilayer with a suitable sugar such as trehalose [32]. Liposomes and even simple lipids have also been shown to promote trans-alveolar permeation of drugs. For example, it has been shown by Mitra et al. [33] that the mere presence of lipids co-administered to the lung along with insulin increased the bioavailability of insulin by 40%. Similar enhancements have also been reported by the same group for liposomes containing insulin. It therefore appears that liposomes are a good choice for core nanoparticles.

2.2.1.1. Preparation of liposomes

Factors that influence the hydration of the lipids and the vesicle formation process are the size of the raw lipid material, the hydration temperature and the bilayer phase transition temperature, shear forces, composition of the hydration medium and time [30]. Vesicle formation is greatly accelerated when the hydrated lipids are in the liquid crystalline state above their main transition

temperature (T_m). The vesicles formed are predominantly multilamellar vesicles (MLVs). When a drug is dispersed with the dry phospholipids or in the hydration buffer, encapsulation will occur during the vesicle formation.

The hydration of the lipids using organic solvents is achieved by injecting an organic solution containing the lipids, which is miscible with water (e.g. ethanol), into an aqueous phase. The resulting dilution of the organic solvent induces MLV vesicle formation. An attractive sizing technique to obtain small, unilamellar vesicles is low-pressure extrusion of the liposomal suspension under moderate pressures (<1 MPa) through polycarbonate membranes with well-defined pore diameters. Polycarbonate filters with pore sizes ranging from 0.8 down to 0.03 μm are available. The resulting vesicle size and lamellarity are related with the pore size, although effects of the medium and phospholipid composition are generally observed as well. Extrusion rates depend on the bilayer phase. The highest rates are obtained with phospholipids heated above the T_m , even when cholesterol is present, which abolishes the transition from the gel to the liquid crystalline state. The possible effects of the phospholipid composition on the obtained vesicle size can be minimized by repeated extrusion cycles.

2.2.1.2. Encapsulating drugs within liposomes

Drugs can be encapsulated within liposomes by two different ways: (1) passive encapsulation, where the drug is entrapped within the liposomes during the vesicle formation process, and (2) active or remote loading, where the drug is loaded into preformed vesicles.

Passive encapsulation is suitable for water soluble compounds that do not interact with the bilayer. The encapsulation efficiency directly depends on the

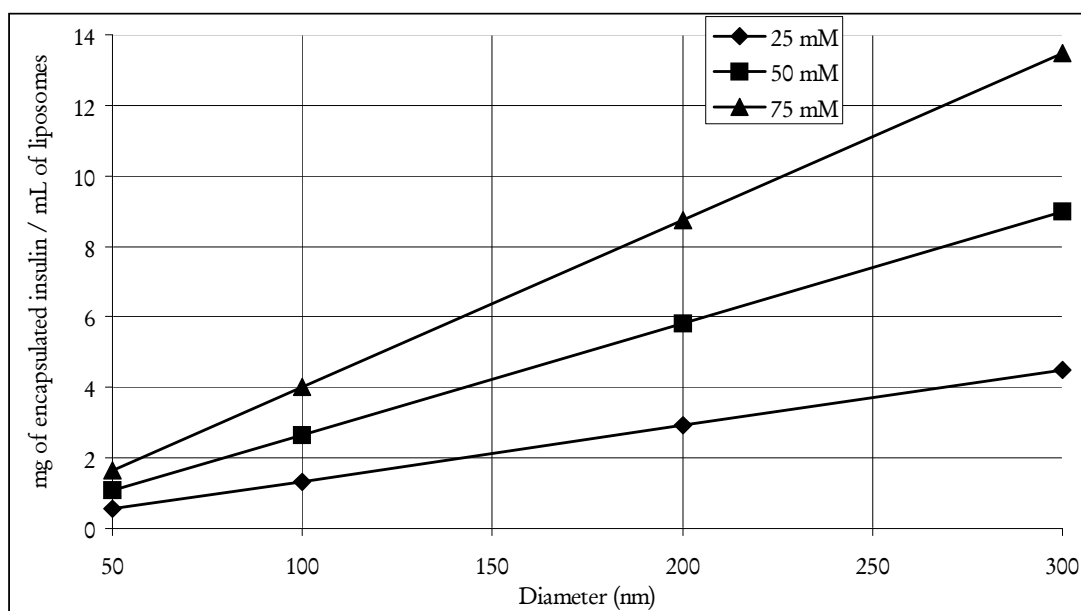


Figure 6. *Dependence of the amount of encapsulated insulin to size of liposomes passively encapsulating insulin from a pool concentration of 30 mg/mL.*

aqueous volume enclosed by the vesicles, which itself depends on the phospholipid composition of the dispersion and the lamellarity and morphology of the vesicles. The encapsulation capacity but not the efficiency can be improved by using a high drug concentration (limited by solubility) during the vesicle formation process. The physical dimensions of lipid molecules and their

contribution to the encapsulation efficiency of liposomes has been described by Lasic [30].

Using insulin as an example, figure 6 shows the portion of a 30 mg/mL pool insulin concentration loaded passively into liposomes as a function of liposome size, and lipid concentration. Assuming a bioavailability of 25% of inhaled insulin [5] and a daily dose of insulin for an adult Type-I diabetic patient of 50 IU (1 mg \approx 27.6 IU), one can readily see that, in the case of 250 nm liposomes with 75 mM lipid content and 30 mg/mL insulin pool concentration, about 0.650 ml of suspension and 35 mg of lipid will be needed to carry the insulin required. While with a polymeric excipient, this load may be unacceptable, with a lipid excipient, one can easily justify this drug:excipient ratio, since the lipids used are already present in the lung in larger quantities than administered with this formulation.

The remote loading depends on a proton gradient along the liposomal bilayer. Partition coefficients of drugs can depend on the pH, and to a lesser extent on the ionic strength of the aqueous medium [28]. 100% of the drug can be effectively encapsulated within liposomes depending on the conditions selected. The earliest drugs characterized for active loading were lipophilic cations or anions [34]. It has been shown by a number of groups [35 – 37] that a zwitterionic drug like Ciprofloxacin can also be actively loaded using an ammonium sulfate ion gradient method. Ciprofloxacin possesses both an amino and a carboxyl functional group. At a pH < 6 it has a net positive charge, whereas above pH 9 it

has a net negative charge. Below or above these pH extremes, Ciprofloxacin is highly soluble in aqueous media, however at physiological pH values it is practically insoluble. In general, a charged species cannot cross the bilayer at a significant rate; consequently it is the uncharged species that is able to diffuse into the vesicle down its concentration gradient.

In a two chamber aqueous system separated by a membrane as illustrated in figure 7 using doxorubicin as an example, accumulation will occur at the low pH side under dynamic equilibrium conditions. A transmembrane pH-gradient causes accumulation of doxorubicin ($pK_a=8.1$) in the low pH interior. In the unprotonated form, doxorubicin can diffuse through the bilayer. At the low pH-side the molecules are predominantly protonated, which lowers the concentration of this drug in the unprotonated form, and thus promotes the diffusion of doxorubicin to the low-pH side of the bilayer from the external side.

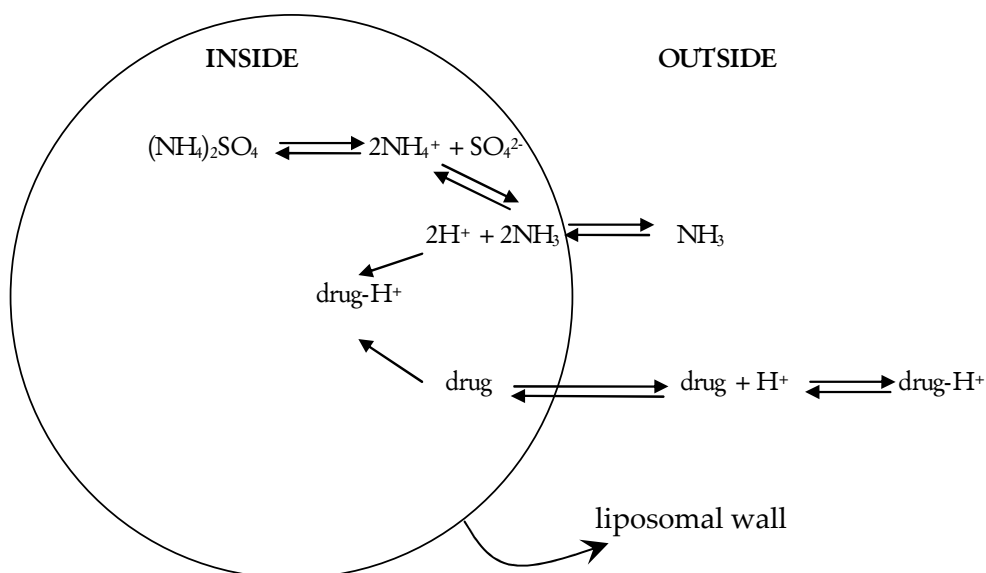


Figure 7. Schematic representation of the active loading technique.

2.2.1.3. Tether selection for agglomeration

The density and porosity of the agglomerates are clearly a function of the spacer length chosen and the size of the starting particles. Further, the more rigid this spacer is, the more rigid the agglomerate will be. However, a rigid, non-flexible spacer would limit the efficiency of agglomerate formation since the terminal ligands, constituting the reactive groups that help the nanoparticles agglomerate, would not be free to move in all directions and seek other reactive groups during the reaction step. The reaction rate would therefore be limited by the diffusion of the relatively large, slow moving liposomes. It is not clear at this time, what the ideal choice of spacer for any given application would be, and the effect of different tethers is a topic of ongoing investigation. In the present work, polyethylene-glycol (PEG) tethers were chosen since: (1) they are readily available conjugated to lipids and (2) much is known about the safety of PEG-lipids.

2.2.1.4. Agglomeration chemistries

Cross-linking chemistries are well known in bioconjugation of proteins and other molecules [21]. These techniques have been utilized to couple particles together. In earlier studies carbodiimide, NHS ester, and imidoester linkers have been used for agglomerating both polymer particles and liposomes [38].

In this work the following imidoester and NHS linker chemistries have been investigated for cross-linking liposomes:

a) DTBP (dimethyl 3,3'-dithiobispropionimidate•2HCl) is a homobifunctional imidoester that reacts with primary amines to form stable

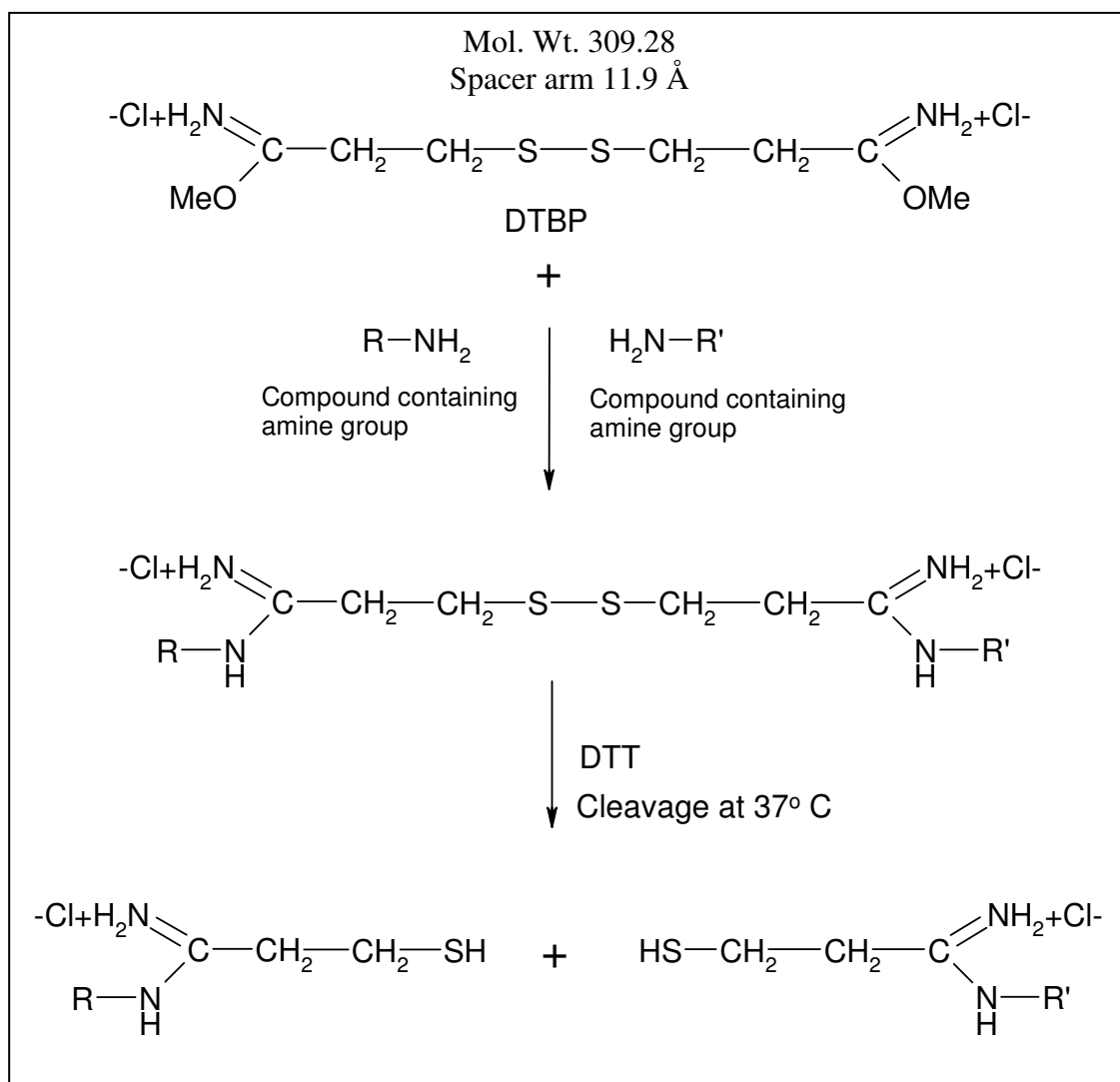


Figure 8. Reaction scheme for DTBP agglomeration [21] followed by cleavage with DTT.

covalent bonds. In mildly alkaline pH's (7-10), DTBP reacts with amine-containing molecules forming charged amidine bonds. The disulfide bond on the

linked conjugate can be cleaved with a strong thiol like DTT (Dithiothreitol) at 37 °C. The reaction scheme for DTBP is illustrated in figure 8.

b) DTSSP (Dithiobis[succinimidylpropionate]) is a water-soluble, homobifunctional N-hydroxysuccinimide (NHS) ester. This cross-linker is active towards the primary amines resulting in a covalent amide bond and the release of N-hydroxysuccinimide. The reaction scheme is illustrated below in figure 9. This is also a thiol cleavable linker well known to be cleavable by DTT.

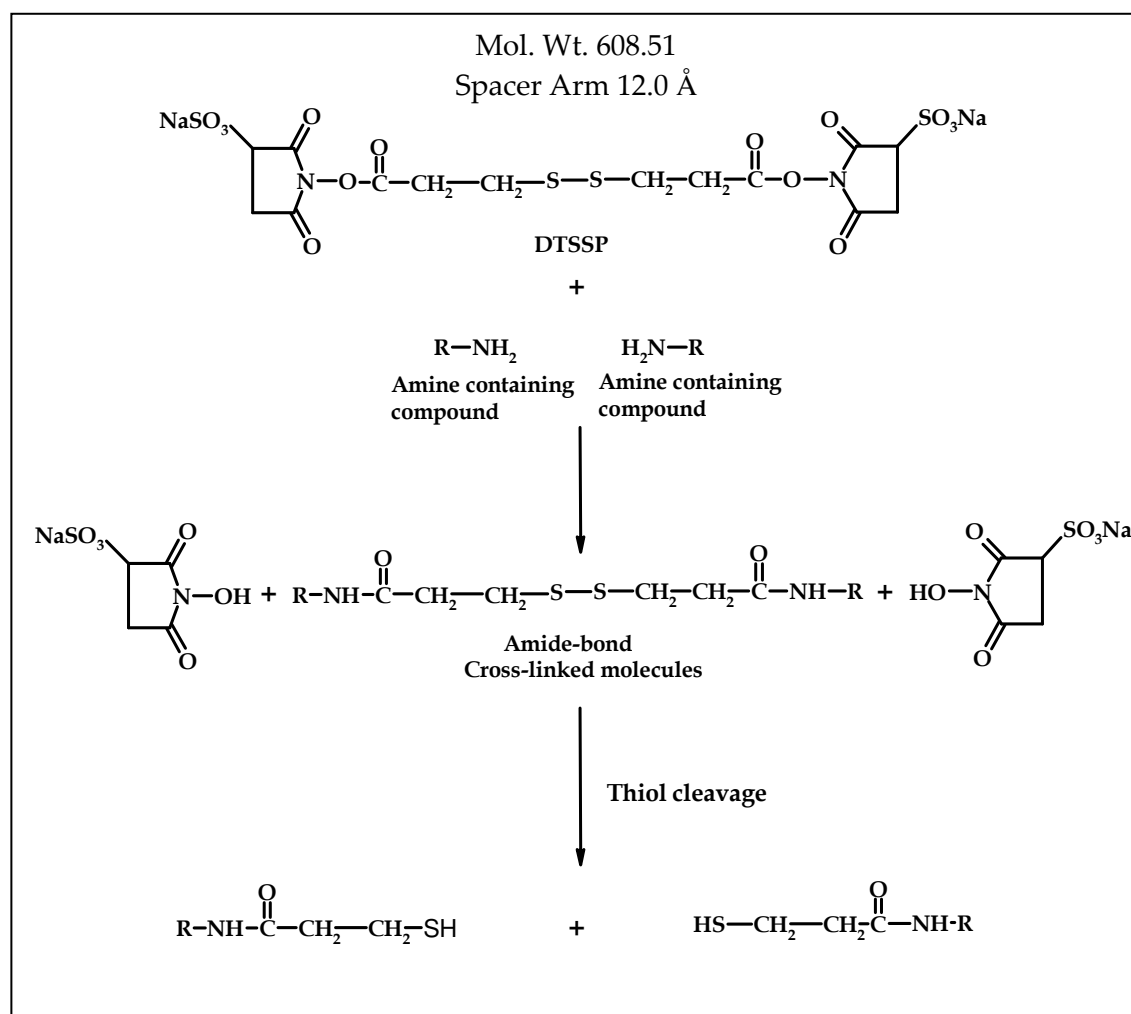


Figure 9. Agglomeration scheme for DTSSP agglomeration [21].

It was found that this linker is also cleavable by a mild thiol like cysteine,

as witnessed by the size reduction of agglomerates made with DTSSP on incubation with cysteine.

2.2.2. *Triggered release of drug*

With the goal of ‘in vivo’ post-inhalation modulation of drug release rate, a DTB-urethane conjugate cleavable by an ‘in vivo’ acceptable compound such as cysteine [27] was developed in our lab. In vitro results showing release and size reduction was demonstrated [8]. However, with the finding that DTSSP, a commercially available cross-linker, is cleavable by cysteine, and also the limited success with the synthesis of a clean DTB-urethane conjugate in considerable quantities for the studies to be undertaken, the triggered release studies in animals were done based solely on the DTSSP linkage with no DTB coupled to the PEG-lipid.

2.2.2.1. Using cysteine as a trigger

In order for cysteine to act effectively as a cleaving agent to the AVT particle, the required concentration of cysteine in the lung surfactant should be below 300 mM representing a total amount of about 1 gram. L-cysteine and its derivative N-acetyl-L-cysteine (NAC) are available as commercial dietary supplements from numerous manufacturers. Cysteine is an amino acid which is commonly found in food and synthesized by the body. NAC helps break down

mucus (for that reason, inhaled NAC is used in hospitals to treat bronchitis), increase levels of the antioxidant glutathione, and detoxify harmful substances in the body. Mucomyst® brand of acetyl-cysteine (Bristol Laboratories), a mucolytic agent for inhalation, requires a maintenance dose of 6 grams for an adult with a body weight of 80 kg. Hence, the needed dose of cysteine as a cleaving agent is not considered forbidden for 'in vivo' use at this preliminary stage of this work.

Chapter 3

Methods and Experimental Procedures

3.1. Analytical Methods

The methods and techniques that were used in the study for characterizing the particles and assaying the drug are discussed briefly here.

3.1.1. *Dynamic Light Scattering*

The parent liposomes that were fabricated and used in the study were in the submicron range. For measuring such small particles, Dynamic Light Scattering (DLS) is a very popular and useful technique [39]. Light incident on particles in solution is scattered in all directions. The light scattered by different particles is of different phase. The DLS technique is dependent on the molecular diffusion rate, and monitors the time-dependence of intensity of light scattered

from the particles. The rate at which the intensity fluctuates about its average value is dependent on the rate at which the molecules move in solution. The timescale on which the intensity domain fluctuation takes place is approximately equal to the time required by two molecules to diffuse far enough relative to each other such that the phase difference between the two, changes from zero to π radians. The intensity domain output is transformed into a time domain output by autocorrelation. The measured autocorrelation function $G(\tau)$ is given as

$$G(\tau) = A[1 + B | g(\tau) |^2] \quad \dots \quad (3.1)$$

where,

$A \rightarrow$ baseline value,

$B \rightarrow$ machine constant,

$g(\tau) \rightarrow$ normalized first-order autocorrelation function.

For a monodisperse system of particles $g(\tau)$ becomes a simple exponential decay, and equation (3.1) is transformed to:

$$G(\tau) = A[1 + B \exp(-2Dq^2\tau)] \quad \dots \quad (3.2)$$

where,

$D \rightarrow$ coefficient of diffusion,

$q \rightarrow$ scattering vector [$q = (4\pi/\lambda)\sin(\theta/2)$],

$\lambda \rightarrow$ wavelength of laser in air,

$\theta \rightarrow$ angle of scatter,

$\tau \rightarrow$ time.

For a Newtonian fluid and spherical particles, the diffusion coefficients are related to the hydrodynamic diameter of the particles by the Stokes-Einstein equation as,

$$D = k_B T / (3\pi\eta d) \quad \dots \quad (3.3)$$

where,

$k_B \rightarrow$ Boltzmann's constant,

$T \rightarrow$ absolute temperature in $^{\circ}\text{K}$,

$\eta \rightarrow$ viscosity of the liquid,

$d \rightarrow$ particle diameter.

The DLS measurements for this study were done on a Brookhaven Instruments BI-9000AT Digital Autocorrelator, a BI-200SM goniometer and a Hamamatsu photomultiplier (Brookhaven Instruments Corp., Holtsville, NY, USA). The light source was a 532 nm, Ti-sapphire, frequency doubled laser. For the DLS measurement, the liposomal suspensions were appropriately diluted in the buffer used to prepare the liposomes.

3.1.2. Fraunhofer Diffraction Pattern Analysis

Fraunhofer diffraction is widely used for characterizing particles in the 1-

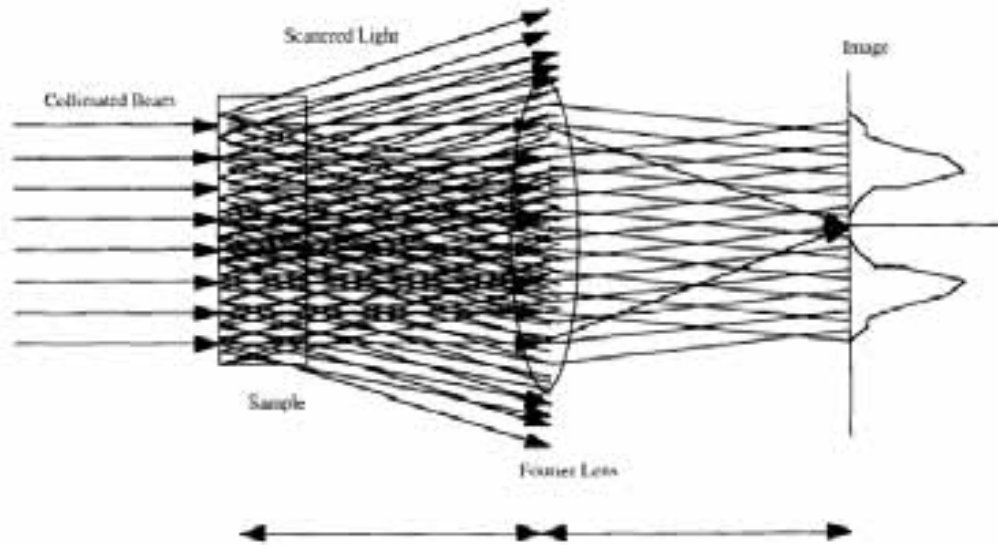


Figure 10. Fraunhofer Diffraction Pattern Analysis system [41].

200 μm size range [40, 41]. The sample is normally a liquid or gas suspension of particles whose size distribution is to be determined. Laser energy from the source is scattered by the particles, resulting in a characteristic energy distribution at small angles of deviation from the forward beam. A portion of this scattered pattern is focused onto a detector by a lens of known focal length. A schematic of a typical Fraunhofer diffraction experiment is shown in figure 10. The detector response is averaged over a period of time and recorded. The size distributions are determined by numerically inverting the recorded pattern. For a monodisperse system of spherical particles in the sample which are larger than the wavelength of the light used, the diffraction pattern would be described by the characteristic Airy diffraction equation:

$$I(\theta) = I_o \int_0^\infty \frac{\pi^2 D^4}{16\lambda^2} \left[\frac{2J_1\left(\frac{\pi D \theta}{\lambda}\right)}{\frac{\pi D \theta}{\lambda}} \right]^2 n(D) dD \quad \dots (3.4)$$

$I(\theta)$ is the scattered intensity at any angle θ , λ the wavelength of the incident light, D the diameter of the particles in the sample, and $n(D)$ the particle size (number) distribution.

This pattern is then refracted by a transform lens (of finite aperture) onto a detector of finite diameter. Neglecting the aberrations due to finite aperture, the transformed pattern can be obtained by the following transformation:

$$r = f\theta \quad \dots (3.5)$$

Where, f is the focal length of the lens and r is the radial position of the pattern.

The light energy within any detector ring on the focal plane bounded by radii s_1, s_2 due to a particle of radius r is given by:

$$L_{s_1, s_2} = E \{ J_0^2(krs_1/f) + J_1^2(krs_1/f) - J_0^2(krs_2/f) - J_1^2(krs_2/f) \} \quad \dots (3.6)$$

where,

$f \rightarrow$ focal length,

$E \rightarrow$ energy falling on the particle that is proportional to the cross sectional area of the particle,

$J_0, J_1 \rightarrow$ Bessel functions of the zeroth and first order respectively and first kind.

For a collection of particles of different sizes, the total energy is a sum over all the sizes and is given as:

$$L_{S_1, S_2} = C \sum_i^M N_i \{ (J_o^2 + J_1^2)_{s_1} - (J_o^2 + J_1^2)_{s_2} \} \quad \dots (3.7)$$

where,

$C \rightarrow$ proportionality constant,

$N_i \rightarrow$ number of particles of a particular size.

The detector response (normally a voltage or a current, depending on the energizing and analysis circuitry), which is proportional to the incident energy is then given by;

$$V_{S_1, S_2} = C' . L_{S_1, S_2} \quad \dots (3.8)$$

The size distribution can then be calculated from the detector response by using several methods. The two most popular methods used are the model-dependent and the model-independent methods. The model dependent method assumes a model such as the Log-Normal or Rosin-Rammler for the size distribution. The utility of the model-dependent inversion technique is limited to unimodal distributions. The model-independent technique tackles the more general multimodal distributions which makes no such assumptions. However, the number of available detector channels also limits the number of size classes which can be included in the model-independent analyses. This is normally 32 classes.

The Fraunhofer Diffraction Pattern Analysis method works very well for unimodal systems. For sharp-peaked multimodal systems, there is a strong tendency to skew the distribution towards the mode that contributes the strongest peak in the diffraction pattern. In the presence of small particles ($<1\text{ }\mu\text{m}$, just below the lower limit of the FDPA system), the modes of multimodal distributions can be assigned incorrect mass fractions.

It should be noted that the Fraunhofer theory is based on the ideal case of hypothetical particles. In reality, particles could be non-spherical, and possess refractive indices that are close to that of the medium. If the particles were multimodal with a mode larger than the upper limit on size, the measurement would be inaccurate.

A Malvern Mastersizer (Malvern Instruments Inc., Southborough, MA, USA) with a 100 mm lens was used to do the FDPA on the agglomerated liposomes.

3.1.3. *Cascade impaction for aerodynamic characterization of aerosols*

Aerosol particles can be spherical or highly irregular in shape. Due to a variety of shapes, it is difficult to describe an aerosol particle by a single number like diameter. One way of describing the size of a particle is by the description of equivalent aerodynamic diameter. The aerodynamic diameter of a sphere can be equated to its geometric diameter by deriving from Stokes Law as,

$$D_{\text{aer}} = D_{\text{geo}} \cdot \sqrt{\varrho} \quad \dots (3.9)$$

where, D_{aer} is the aerodynamic diameter, D_{geo} is the geometric diameter, and ϱ is the specific gravity of the particle with respect to water.

Cascade impactors have been widely used to characterize the aerodynamic size distribution of aerosol particles. The working principle involves the drawing of ambient air through the inlet port into a series of stages connected by successive smaller orifices. The number of stages is typically 6 to 7. As the aerosol particles flow through the stages of the device, they are propelled toward the collection plates on each stage with increasingly higher inertia. If the particle has sufficient inertia, it will impact the plate; else it will be carried by the air flow into the successive stage. Submicron particles that are not collected on the last collection plate are caught up in the backup filter, immediately downstream from the last stage. Once the sampling is complete, the amount deposited on each stage is determined. The measurement results in a size distribution of the aerosol particles.

An Andersen Cascade Impactor, series 20-800, 1 ACFM non-viable sampler (Thermo Electron Corp., Waltham, MA, USA) was used to determine the aerodynamic diameters of the agglomerates.

3.1.4. *Microscopy*

Microscopy is a widely used technique that produces visible images of structures or details that are too small to be seen by the eye, by using either a microscope or a magnification tool.

In conventional microscopy, the resolution of the image depends on the wavelength of the incident radiation, which could be light, electron beam, or an X-ray. The lower wavelength of electron beam results in an image with higher resolution.

The techniques discussed below were used to evaluate the morphology and size of the agglomerates:

3.1.4.1. Confocal Laser Scanning Microscopy

Confocal laser scanning microscopy (CLSM) is a valuable tool for obtaining high resolution images and 3-D reconstructions. The key feature of confocal microscopy is its ability to produce blur-free images of thick specimens at various depths. Images are taken point-by-point and reconstructed with a computer, rather than projected through an eyepiece.

In a laser scanning confocal microscope, a laser beam passes a light source aperture and is then focused by an objective lens into a small (ideally diffraction-limited) focal volume within a fluorescent specimen. A mixture of emitted fluorescent light as well as reflected laser light from the illuminated spot is then

recollected by the objective lens. A beam splitter separates the light mixture by allowing only the laser light to pass through and reflecting the fluorescent light into the detection apparatus. After passing a pinhole, the fluorescent light is detected by a photo-detection device [photomultiplier tube (PMT)] transforming the light signal into an electrical one which is recorded by a computer

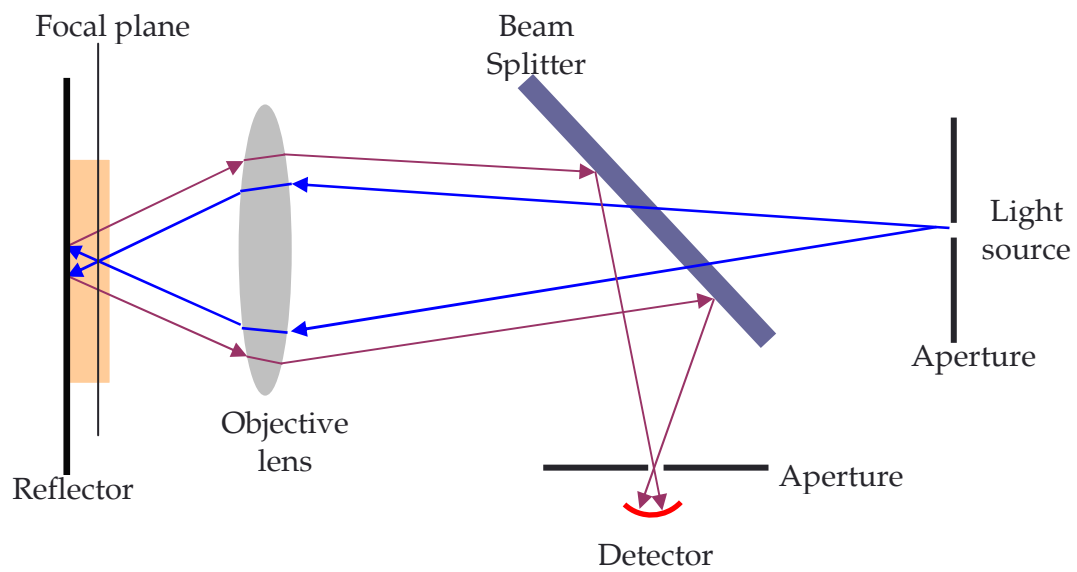


Figure 11. Working principle of confocal microscopy.

The agglomerates (encapsulating carboxyfluorescein dye) in this study were imaged with a Zeiss LSM 510 META confocal microscope using a $\times 63$ immersion oil objective (Carl Zeiss, Germany).

3.1.4.2. Negative Staining Electron Microscopy

Electron microscopes were developed to overcome the limitations of light microscopes, which are limited by the physics of light to 1000X magnification and a resolution of 0.2 μm . They are able to achieve 10,000X plus magnifications that are just not possible using light microscopes. By achieving these magnifications, finer details of a specimen can be observed with a resolution in the nanoscale length limits.

An electron microscope uses a highly energetic beam of electrons that is focused on a specimen to examine objects on a very fine scale. The examination can yield information on; (1) the surface features of the object (topography), (2) shape and size of the particles that make up the object (morphology), (3) the elements and compounds that make up the object (composition), and (4) the crystallographic information of the specimen.

Most biological materials show little contrast with their surroundings unless they are stained. In the case of light microscopy, contrast can be enhanced by using colored stains which selectively absorb certain wavelengths. The electrons in the electron microscope are absorbed very little by biological material and contrast is obtained mainly by electron scattering.

To heighten the contrast between the specimen and the background, electron-dense "stains" are used. These are usually compounds of heavy metals of high atomic number (for e.g. uranium salts), that serve to scatter the electrons from regions covered with the stain. If particles are coated with stain (positive

staining), fine details may be obscured. Negative staining overcomes this problem by staining the background and leaving the particle relatively untouched. The negative stain is molded round the particle, outlining its structure, and is also able to penetrate between small surface projections and to delineate them.

In this study, negative stained electron micrographs of agglomerates and liposomes were taken with a JEOL JEM1230 electron microscope operating at 80 kV and 56 μ A beam current.

3.1.5. HPLC assay

Chromatography is a general technique that separates a mixture into its individual components in order to evaluate each component, free from interference, from the other components. Chromatography can be coupled with a detection system that would enable a characterization of each component. High performance liquid chromatography (HPLC) is one such method. It is used to analyze liquid samples or the liquid extract of a sample.

The fundamental basis for HPLC consists of passing a sample (chemical mixture) in a high pressure solvent (the mobile phase) through a packed bed of adsorbents (the stationary phase). As the chemical entities pass through the column they interact between the two phases; mobile and stationary, at different rates. The difference in rates is primarily due to different polarities of the

components. The components that have the least amount of interaction with the stationary phase or the most amount of interaction with the mobile phase will exit the column faster. Repeated interactions along the length of the column result in a separation of the entities. Various mixtures of the chemicals can be analyzed by changing the polarities of the stationary phase and the mobile phase.

The stationary phase is typically bonded to a support phase, usually consisting of porous beads. The pore sizes can be varied to control the elution rate of different species. Furthermore, the dimensions of the column can also be varied to enable further control over the separation.

A change in the polarity of the mobile phase can significantly affect the efficiency of any HPLC separation. The mobile phase polarity is generally the opposite of the stationary phase. The rate at which the polarity is changed defines the "gradient." This gradient technique helps to further separate mixtures of variously polar components.

As the components exit the column, they can be detected by various means. Refractive index, electrochemical, or ultraviolet-absorbance changes in the mobile phase can indicate the presence of a component. The amount of the particular component leaving the column will determine the intensity of the signal produced in the detector. The detector measures a signal peak as each component leaves the column. By comparing the time it takes for the peak to show up (the retention time) with the retention times for a mixture of known

compounds, the components of unknown sample mixtures can be identified. By measuring the signal intensity (response) and comparing it to the response of a known amount of that particular component, the amount of the component in the mixture can be determined.

The HPLC system used in the studies for assaying Ciprofloxacin consisted of a Shimadzu SCL-10Avp liquid chromatograph, SPD-10Avp UV-Vis detector (278 nm) and SIL-10Advp auto-injector (Shimadzu Scientific Instruments, Columbia, MD, USA). The chromatographic conditions were as follows: Chromatography was carried out with a Waters Symmetry 5 μ C18 column, 150 x 4.6 mm (Waters Corp, Milford, MA, USA); The column temperature was maintained at 28°C and the flow rate was 1.0 mL per minute; The mobile phase was a mixture of 15% (v/v) acetonitrile and 85% (v/v) 25 mM sodium phosphate buffer at pH ~ 2.3. The sample injection volume was 20 μ L. Ciprofloxacin eluted within 10 minutes, under these assay conditions.

3.2. Experimental procedures of the 1st generation of AVT (in vivo non-cleavable)

In this section preliminary experiments that were undertaken are described. The early studies were done with blank liposomes (no drug encapsulated). The focus of these studies was to see how different reaction conditions, such as the amount of reacting groups, and pH of the reaction,

affected the agglomeration of liposomes. Ciprofloxacin was used as a model drug to investigate in vitro release characteristics of the agglomerates in addition to the aerodynamic properties of the agglomerated vesicles. Finally the agglomerates of DTBP (in vivo non-cleavable) encapsulating Ciprofloxacin were evaluated for drug release properties in vivo, by instilling formulations in the lungs of normal rabbits.

3.2.1. *In vitro experiments with blank liposomes*

3.2.1.1. Materials

1,2-Dipalmitoyl-sn-Glycero-3-Phosphatidylcholine (DPPC) was purchased from Genzyme Pharmaceuticals (Cambridge, MA, USA). Cholesterol was purchased from Sigma-Aldrich (St. Louis, MO, USA). Distearoyl phosphoethanolamine [Amino (polyethylene glycol)] (DSPE-PEG-NH₂) conjugate was purchased from Avanti Polar Lipids Inc (Alabaster, AL, USA). The cross-linker DTBP was purchased from Pierce (Rockford, IL, USA). All the rest of the reagents were purchased from Fisher Scientific.

3.2.1.2. Fabrication and characterization of liposomes

The liposomes were made by extruding a suspension of dissolved hydrated lipids through a single 400 nm Whatman Nuclepore polycarbonate

trach-etch membrane in a Lipex Biomembranes extruder (Vancouver, British Columbia, Canada). A lipid composition of 57-58% DPPC, 40% Cholesterol, and 2-3% DSPE-PEG-NH₂ conjugate was used. The lipids were dissolved in ethanol at 50-60^o C and then hydrated with sodium citrate buffer (ethanol volume not exceeding more than 10% of the final volume), the lipid concentration in the final mixture being 50-100 mM. The suspension was then passed 7-10 times through the extruder at 50-54^oC and a pressure of approximately 100 psi.

Assuming 51% of the DSPE-PEG-NH₂ to be on the outer leaflet of the bilayer, the number of amine groups available for coupling with the cross-linker were estimated to be 0.26×10^{-6} moles/ml (10 mM lipid), 0.51×10^{-6} moles/ml (20 mM lipid), and 1.28×10^{-6} moles/ml (50 mM lipid). The liposomes were characterized by Dynamic Light Scattering (DLS).

3.2.1.3. Fabrication and characterization of agglomerates

Liposomes were agglomerated using DTBP. Liposomes at a lipid molarity of 10, 20, and 50 mM were used for the agglomeration. The amount of DTBP used in the reactions were 25, 50, and 100 fold molar excess over the number of PEG-NH₂ groups on the outer leaflet of the liposomes. The pH of the liposomes was monitored and maintained at ~8.15 (the optimal pH for DTBP activity is in the 8-9 range) with NaOH solution, and the linker was added to the liposomes with constant stirring for over 3 hours. The reaction was carried at room temperature.

To investigate the extent of the agglomeration process at various time points, aliquots of the reaction mixtures were taken and added to a buffered solution of 300 mM Tris. Tris is used as a quencher to arrest the reaction of the imidoester - DTBP, by providing free primary amines to the cross-linker.

The sizes of the agglomerates were determined by the Fraunhofer diffraction technique.

3.2.2. *In vitro studies with Ciprofloxacin loaded liposomes*

3.2.2.1. Materials

DPPC was purchased from Genzyme Pharmaceuticals (Cambridge, MA, USA). Cholesterol was purchased from Sigma-Aldrich (St. Louis, MO, USA). DSPE-PEG-NH₂ conjugate was purchased from Avanti Polar Lipids Inc (Alabaster, AL, USA). The cross-linker DTBP was purchased from Pierce (Rockford, IL, USA). Ciprofloxacin (Bayer Pharmaceutical Corp, West Haven, CT, USA) was purchased from a local pharmacy as Cipro-I.V. solution and purified as follows: The pH of Cipro-I.V. solution was raised from 2.1 to 7 with sodium hydroxide to precipitate the Ciprofloxacin. The suspension was then centrifuged at 1500 x g (4000 rpm) for 10 minutes, and the supernatant discarded. The powder was then washed with DI water and centrifuged 4 times to remove lactic acid (an inert excipient in the i.v. solution). A final wash and centrifugation with ethanol yielded a wet powder which was collected and dried in a vacuum

desiccator. Ciprofloxacin yield was 90%. Survanta[®] was purchased from Abbot Laboratories (Abbott Park, Illinois, USA). All the rest of the reagents were purchased from Fisher Scientific (Hampton, NH, USA).

3.2.2.2. Fabrication and characterization of liposomes

The liposomes were made by extruding a suspension of dissolved hydrated lipids through a single 400 nm Whatman Nuclepore polycarbonate track-etch membrane in a Lipex Biomembranes Extruder. A lipid composition of 55% DPPC, 40% Cholesterol, and 5% DSPE-PEG-NH₂ conjugate was used. The lipids were dissolved in ethanol at 50-60^o C and then hydrated with 300 mM ammonium sulfate solution (ethanol volume not exceeding more than 10% of the final volume), the lipid concentration in the final mixture being 75 mM. The suspension was then extruded 7 times at 50-60^oC and a pressure of approximately 100 psi.

Assuming 51% of the DSPE-PEG-NH₂ to be on the outer leaflet of the bilayer, the number of amine groups available for coupling was estimated to be 1.92×10^{-6} moles/ml (75 mM lipid). The liposomes were characterized by DLS.

3.2.2.3. Loading of liposomes with ciprofloxacin

Ciprofloxacin was loaded into liposomes of 75 mM lipid content by the ammonium sulfate gradient method [36]. Blank liposomes were prepared in a 300 mM ammonium sulfate solution. 10 mL of the liposomes were dialyzed

(using 100,000 MWCO dialysis tubing) for 4 hours against 300 mL of saline at pH of 5.2 (adjusted by HCl) in order to remove ethanol and ammonium sulfate from the external phase of the liposomes and to establish the proton/sulfate gradient. Ciprofloxacin was dissolved in saline at pH 4.2 and 52°C. The solution of Ciprofloxacin (15 mL) was added gradually to the liposomal suspension (15 mL) and the temperature was maintained at 52°C. The remote loading procedure was terminated after 1 hour by rapidly dropping the temperature using an ice bath. The drop in temperature reduces the permeability of the liposome bilayer thus preventing the transfer of species across the bilayer and entrapping the loaded drug. Finally, the liposomal suspension was dialyzed for 4 hours against 300 mL of saline at pH 5.2 to remove unencapsulated Ciprofloxacin. The final lipid content of the Ciprofloxacin-loaded liposomes was 37.5 mM.

Dialysis (using 100,000 Dalton MWCO tubing) was used to evaluate the encapsulated fraction of drug. The Ciprofloxacin-loaded formulations were dialyzed against saline at pH 5.2. The volume of the external buffer was 100 times the volume of the liposomal formulation. Samples were taken from the external phase and were assayed. Complete removal of the unencapsulated drug was considered to be achieved, when the external phase concentration remained unchanged for 6 hours. Then, the formulation was removed from the dialysis tubing, lysed with methanol (30% of total volume), and assayed by HPLC to measure the encapsulated amount of drug.

3.2.2.4. Agglomeration and characterization of Ciprofloxacin-loaded liposomes

Liposomes were agglomerated using DTBP. The coupling reaction of the PEG-amines with DTBP was carried out in pH of 5.2 (same pH as for Ciprofloxacin loading) or 8.5 (optimal pH for linker activity) in saline. This was done to determine the pH that would be best suited for the agglomeration and at the same time would not result in drug leakage. The amount of DTBP used was 100-fold molar excess of the NH₂ groups on the PEG.

The cleavage of the DTBP agglomerates was accomplished with dithiothreitol (DTT) at 37 °C. The sizes of the agglomerates were determined by the Fraunhofer diffraction technique.

3.2.2.5. Aerodynamic properties of agglomerates

The aerodynamic properties of the agglomerated liposomes containing Ciprofloxacin were evaluated by nebulizing 2 ml of the formulation into an Andersen Cascade Impactor (Series 20-800, 1 ACFM non-viable sampler). A Parijet LC nebulizer was used for the cascade impactor study. The impactor was operated under ambient conditions (24 ± 1 °C and ~ 55% relative humidity) at constant flow rate of 28.3 L/min (calibrated by the supplier). The vacuum pump connected to the impactor was started and the sample was nebulized into the cascade impactor for 15 minutes, sufficient to nebulize the entire contents. Finlay

et al. have emphasized the problems of droplet undersizing [42, 43] in a cascade impactor run at ambient conditions, due to heating of the nebulized air. They demonstrate mass mean aerodynamic diameters (MMADs) under ambient conditions to be 1 μm lower than under saturated air conditions. However, it is also known that this shrinkage will be less in a larger droplet due to the lower surface area/unit volume. We have therefore operated the nebulizer and cascade impactor at ambient conditions, which is consistent with the USP method (USP 23, NF 18, <610>, 1995).

At the end of the nebulization run, each plate of the impactor, the elbow piece, and the filter paper at the end of the last stage were washed several times with 10 ml of saline at pH ~ 5.2. Methanol (30% of total wash buffer by volume) was used to lyse the liposomes collected on each stage. These washes were then analyzed by HPLC to determine the amount of Ciprofloxacin collected on each stage. The amount of Ciprofloxacin on each stage was then assigned to the corresponding aerodynamic diameter of each stage to determine the aerodynamic size distribution.

The weight of the nebulizer containing the formulation was recorded prior to and at the end of the nebulization in order to estimate the amount of formulation nebulized into the cascade impactor. It was estimated that more than 95% of the initial charge was nebulized.

3.2.2.6. Stability upon nebulization

The effects of nebulization on the size and encapsulation of Ciprofloxacin were investigated. For this, the core liposomes and agglomerated formulations were nebulized, using a Parijet LC nebulizer, for a specific time into a conical flask, (figure 12) which contained 30 mL of saline. The secondary aim of this experiment was also to determine if the nebulizer was able to deliver the agglomerates.

The nebulizer loaded with the formulation was weighed before and after every nebulization. After every nebulization, the device was weighed and a sample was taken for HPLC analysis of Ciprofloxacin content. This was used to determine the total amount of formulation nebulized into the flask. At the end of the experiment, the amount of Ciprofloxacin in the collected nebulisate was analyzed by HPLC. This was done to estimate the fraction of nebulized material collected in saline.

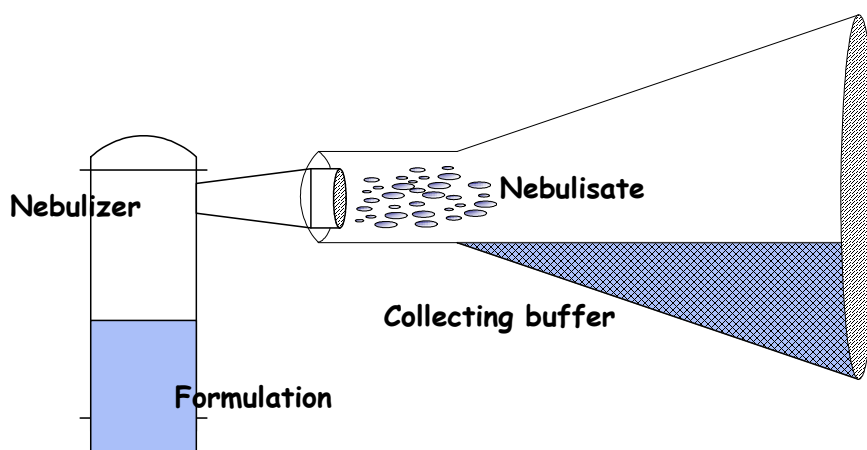


Figure 12. Schematic for collecting nebulized formulations of liposomes and agglomerates for evaluating effects upon nebulization.

The size of liposomes in the collected nebulisate was determined by DLS, and the size of the agglomerates in the collected nebulisate was analyzed by Fraunhofer diffraction. The loss of encapsulated Ciprofloxacin from the liposomes and agglomerates was evaluated by dialysis (as described previously) of the collected nebulisate.

3.2.2.7. In vitro release studies

The release of Ciprofloxacin from agglomerates and liposomes was evaluated in-vitro. The commercial pulmonary surfactant replacement Survanta® was used to simulate the lung environment. Ciprofloxacin-loaded liposomes/agglomerates and Survanta® (3:1 volumetric ratio respectively) were incubated at 37 °C in a dialysis bag (100,000 MWCO) immersed in PBS at a pH of 7.4. The volume of the external phase was 25 times that of the internal phase. Samples from the external phase were taken and were assayed for Ciprofloxacin in the HPLC. At the end of the experiment the contents of the dialysis bag were also assayed for Ciprofloxacin content.

3.2.3. In vivo studies of Ciprofloxacin loaded liposomes

To evaluate the drug release properties of the agglomerates made with DTBP (in vivo non-cleavable) in vivo, formulations of liposomes and

agglomerates were instilled in the lungs of rabbits. The experimental procedures are noted below.

3.2.3.1. Materials

DPPC and methoxypoly (ethylene glycol) distearoylphosphatidyl ethanolamine (MPEG-DSPE) were purchased from Genzyme Pharmaceuticals (Cambridge, MA, USA). Cholesterol (CHOL) was purchased from Sigma-Aldrich (St. Louis, MO, USA). DSPE-PEG-NH₂ conjugate was purchased from Avanti Polar Lipids (Alabaster, AL, USA). DTBP was purchased from Pierce (Rockford, IL, USA). Ciprofloxacin (Bayer Pharmaceutical Corp., West Haven, CT, USA) was purchased from a local pharmacy as Cipro-I.V. solution and was purified as described in section 3.2.2.1. All other reagents were purchased from Fisher Scientific (Hampton, NH, USA).

3.2.3.2. Animals

New Zealand White male rabbits (2.9 ± 0.5 kg) were purchased from Myrtle Rabbitry (Thompson Station, TN, USA). The use of animals for this study was approved by the Center for Laboratory Animal Medicine and Care (CLAMC) of UTHSC-Houston. Care and handling of the animals was in accordance with all policies of the United States Department of Agriculture (USDA) and U.S. Public Health Service (PHS).

3.2.3.3. Fabrication and characterization of liposomes

Two separate batches of liposomes (~120 mM lipid content) were prepared. A lipid composition of DPPC:CHOL:DSPE-MPEG (57:40:3, mol%) (MPEG terminated, for studies with liposomes), and DPPC:CHOL:DSPE-PEG-NH₂ (57:40:3, mol%) (amino terminated, for making AVT) was used. The lipids were dissolved in ethanol at 55^o C and then hydrated with a 400 mM ammonium sulfate solution (ethanol volume not exceeding more than 10% of the final volume). The liposomes were made by extruding the suspension of the hydrated dissolved lipids through a single 400 nm Whatman Nuclepore polycarbonate track-etch membrane in a Lipex Biomembranes extruder (Vancouver, British Columbia, Canada). The suspension was then passed 7-10 times through the extruder at 50-54 ^oC and a pressure of approximately 100 psi. The liposomes were characterized by DLS.

3.2.3.4. Loading of liposomes with Ciprofloxacin

Ciprofloxacin was loaded into liposomes by the ammonium sulfate gradient method [36]. Liposomes were diafiltered for 1-2 hours using 50 nm cutoff tubings with the external phase of the liposomes being replaced with saline (150 mM) at pH of ~5.3 in order to remove ethanol and non-encapsulated ammonium sulfate. For the remote loading procedure, Ciprofloxacin was

dissolved in saline (60 mg/ml) at pH 4.2 and 60°C, and was gradually added (0.5 ml added every 3-5 minutes) to the liposomal suspension with the temperature maintained at 60°C. The loading was terminated after 1 hour by rapidly dropping the temperature using an ice bath. The drop in temperature reduces the permeability of the liposome bilayer thus preventing the transfer of species across the bilayer and entrapping the loaded drug. Finally, the suspension was separated from unencapsulated Ciprofloxacin by overnight dialysis against saline solution (100 times volume of liposomes) at pH 5.3.

3.2.3.5. Agglomeration and characterization of Ciprofloxacin-loaded liposomes

Liposomes containing 3% PEG-NH₂ conjugate in the lipid bilayer were agglomerated using DTBP as the linker. The amount of DTBP used was a 50 fold molar excess over the number of PEG-NH₂ groups on the outer leaflet of the liposomes. The pH of the liposomes was raised from 5.3 to 8.5 (the optimal pH for DTBP activity is in the 8-9 range) with NaOH solution, and the linker was added to the liposomes with constant stirring for 1.5 hours after which the pH was dropped to 5.3 to arrest the cross-linking reaction.

The sizes of the agglomerates were determined by the Fraunhofer diffraction technique.

3.2.3.6. Pharmacokinetic study in rabbits

Rabbits were anesthetized by a subcutaneous injection of ketamine/xylazine (40-50/5-10 mg/kg). The rabbits were maintained on 2% isoflurane and O₂ (1 lit/minute). The heart rate, temperature and O₂ were monitored periodically, and remained stable throughout the course of the experiment.

The marginal ear vein was accessed via an i.v. catheter (24 G). The catheter was taped to the ear. Using a laryngoscope, an endotracheal tube (size 3) was inserted into the trachea, with a urinary catheter acting as a guide. Insertion into trachea was confirmed with a stethoscope, by pumping air into the lungs. The cuff of the endotracheal tube was filled with air to maintain the tube in the trachea. Additionally, the tube was tied to the mouth to retain it in place.

The rabbit's head was maintained in an upright position and drug formulation was instilled into the lungs with a syringe. The formulation was pushed down by forcing air into the lungs with the syringe several times. 2.2 to 2.8 ml of formulation (corresponding to Ciprofloxacin doses of 17 ± 1.6 mg/kg) was instilled.

Blood was drawn from the ear vein before (time 0) and after instillation of drug formulation. Blood samples were centrifuged at 13,400 rpm for 15 minutes to separate the plasma from cell components. The plasma was then diluted 1:4 times with methanol: phosphate buffer (9:1 v/v) to precipitate the proteins

present in the sample. The resulting suspension was then centrifuged at 13,400 rpm in a microcentrifuge for 15 minutes and the supernatant was assayed for Ciprofloxacin content by HPLC. Standard curve for Ciprofloxacin was determined by spiking known amounts of Ciprofloxacin in rabbit plasma. The lowest detection limit by HPLC was 0.05 µg/ml.

The following formulations were instilled into the lungs:

a) Free Ciprofloxacin solution.

Ciprofloxacin was dissolved in normal saline at a concentration of 21.9 mg/ml. The pH of the solution was adjusted to approximately 3.1 to maintain Ciprofloxacin in solution. This solution was then instilled into the lungs of the rabbits as described above.

b) Liposome-encapsulated Ciprofloxacin

The instillation of the Stealth® liposomes was as described by the procedure above. The final lipid content of the liposomes that were instilled was ~110 mM.

c) AVT1

AVT particles made with the cross-linker DTBP that were used for the pharmacokinetic studies in rabbits are referred to as AVT1. These agglomerates are not susceptible to cysteine cleavage. They were instilled according to the procedure described above. The final lipid content of the AVT1 that was instilled was ~50 mM.

3.2.4. *In silico study of Ciprofloxacin pharmacokinetics of the 1st generation AVT*

A deterministic compartmental model was employed to analyze the Ciprofloxacin profiles obtained from the pharmacokinetic studies. The model shown in Figure 13 consisted of 4 compartments with most of pharmacokinetics being assumed first order. In order to understand the pharmacological phenomena and the related physiological meaning, possible release mechanisms of Ciprofloxacin from the AVT particle were proposed by introducing the “particle” compartment.

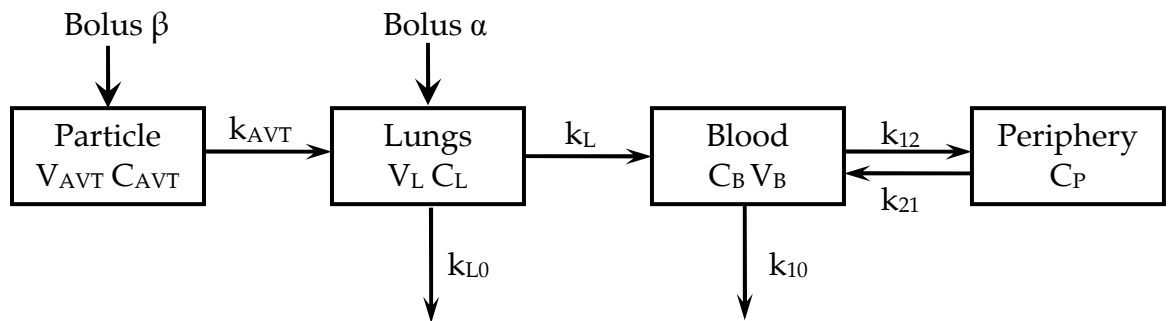


Figure 13. Sketch of the compartmental model.

It was hypothesized that 2 mechanisms are important to describe the release from the liposomes and AVT particles:

1. Once the liposomes and agglomerate microparticles were instilled into the lungs of the rabbit, forces due to motion of the lungs caused a degree of fragmentation resulting in immediate release of a portion of the encapsulated drug. Therefore, the input amount into the “particle” compartment was the total load of Ciprofloxacin into the particle subtracted by “ α ” which is used to represent the amount leaked from the AVT particle due to fragmentation (equation 1). It is assumed that shear forces are experienced by the particle until the particle comfortably reorients itself. The reorientation was assumed to occur instantaneously upon deposition in the lungs.
2. The second mechanism of release was attributed to a diffusion process represented with the first order rate constant k_{AVT} in equation 2. The drug molecule is assumed to diffuse initially through the liposomal wall and then through the matrix of the agglomerate.

$$\text{Input Bolus} = \beta = \frac{D - \alpha}{V_{AVT}} \quad (1)$$

D *initial dose of Ciprofloxacin (μg)*
 α *amount of Ciprofloxacin leaked from particles due to disruption (μg)*
 V_{AVT} *internal volume of the liposomes (ml)*

$$\frac{dC_{AVT}}{dt} = -k_{AVT} \cdot C_{AVT} \quad (2)$$

C_{AVT} *Ciprofloxacin concentration in the “particle” compartment ($\mu\text{g/ml}$)*
 k_{AVT} *first order constant to the “lung” compartment (hr^{-1})*

In the case of the liposomes, the subscripts with “AVT” are replaced with “Lips”.

In the case of the “lung” compartment, the elimination rate could be attributed to (a) transport of the Ciprofloxacin molecule to the lymphatic circulation, and (b) macrophage uptake of liposomes, and agglomerates when their fragments fall into geometrical sizes (due to size decrease induced by rupture due to the motion of the lungs) within the macrophage uptake range. The total clearance is described via the first order elimination process (k_{L0}). Besides the elimination rate and the flux towards the “blood” compartment (both first order), a bolus input (α) was introduced which represents the amount of drug that leaked from the AVT particles (or liposomes) during reorientation/fragmentation.

$$\text{Input Bolus} = \frac{\alpha}{V_L} \quad (4)$$

$$\frac{dC_L}{dt} = k_{AVT} \cdot C_{AVT} - (k_L + k_{L0}) \cdot C_L \quad (5)$$

V_L volume of the pulmonary surfactant (mL)

C_L Ciprofloxacin concentration in the “lung” compartment ($\mu\text{g/ml}$)

k_{L0} first order elimination constant (hr^{-1})

k_L first order constant towards the “blood” compartment (hr^{-1})

The “blood” compartment was assumed to communicate with the lung compartment and a “periphery” compartment with elimination of the drug due to hepatic and renal clearance mechanisms.

$$\frac{dC_B}{dt} = k_L \cdot C_L - (k_{10} + k_{12}) \cdot C_B + k_{21} \cdot C_P \quad (6)$$

$$\frac{dC_P}{dt} = k_{12} \cdot C_B - k_{21} \cdot C_P \quad (7)$$

- C_B Ciprofloxacin concentration in the “blood” compartment ($\mu\text{g/ml}$)
 V_B blood volume (mL)
 C_P Ciprofloxacin concentration in the “periphery” compartment ($\mu\text{g/ml}$)
 k_{12}, k_{21} first order constant towards and from the “periphery” compartment (hr^{-1})
 k_{10} first order constant for elimination of drug from blood compartment (hr^{-1})

Colino et al. investigated the response of i.v. injection of Ciprofloxacin in rabbits [44]. The parameters that were estimated in the study were fixed in this work and are tabulated in table 1. The model given by equations (1)-(7) was fitted to the Ciprofloxacin levels in the blood of animals treated with the liposomes, and AVT. For the estimation of the PK parameters a non-linear extended least squares regression analysis, as implemented in the SAAM II software (University of Washington and SAAM institute, Seattle, WA) was used.

Table 1. Pharmacokinetic parameters fixed from literature

Parameter	Value
k_{12}	3.06 (hr^{-1})
k_{21}	1.25 (hr^{-1})
k_{10}	1.7 (hr^{-1})

The integrator was based on the Rosenbrock method and the optimizer was a modification of Gauss-Newton method [45-47]. The objective function that was minimized was the following extended least squares function:

$$\text{OBJ} = \frac{1}{M} \sum_{j=1}^J \sum_{i=1}^{N_j} \left\{ \frac{[y_{i,j} - s(p, t_{i,j})]^2}{V_{i,j}[s(p, t_{i,j}), y_{i,j}, v_{i,j}]} + \log V_{i,j}[s(p, t_{i,j}), y_{i,j}, v_{i,j}] \right\} \quad (8)$$

- M *the sum of all data points across all data sets*
- $y_{i,j} \ t_{i,j}$ *the i -th data and time point in the j -th data set*
- p *vector of the estimated parameters*
- $s(p, t_{i,j})$ *the model prediction at time i in the j -th data set*
- $V_{i,j}$ *the measurement error at time i in the j -th data set*
- v_j *the posteriori variance factor of the j -th data set*

In our case the model was used to fit one set of experimental data. Since the data were expressed as mean value (\pm standard deviation), the model accounted for the error of the data.

$$y_{\text{obs}}(t_i) = y_{\text{calc}}(t_i, p) + e_i, i = 1, \dots, n \quad (9)$$

- y_{obs} *the random vector of measurements*
- y_{calc} *known function describing the kinetics*
- p *the random vector for kinetic model parameters*
- e_j *the measurement error random vector*

The objective function was optimized in order to minimize the difference between the experimental and the simulated data. Therefore, the objective function was weighted by the error variance and hence the parameter confidence limits would be a function of data reliability.

$$\text{OBJ} = \sum_{i=1}^n \left\{ \left[\frac{y_{\text{obs}}(t_i) - y_{\text{calc}}(t_i)}{SD(t_i)} \right]^2 + \ln[SD^2(t_i)] \right\} \quad (10)$$

$$\text{Variance} = v = SD^2$$

$$\text{Weight} = w = \frac{1}{v} = \frac{1}{SD^2}$$

$$\text{res}(t_i) = y_{\text{obs}}(t_i) - y_{\text{calc}}(t_i)$$

$$\text{wres}(t_i) = \sqrt{w_i} [y_{\text{obs}}(t_i) - y_{\text{calc}}(t_i)]$$

The minimum number of calculation intervals was set at 200 and the maximum number of fit iterations was set at 50 based on central difference derivative. The convergence criterion was set to 10^{-7} . Convergence was achieved when one of the two criteria was satisfied:

1. The difference between the value of the linear approximation of the objective function at the current parameter estimate and the minimum value of the linear approximation was less than ε , where ε equaled 10^{-7} times the value of the linear approximation at the current parameter estimate.
2. The solution to a linear approximation of the objective function was within δ for each parameter, where the default value of δ equaled 10^{-7} times the difference between the upper and lower bounds for that parameter.

3.3. Experimental procedures of the 2nd generation of AVT (in vivo cleavable)

In this section the in vitro and in vivo experiments that were undertaken to demonstrate modulation of release after cleavage with cysteine are described. The aliphatic disulfide cross-linker dithiobis[succinimidylpropionate] (DTSSP) was used in making the agglomerates.

3.3.1. *In vitro studies with blank liposomes*

3.3.1.1. Materials

DPPC was purchased from Genzyme Pharmaceuticals (Cambridge, MA, USA). Cholesterol was purchased from Sigma-Aldrich (St. Louis, MO, USA). DSPE-PEG-NH₂ conjugate was purchased from Avanti Polar Lipids Inc (Alabaster, AL, USA). The cross-linker DTSSP was purchased from Pierce (Rockford, IL, USA). All the rest of the reagents were purchased from Fisher Scientific.

3.3.1.2. Fabrication and characterization of liposomes

The liposomes were made by extruding a suspension of dissolved hydrated lipids through a single 400 nm Whatman Nuclepore polycarbonate track-etch membrane in a Lipex Biomembranes extruder (Vancouver, British Columbia, Canada). A lipid composition of 57% DPPC, 40% Cholesterol, and 3% DSPE-PEG-NH₂ conjugate was used. The lipids were dissolved in ethanol at 50-

60⁰ C and then hydrated with sodium citrate buffer (ethanol volume not exceeding more than 10% of the final volume), the lipid concentration in the final mixture being 100 mM. The suspension was then passed 7-10 times through the extruder at 50-54⁰C and a pressure of approximately 100 psi. The liposomes were characterized by DLS.

3.3.1.3. Agglomeration and characterization of blank agglomerates

Liposomes (~50 mM lipid content) were agglomerated using DTSSP as the linker. The amount of DTSSP used was a 20 fold molar excess over the number of PEG-NH₂ groups on the outer leaflet of the liposomes. The pH of the reaction mixture was maintained at ~ 7.4 (the optimal pH for DTSSP activity is in the 7-8.5 range). The linker was added slowly over 10 minutes to the liposomes with constant stirring, with the agitation maintained for 1.5 hours.

The agglomerates were split into batches and treated with different amounts of cysteine at 37 ⁰C to induce cleavage of the disulfide linkage in the cross-linker. The sizes of the agglomerates before and after cleavage were measured Fraunhofer diffraction.

3.3.2. *In vitro studies with carboxyfluorescein loaded liposomes*

3.3.2.1. Materials

DPPC was purchased from Genzyme Pharmaceuticals (Cambridge, MA, USA). Cholesterol and 1,4-diazabicyclo[2.2.2]octane (Dabco) was purchased from Sigma-Aldrich (St. Louis, MO, USA). DSPE-PEG-NH₂ conjugate was purchased from Avanti Polar Lipids Inc (Alabaster, AL, USA). The cross-linker DTSSP was purchased from Pierce (Rockford, IL, USA). 5-(and-6)-carboxyfluorescein was purchased from Invitrogen Corp. (Carlsbad, CA, USA). The other reagents were purchased from Fisher Scientific.

3.3.2.2. Fabrication and characterization of liposomes

A lipid composition of 57% DPPC, 40% Cholesterol, and 3% DSPE-PEG-NH₂ conjugate was used. The lipids were dissolved in ethanol at 55^o C and then hydrated with a 5 mM carboxyfluorescein solution made in saline (150 mM NaCl) (ethanol volume not exceeding more than 10% of the final volume). The liposomes were made by extruding the suspension of the hydrated dissolved lipids through a single 400 nm Whatman Nuclepore polycarbonate track-etch membrane in a Lipex Biomembranes extruder (Vancouver, British Columbia, Canada). The lipid concentration in the mixture was 100 mM. The suspension was then passed 7-10 times through the extruder at 50-54 ^oC and a pressure of approximately 100 psi.

The extruded liposomes were then diafiltered for over 3 hours using 50 nm cutoff tubings with the external phase of the liposomes being replaced with saline (150 mM) at pH of ~7.2 in order to remove ethanol and unencapsulated carboxyfluorescein. The diafiltration was stopped when the external phase collected during the diafiltration was colorless. The liposomes were characterized for size by DLS.

3.3.2.3. Agglomeration and characterization of carboxyfluorescein agglomerates

Liposomes (~50 mM lipid content) were agglomerated using DTSSP as the linker. The amount of DTSSP used was a 20 fold molar excess over the number of PEG-NH₂ groups on the outer leaflet of the liposomes. The pH of the reaction mixture was maintained at ~ 7.4 (the optimal pH for DTSSP activity is in the 7 - 8.5 range). The linker was added slowly over 10 minutes to the liposomes with constant stirring, with the agitation maintained for 1.5 hours.

The sizes of the agglomerates were characterized by Fraunhofer diffraction.

3.3.2.4. Visual analysis of agglomerates by Confocal microscopy

The agglomerates were diluted in saline containing 25 g/L of Dabco to inhibit the photobleaching of the fluorescent dye. A drop of the diluted

agglomerates was placed on a glass slide and a cover slip was placed over it. The agglomerates were observed under a Zeiss LSM 510 META confocal microscope using a $\times 63$ immersion oil objective (Carl Zeiss, Germany) in the multi-track scanning mode with excitation wavelengths set at 488 nm (Argon laser); emission wavelengths were 505 to 530 nm for signal detection. Single optical slices were set to 0.8 μm and Z-stack slices to 0.5 μm .

3.3.3. *In vitro studies with Ciprofloxacin loaded liposomes*

3.3.3.1. Materials

DPPC was purchased from Genzyme Pharmaceuticals (Cambridge, MA, USA). Cholesterol was purchased from Sigma-Aldrich (St. Louis, MO, USA). DSPE-PEG-NH₂ conjugate was purchased from Avanti Polar Lipids Inc (Alabaster, AL, USA). The cross-linker DTSSP was purchased from Pierce (Rockford, IL, USA). Ciprofloxacin (Bayer Pharmaceutical Corp, West Haven, CT, USA) was purchased from a local pharmacy as Cipro-I.V. solution and purified as follows: The pH of Cipro-I.V. solution was raised from 2.1 to 7 with sodium hydroxide to precipitate the Ciprofloxacin. The suspension was then centrifuged at 1500 \times g (4000 rpm) for 10 minutes, and the supernatant discarded. The powder was then washed with DI water and centrifuged 4 times to remove lactic acid (an inert excipient in the i.v. solution). A final wash and centrifugation with ethanol yielded a wet powder which was collected and dried in a vacuum

desiccator. Ciprofloxacin yield was 90%. Survanta[®] was purchased from Abbot Laboratories (Abbott Park, Illinois, USA). All the rest of the reagents were purchased from Fisher Scientific (Hampton, NH, USA).

3.3.3.2. Fabrication and characterization of liposomes

A lipid composition of 57% DPPC, 40% Cholesterol, and 3% DSPE-PEG-NH₂ conjugate was used. The lipids were dissolved in ethanol at 55⁰ C and then hydrated with a 400 mM ammonium sulfate solution (ethanol volume not exceeding more than 10% of the final volume). The liposomes were made by extruding the suspension of the hydrated dissolved lipids through a single 400 nm Whatman Nuclepore polycarbonate track-etch membrane in a Lipex Biomembranes extruder (Vancouver, British Columbia, Canada). The suspension was then passed 7 times through the extruder at 50-54 ⁰C and a pressure of approximately 100 psi. The liposomes were characterized by DLS.

3.3.3.3. Loading of liposomes with Ciprofloxacin

Ciprofloxacin was loaded into liposomes by the ammonium sulfate gradient method [36]. Liposomes were diafiltered for 1-2 hours using 50 nm cutoff tubings with the external phase of the liposomes being replaced with saline (150 mM) at pH of ~5.3 in order to remove ethanol and unencapsulated ammonium sulfate. For the remote loading procedure, Ciprofloxacin was dissolved in saline (60 mg/ml) at pH 4.2 and 60⁰C, and was gradually added (0.5 ml added every 3-5 minutes) to the liposomal suspension with the temperature

maintained at 60°C. The loading was terminated after 1 hour by rapidly dropping the temperature using an ice bath. The drop in temperature reduces the permeability of the liposome bilayer thus preventing the transfer of species across the bilayer and entrapping the loaded drug. Finally, the suspension was separated from unencapsulated Ciprofloxacin by overnight dialysis against saline solution (100 times volume of liposomes) at pH 5.3.

3.3.3.4. Agglomeration and characterization of Ciprofloxacin loaded liposomes

Liposomes were agglomerated using DTSSP as the linker. The amount of DTSSP used was a 10 – 20 fold molar excess over the number of PEG-NH₂ groups on the outer leaflet of the liposomes. The pH of the reaction mixture was maintained at ~ 7.4 (the optimal pH for DTSSP activity is in the 7-8.5 range). The agglomerates were characterized for size by Fraunhofer diffraction.

3.3.3.5. Visual analysis of agglomerates by negative stain electron microscopy

The morphology of the agglomerates of DTSSP preparations was examined by negative staining electron microscopy (EM). Copper grids coated with colloid-ion-carbon and freshly glow discharged were used for sample adsorption. Each grid was floated on a drop of sample for 5 min. Excess fluid was removed by blotting with a filter paper, and the grid was washed for 2

seconds on a drop of water, floated on a drop of 1% uranyl acetate for 15 seconds, and air dried for 2-5 minutes. All electron micrographs were taken with a JEOL JEM1230 electron microscope operating at 80 kV and 56 μ A beam current.

3.3.3.6. Release studies

The release of Ciprofloxacin from agglomerates before and after cleavage with cysteine was evaluated in vitro. 1 ml of Ciprofloxacin loaded agglomerates (14 mM lipid) and 400 μ l Survanta® was incubated at 37 °C in a dialysis bag (100,000 MWCO) immersed in PBS at a pH of 7.4. The volume of the external phase was 20 times that of the internal phase. Samples from the external phase were taken and were assayed for Ciprofloxacin in the HPLC.

At different time points cysteine (8.7 mg/ml in total volume of dialysis bag equivalent to 70 mM) was spiked into the dialysis bag, in an attempt to trigger the release. To show that the modified release from the agglomerates was due to cysteine and not due to any other factors, a separate study was done where a volume of plain buffer equivalent to that of cysteine (50 μ l) was introduced at similar time points. At the end of the experiment the contents of the dialysis bag were also assayed for Ciprofloxacin content.

3.3.4. *In vivo* cysteine triggered release studies

3.3.4.1. Materials

DPPC was purchased from Genzyme Pharmaceuticals (Cambridge, MA, USA). Cholesterol was purchased from Sigma-Aldrich (St. Louis, MO, USA). DSPE-PEG-NH₂ conjugate was purchased from Avanti Polar Lipids Inc (Alabaster, AL, USA). The cross-linker DTSSP was purchased from Pierce (Rockford, IL, USA). Fluorescently tagged lipid, N- (7-nitrobenz-2-oxa-1, 3-diazol-4-yl)-1, 2-dihexadecanoyl-sn-glycero-3-phosphoethanolamine (NBD-PE) was purchased from Invitrogen Corp. (Carlsbad, CA, USA). Ciprofloxacin (Bayer Pharmaceutical Corp, West Haven, CT, USA) was purchased from a local pharmacy as Cipro-I.V. solution and was purified as described in section 3.3.3.1.

3.3.4.2. Animals

New Zealand White male rabbits (2.9 ± 0.5 kg) were purchased from Myrtle Rabbitry (Thompson Station, TN, USA). Male Sprague Dawley rats (330 – 350 gm) were purchased from Harlan (Indianapolis, IN, USA). The use of animals for this study was approved by the Center for Laboratory Animal Medicine and Care (CLAMC) of UTHSC-Houston. Care and handling of the animals was in accordance with all policies of the United States Department of Agriculture (USDA) and U.S. Public Health Service (PHS).

3.3.4.3. Fabrication and characterization of liposomes

3.3.4.3.1. *Ciprofloxacin loaded liposomes*

A lipid composition of 57% DPPC, 40% Cholesterol, and 3% DSPE-PEG-NH₂ conjugate was used. The liposomes were made by following the procedure described in section 3.3.3.2. The liposomes were remotely loaded with Ciprofloxacin following the same steps as in section 3.3.3.3.

3.3.4.3.2. *Liposomes with fluorescent labeled lipid*

A lipid composition of DPPC:CHOL:DSPE-PEG-NH₂:NBD-PE (56:40:3:1, mol%) was used. After ethanol dissolution the lipids were hydrated with 150 mM NaCl solution (ethanol volume not exceeding more than 10% of the final volume). The liposomes were made by extruding the suspension of the hydrated lipids 7 times through a single 400 nm Whatman Nuclepore polycarbonate track-etch membrane in a Lipex Biomembranes extruder at 50-54 °C and a pressure of approximately 100 psi. The liposomes were size characterized by DLS.

3.3.4.4. Preparation and characterization of agglomerated liposomes

Liposomes with a lipid content of 50 mM were agglomerated using DTSSP as the linker. The amount of DTSSP used for the agglomeration was a 10 - 20 fold molar excess over the PEG-NH₂ groups on the outer leaflet of the liposomes. The cross-linking reaction was carried out at a pH of 7.4 (optimal for cross-linking

activity of DTSSP) with constant stirring for 1.5 hours. The size distribution of the agglomerates was determined using the Fraunhofer diffraction technique.

3.3.4.5. Pharmacokinetic study in rabbits

Rabbits were anesthetized by a subcutaneous injection of ketamine/xylazine (40-50/5-10 mg/kg). The rabbits were maintained on 2% isoflurane and O₂ (1 lit/minute). The heart rate, temperature and O₂ were monitored periodically, and remained stable throughout the course of the experiment.

The marginal ear vein was accessed via an i.v. catheter (24 G). The catheter was taped to the ear. Using a laryngoscope, an endotracheal tube (size 3) was inserted into the trachea, with a urinary catheter acting as a guide. Insertion into trachea was confirmed with a stethoscope, by pumping air into the lungs. The cuff of the endotracheal tube was filled with air to maintain the tube in the trachea. Additionally, the tube was tied to the mouth to retain it in place.

The rabbit's head was maintained in an upright position and drug formulation was instilled into the lungs with a syringe. The formulation was pushed down by forcing air into the lungs with the syringe several times. 2.2 to 2.8 ml of formulation (corresponding to Ciprofloxacin doses of 17 ± 1.6 mg/kg) was instilled.

Blood was drawn from the ear vein before (time 0) and after instillation of drug formulation. Blood samples were centrifuged at 13,400 rpm for 15 minutes to separate the plasma from cell components. The plasma was then diluted 1:4 times with methanol: phosphate buffer (9:1 v/v) to precipitate the proteins present in the sample. The resulting suspension was then centrifuged at 13,400 rpm in a microcentrifuge for 15 minutes and the supernatant was assayed for Ciprofloxacin content by HPLC. Standard curve for Ciprofloxacin was determined by spiking known amounts of Ciprofloxacin in rabbit plasma. The lowest detection limit by HPLC was 0.05 µg/ml.

The agglomerates made with the cross-linker DTSSP that were used in the in vivo pharmacokinetic studies are termed as AVT2. Two sets of studies were done with these agglomerates. In the first study the agglomerates were instilled as described above, and their drug release was monitored.

In the second study, 1 ml cysteine (60 mg/ml) was introduced in to the lungs 90 minutes after instillation of AVT2, to cleave the agglomerates and alter the release of Ciprofloxacin into the blood. The rabbits recovered from anesthesia and were returned to their cages after 6 hours. After 24 hours, the rabbits were anesthetized and intubated again and cysteine solution was instilled again. Blood was drawn at all the time points as described earlier.

3.3.4.6. Lipid assay of instilled formulations in rat lungs

To measure lipid elimination as a function of particle size and correlate it to drug release, fluorescently tagged liposomes and agglomerates were instilled in the lungs of rats and the residual fluorescence in lung tissue assayed over a 48 hour period.

Male Sprague Dawley rats were anesthetized with an intraperitoneal (i.p.) injection of ketamine (80 mg/kg body wt.) and xylazine (10 mg/kg body wt.). The rats were endotracheally intubated with a 16 G catheter. The endotracheal tube was then connected to a ventilator and under forced ventilation; successful intubation was confirmed if the chest of the rat expanded with the same frequency as the ventilator. 200 μ L of the liposomal and agglomerate formulation (50 mM lipid content) with the fluorescent tagged lipids were instilled into the lungs of the rats. The total lipid dosed was 4078.78 ± 506.07 μ g/gm of lung wt. In a separate study 100 μ L of cysteine (60mg/ml) was instilled after 4 minutes from the instillation of the cleavable agglomerates (made with DTSSP). At 2, 24, and 48 hours post-instillation of the liposomes and agglomerates, the rats were euthanized with an overdose of pentobarbital (200 mg/kg) administered i.p. and the lungs were collected for the lipid assay.

The collected lungs were refrigerated and were processed within a few hours of extraction. For the lipid extraction a modification of the method of Matot et al. [48] was used. Briefly, the lungs were weighed, chopped and then

homogenized in cold chloroform/methanol (2:1 vol.) mixture. The homogenized tissue was filtered through Whatman filter paper no. 1. The collected filtrate was then assayed for fluorescence in a SpectraMax GeminiXS spectrofluorometer (Molecular Devices Corp, Sunnyvale, CA, USA) with filter settings of 463 nm excitation and 530 nm emission wavelengths. (Calibration standards were made by spiking known amounts of the tagged liposomes into the filtrate collected from the lungs of untreated rats.) The fluorescence intensity associated with the known lipid from the liposomes was used to determine the amount of lipid that remained in the lungs after instillation of the liposomes and the agglomerates.

3.3.4.7. Histology of rat lungs to assess inflammation

Male Sprague Dawley rats were anesthetized with an i.p. injection of ketamine (80 mg/kg body wt.) and xylazine (10 mg/kg body wt.). The rats were endotracheally intubated with a 16 G catheter following the same procedure as described in section 3.3.4.6. In separate studies, formulations of (1) 20 μ L of saline (-ve control), (2) 40 μ L of ConA solution (+ve control) containing 2.4 mg ConA/kg body weight, (3) 20 μ L of liposomes containing 0.41 mg of lipids/kg body weight, and (4) 30 μ L of AVT particles containing 1.74 mg of lipids/kg body weight were instilled in the lungs of the rats. The rats were recovered from anesthesia and returned to their cages.

After 24 hours post-instillation the rats were euthanized with an overdose of pentobarbital (200 mg/kg) administered via an i.p. injection and the lungs were collected. The lungs were gently inflated with 10% neutral buffered formalin until resistance was appreciated, and then immersed in formalin overnight. The next day, the lungs were serially sectioned and submitted for routine histological processing and paraffin embedding. Five micron-thick sections were cut from each paraffin block and placed on glass slides, which were stained with a standard hematoxylin-eosin (HE) stain. These slides were reviewed by a practicing pathologist and evaluated semi-quantitatively for changes of edema, inflammation and other histological abnormalities. The inflammation triggered by the preparations was rank-ordered by the pathologist.

3.3.4.8. Cytokine assay from rat lungs as a measure of inflammation

Male Sprague Dawley rats were anesthetized with an i.p. injection of ketamine (80 mg/kg body wt.) and xylazine (10 mg/kg body wt.). The rats were endotracheally intubated with a 16 G catheter following the same procedure as described in section 3.3.4.6. In separate studies, formulations of (1) 250 μ L of liposomes (50 mM lipids; 34.7 mg lipid/ kg body wt.), (2) 250 μ L AVT (50 mM lipids; 34.7 mg lipid/ kg body wt.), (3) 250 μ L of saline (-ve control), and (4) 50 μ L of ConA solution (+ve control) containing 4.1 mg ConA/kg body wt. were instilled in the lungs of the rats. The Ciprofloxacin content of the liposomes and

AVT was 18 mg/ml. The rats were recovered from anesthesia and returned to their cages.

After 48 hours post-instillation the rats were euthanized with an overdose of pentobarbital (200 mg/kg) administered via an i.p. injection. The trachea was exposed and a Teflon tubing with ~1.2 mm i.d. was inserted into the trachea and held in place with a suture. An 18G needle adapter with a syringe was attached to the tubing. The lungs were lavaged twice with 4 ml of sterile filtered (0.22 micron) PBS (10 mM phosphate, 150 mM NaCl). After instilling the lavage, the chest and the abdomen of the rats were massaged for 30 seconds and then the instilled fluid was aspirated. Total volume of the bronchoalveolar lavage (BAL) collected was between 5-6 mls. The collected BAL was stored on ice till the centrifugation step for ~ 3hrs. The BAL was centrifuged for 5 mins at 1000 g's at 4 °C. The supernatant was collected and stored at -20 °C till the assay for cytokines.

Four cytokines, viz. IL-2, IL-6, TNF- α , and IFN- γ were assayed simultaneously in a multiplex panel using a Bio-Rad Bio-Plex cytokine assay kit (Bio-Rad Laboratories Inc., Hercules, CA, USA). The collected samples were thawed prior to assay. The instructions provided in the manual of the kit were followed to prepare the standards and samples in the suspension plate. The plate contents were read in a Bio-Rad Bio-Plex system powered by Luminex Xmap technology.

3.3.5. *In silico study of Ciprofloxacin pharmacokinetics of the 2nd generation AVT*

A mechanistic/deterministic compartmental model was employed as already described in section 3.2.4 to analyze the Ciprofloxacin profiles obtained from the pharmacokinetic studies.

In addition to the parameters already incorporated in the model, an additional term (α'') was introduced in the input bolus term of the AVT and the lungs. This term takes into account the burst in release of drug from the AVT particle at the time point when exogenous cysteine is introduced into the lungs.

Chapter 4

Results and Discussions

4.1. The 1st Generation of AVT (in vivo non-cleavable)

In this section the results of the efforts undertaken to fabricate the first generation of agglomerated liposomes and test them in vitro and in vivo are presented. The linker (DTBP) that was used to make the agglomerates is not cleavable in vivo.

4.1.1. *In vitro experiments with blank liposomes*

4.1.1.1. Characterization of liposomes

Two sets of blank liposomes of 100 mM lipid content with 2% and 3% PEG-NH₂ conjugate in the bilayer were made. These were utilized to make agglomerates under different conditions. The DLS results of the liposomes extruded through the 400 nm polycarbonate membrane are shown in figure 14.

The DLS analysis suggested that the liposomes with 2% PEG-NH₂ had a size distribution between 180 – 440 nm with a mean diameter of 275.5 nm. The liposomes with 3% PEG-NH₂ showed a broader distribution between 165 – 765 nm with a mean diameter of 264.4 nm. These results are consistent with the extrusion process of liposomes as reported by Sood [49]. The size of the liposomes depends on a number of factors including lipid content, temperature, pressure, buffer, pore size of the membrane, and number of passes.

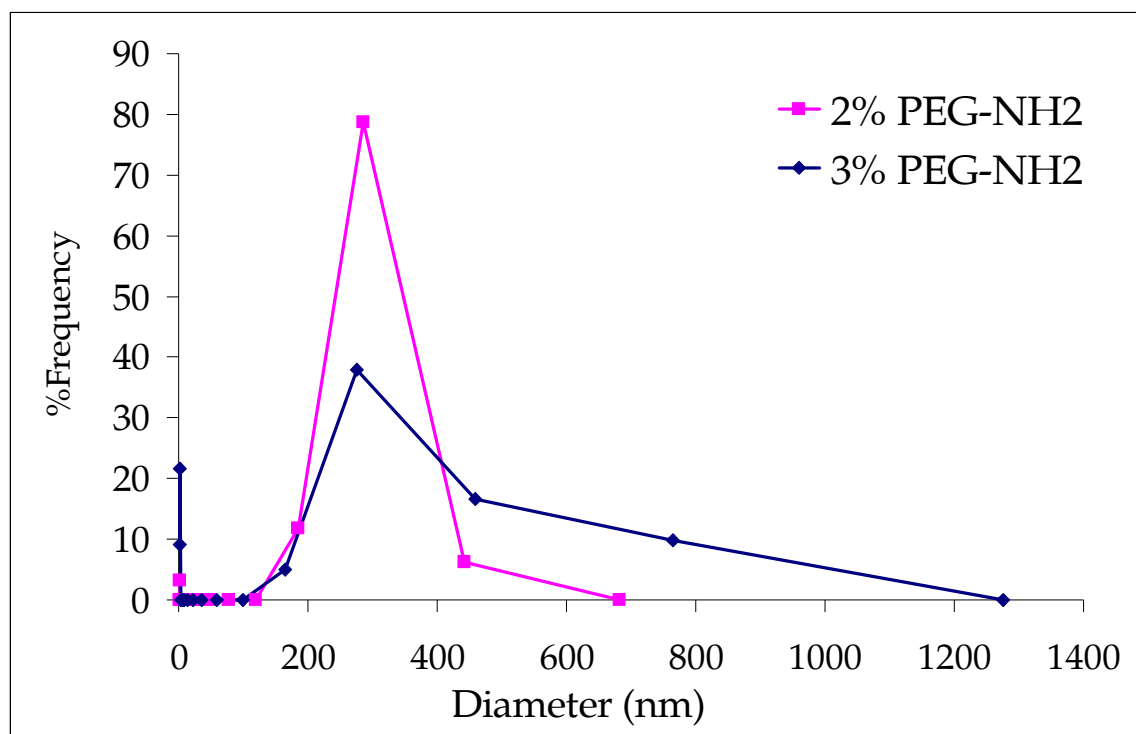


Figure 14. DLS results of blank liposomes with 2% PEG-NH₂ and 3% PEG-NH₂ used for making agglomerates of DTBP.

Particles in the 1-5 nm range were also detected in DLS. These are most likely to be micelles of the DSPE-PEG-NH₂ conjugate that are formed during the hydration process and are not incorporated in the lipid bilayer of the liposomes – a normal occurrence observed with liposomes made with the PEG moiety anchored to a lipid.

4.1.1.2. Agglomeration of liposomes with DTBP

This preliminary study was undertaken to see how the amount of reactants would affect the sizes of the agglomerates formed. In addition to this the time-progression of the agglomeration process was also studied. Table 2 lists

reaction conditions that were utilized for this study. The amount of the cross-linker DTBP used was in excess (molar basis) of the number of reacting groups on the PEG conjugate present on the external surface of the liposomes.

Table 2. Reaction conditions that were used for making the agglomerates of blank liposomes with DTBP cross-linker.

Mol% PEG-NH ₂	Lipid molarity of liposomes (mM)	Molar excess of DTBP used over PEG-NH ₂ present in the external bilayer of the liposomes
2	10	25, 50, and 100 times
	20	25, 50, and 100 times
	50	25, 50, and 100 times
3	10	25, 50, and 100 times
	20	25, 50, and 100 times
	50	25, 50, and 100 times

As an example of the time progression of the agglomeration reaction, figure 15 shows the Fraunhofer diffraction results of liposomes (2% PEG-NH₂) agglomerated with 50 times molar excess of DTBP (figure 15 a), and liposomes (3% PEG-NH₂) agglomerated with a 25 times molar excess of DTBP (figure 15 b). The reactions were stopped by taking aliquots of the reaction mixture and quenching them in a reservoir of Tris buffer (300 mM). During the initial time points (5 mins and 25 mins) the sizes are broadly distributed from the sub-micron range (< 1 μ m) to 100 μ m. As the time of the reaction progressed the particles in the sub-micron range were consumed resulting in bigger sizes as observed by the disappearance of sub-micron sized liposomes. After 2 hours a unimodal distribution was observed with a mode at 6.4 μ m (figure 15a) and 11.1 μ m (figure 15b). Particles bigger than 40 μ m that are observed at 5 and 25

minutes are no longer seen after 1 hour. The reason for this could be the fragmentation of these bigger particles into the smaller size range possibly due to the effects of stirring.

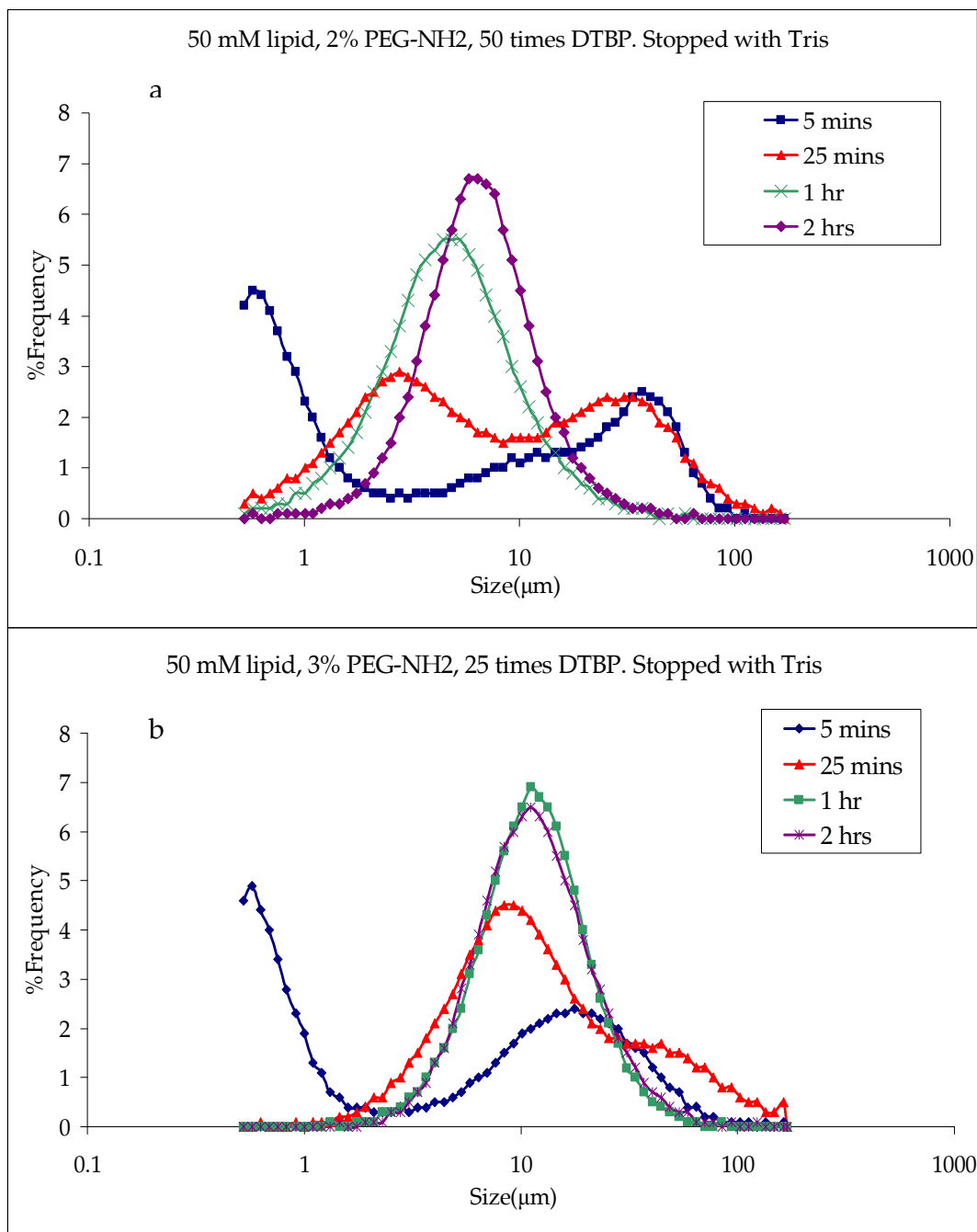


Figure 15. Time progression of agglomeration reaction of liposomes (50 mM lipid) carrying (a) 2% PEG-NH₂ with 50 times DTBP, and (b) 3% PEG-NH₂ with 25 times DTBP. The reactions were stopped with Tris and evaluated by Fraunhofer diffraction.

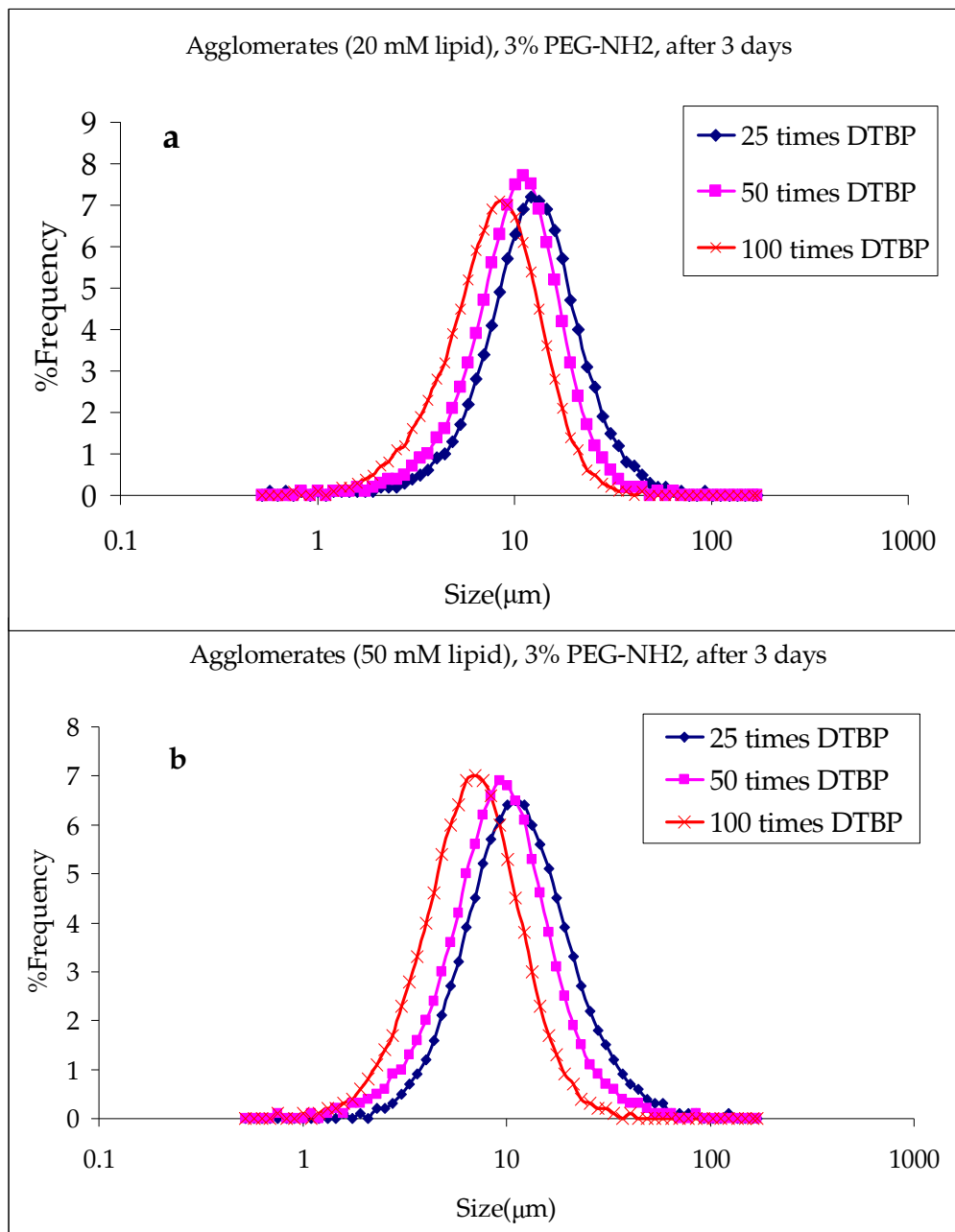


Figure 16. Size distributions of agglomerates obtained by Fraunhofer diffraction after using different molar excess of DTBP linker over 3% PEG-NH₂. Liposomes used were (a) 20 mM lipid, and (b) 50 mM lipid. The agglomerates were measured after 3 days from the start of the reaction.

The agglomerates were analyzed after 3 days from the start of the reaction. The reaction was not quenched with Tris after 2 hours, since the cross-linker loses its activity within a few hours. The sizes of the agglomerates

achieved with different amounts of linker for the same lipid molarity of the liposomes were compared. As an example, figure 16 shows the size distribution of the agglomerates of liposomes (3% PEG-NH₂) having a lipid molarity of 20 mM (figure 16a) and 50 mM (figure 16b) achieved with the different amounts of DTBP. The size distributions were unimodal with the sizes ranging from 3 – 40 μm . In case of the 20 mM lipids (figure 16a), the agglomerates had modes at 13.3, 11.1, and 8.4 μm made with 25, 50, and 100 times DTBP respectively. For the 50 mM lipids (figure 16b), the agglomerates had modes at 12, 9.2, and 7 μm made with 25, 50, and 100 times DTBP respectively.

A common trend was observed wherein; the agglomerates formed with less amount of linker were bigger than the agglomerates formed with higher amounts. A possible explanation to this could be that the higher amount of linker used reacts at a faster rate with the NH₂ groups present on the liposomal surface. Due to the higher bulk concentration of the reactants present at the start, the initial collisions result in the formation of the agglomerates quickly. But as the reaction sites on the liposomal surface start getting consumed by the smaller and faster diffusing cross-linker molecules, no more sites are available for linking the agglomerates formed that have a lower diffusion rate owing to their larger sizes. In the case of the lower amounts of the linker used, the time for this saturation is possibly slower resulting in more interaction between the activated and inactivated sites that results in the formation of slightly bigger agglomerates.

A similar trend was seen when liposomes with different molarities (the lipid molarity is proportional to the number of liposomes of the same size) were reacted with the same molar excess of DTBP. Figure 17 shows an example of the same.

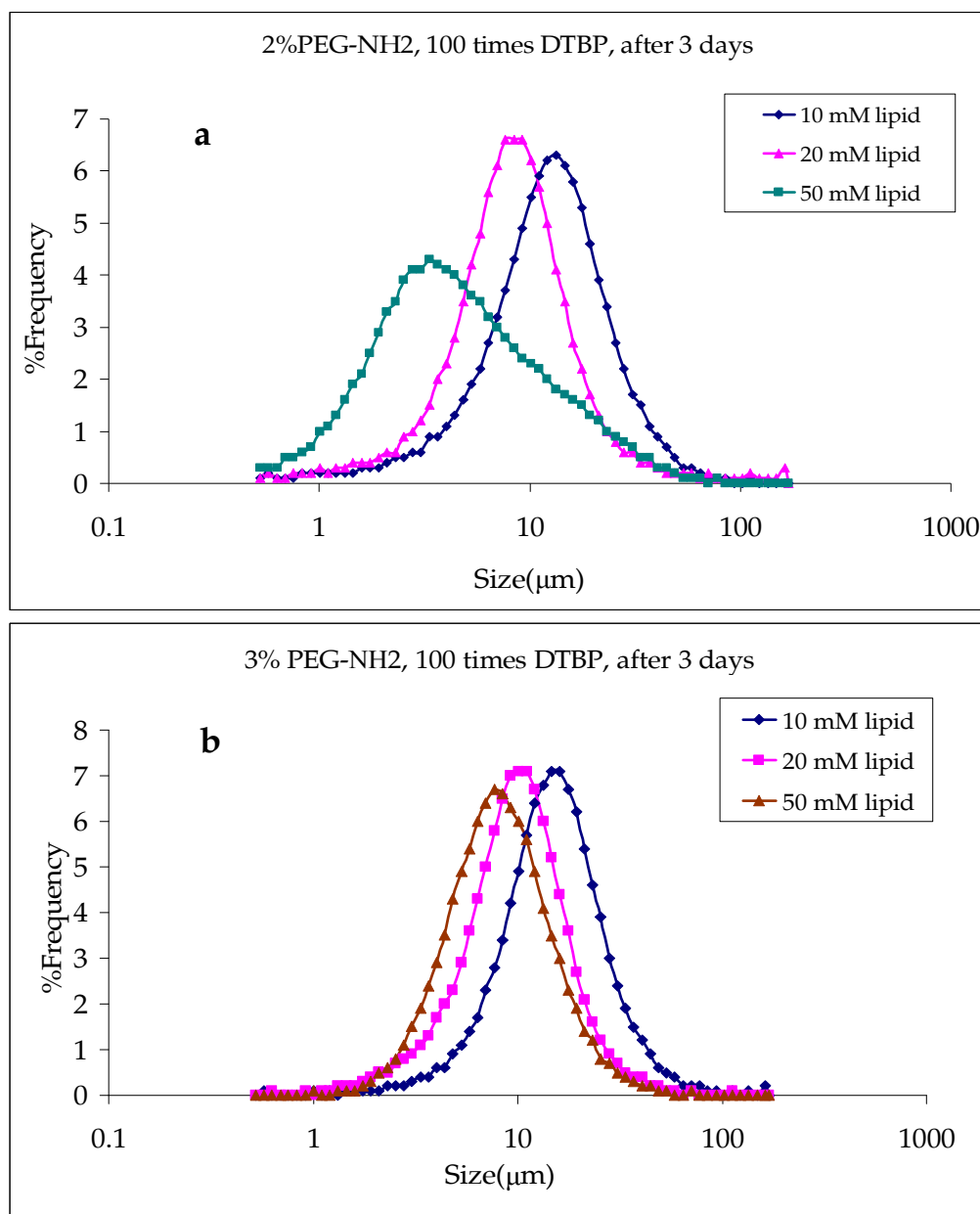


Figure 17. Size distributions of agglomerates obtained by Fraunhofer diffraction after using liposomes with different lipid molarities with 100 molar excess of DTBP over (a) 2% PEG-NH₂, and (b) 3% PEG-NH₂ on liposomes. The agglomerates were measured after 3 days from the start of the reaction.

A lower lipid molarity of the liposomes resulted in larger agglomerates in comparison to a higher lipid molarity. The agglomerates of liposomes with 2% PEG-NH₂ (figure 17a) had a unimodal distribution with modes at 3.35, 8.4, and 13.3 μm for 50, 20, and 10 mM of lipid. The agglomerates of liposomes with 3% PEG-NH₂ (figure 17b) also had a unimodal distribution with modes at 7, 10, and 16 μm for 50, 20, and 10 mM of lipid.

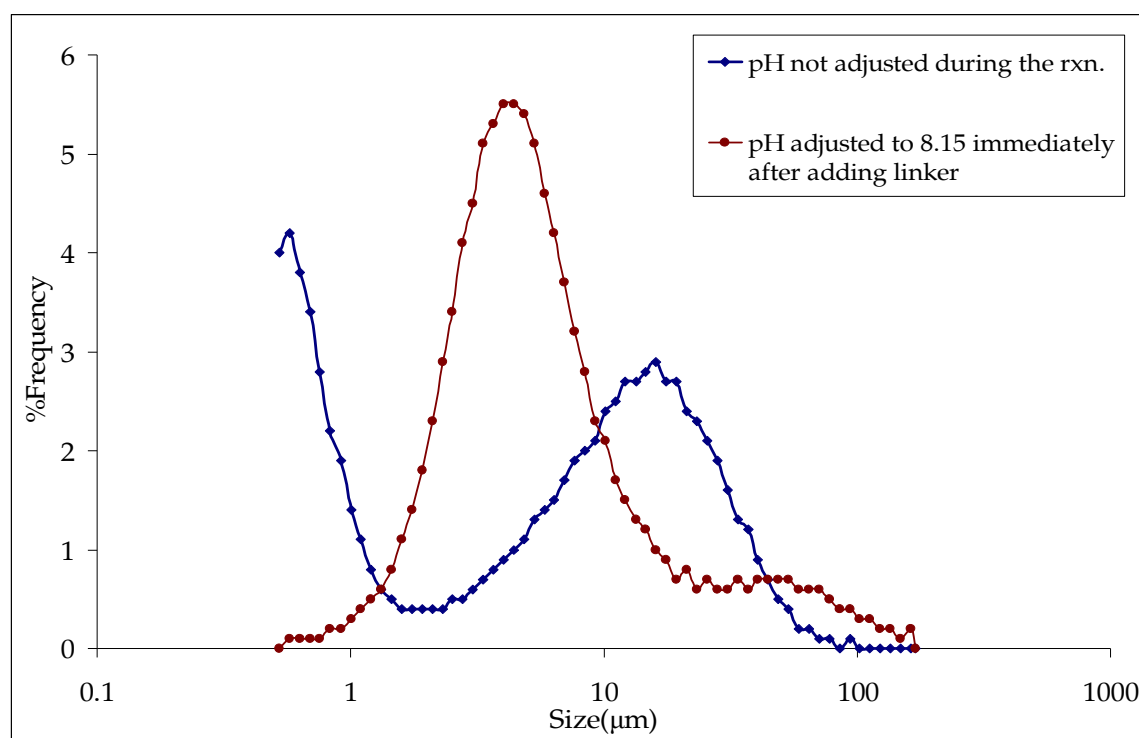


Figure 18. Fraunhofer diffraction results showing the effect of pH on the agglomeration of the liposomes.

During the agglomeration reaction it was observed, that the pH of the mixture drifted from 8.15 to a lower pH of ~ 5.6 after addition of the linker. In the previous results reported the pH was adjusted to 8.15 immediately after the addition of the linker since the cross-linker is active at this point. To test if the drift in pH affects the agglomeration reaction (ultimately affecting the size),

liposomes (50 mM lipid) were reacted with DTBP (100 molar excess). The Fraunhofer diffraction results shown in figure 18 clearly suggest that the pH affects the extent of agglomeration. It was observed that the agglomeration was incomplete when the pH was not adjusted as evidenced by the presence of sub-micron sized liposomes. This suggested that the activity of the cross-linker is lost when the reaction is not carried in the optimal pH range.

4.1.2. *In vitro studies with Ciprofloxacin loaded liposomes*

4.1.2.1. Characterization of Ciprofloxacin loaded liposomes

The size distribution of Ciprofloxacin loaded liposomes is shown in figure 19. The liposomes, extruded through the 400 nm polycarbonate membrane, were in the range of 180-195 nm.

After removal of the unencapsulated Ciprofloxacin, the concentration of the encapsulated drug, determined by HPLC analysis, was 10.5 mg/mL, representing 90% of the initial amount added during the loading procedure.

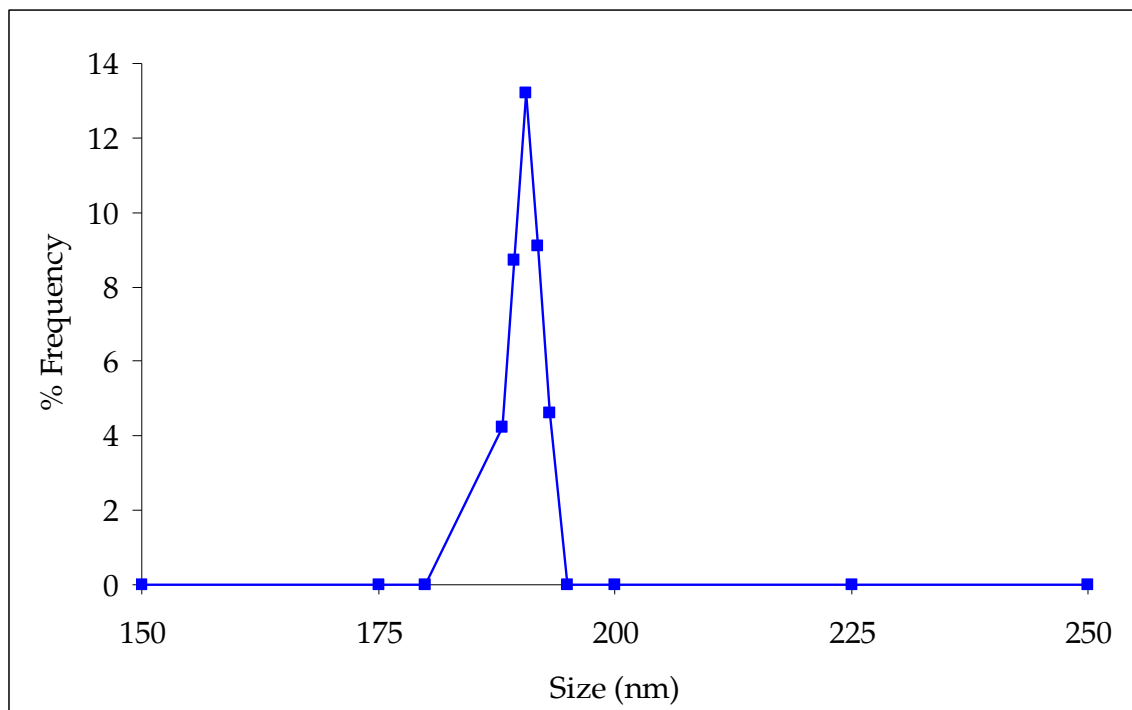


Figure 19. Size distribution of Ciprofloxacin loaded liposomes.

4.1.2.2. Agglomeration of Ciprofloxacin loaded liposomes with DTBP

Figure 20 shows a comparison of the size distribution (measured by Fraunhofer diffraction) Ciprofloxacin loaded liposomes agglomerated with DTBP at pH 5.2 (Prep I) and 8.5 (Prep II). In the case of Prep I, large agglomerates exhibiting sizes between 4 – 60 μm and a mode at 21 μm were seen. A mode at < 1 μm persists, suggesting that the parent liposomes have not been fully agglomerated. In the case of Prep II, it was observed that the agglomerates exhibited a very broad size distribution. These large agglomerates had sizes between 1-160 μm and a mode at 34 μm . It was observed that the mode for unagglomerated liposomes does not appear, implying that the majority of the

parent liposomes have been agglomerated. These results of pH effects on agglomeration are consistent with the studies done with blank liposomes.

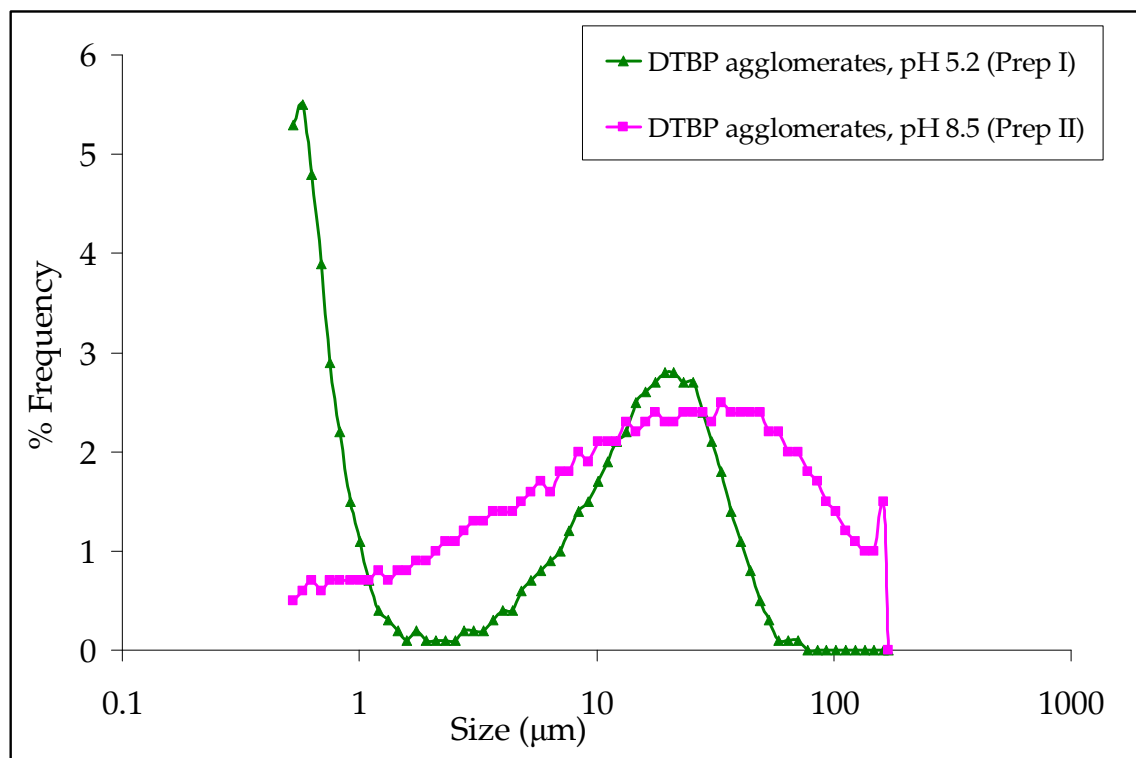


Figure 20. Fraunhofer diffraction results of agglomerates of Ciprofloxacin loaded liposomes made at pH 5.2 and 8.5.

However, the agglomerates of Prep II showed a 70% leakage of the encapsulated Ciprofloxacin even though the pH was brought back to 5.2 after the end of the agglomeration reaction (3 hours). On the other hand, only 10% of the encapsulated ciprofloxacin leaked out from the agglomerates of Prep I, since the pH was maintained at 5.2, which was the pH throughout the remote loading procedure. The leakage was tested by performing a dialysis experiment on the agglomerates preparations and assaying the external phase of the dialysis bag for Ciprofloxacin by HPLC.

DTBP is cleavable by aggressive thiols like DTT (which is not suitable for in vivo use). The Prep II agglomerates were cleaved with different amounts of DTT at 37 °C. The results in figure 21 show that the extent of cleavage was more when more DTT was used. This is evident by the increase in the fraction of particles in the 1-20 μm , and fall in the fraction of agglomerates larger than 40 μm . However, the cleavage was not extensive, i.e. it did not result in the formation of parent liposomes. It was anticipated that this cleavage of the agglomerates would result in accelerated release of the drug.

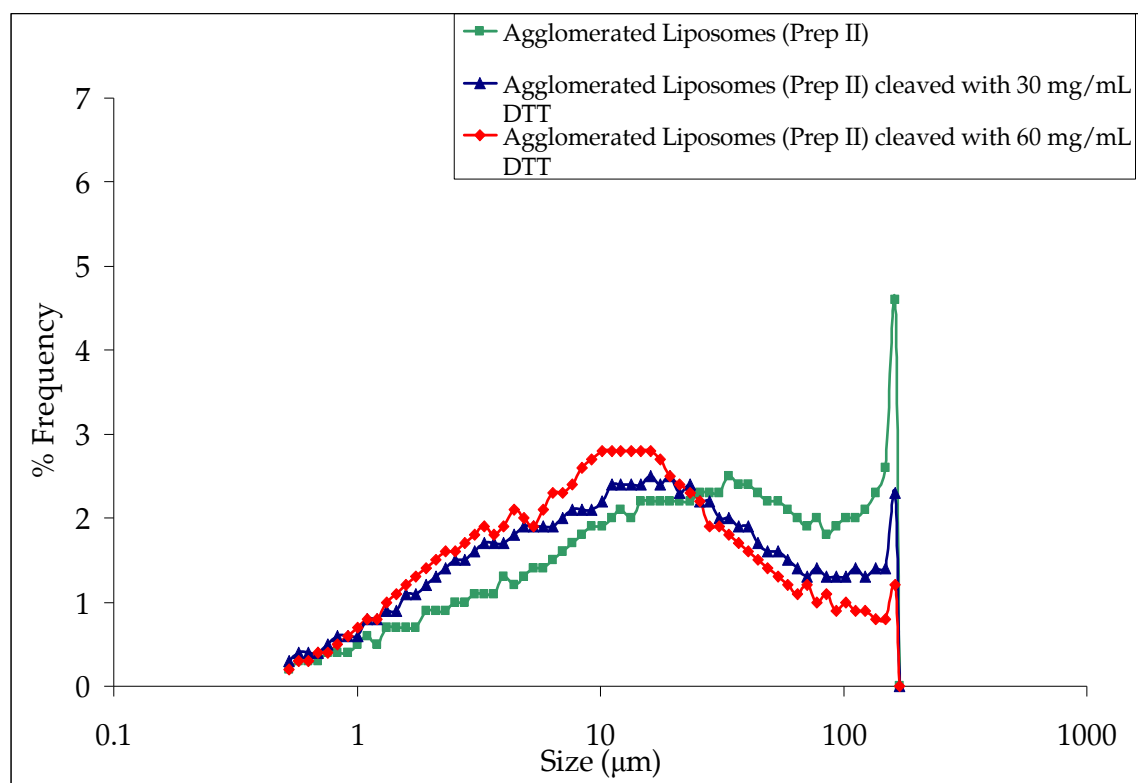


Figure 21. Size analysis of agglomerates of Ciprofloxacin loaded liposomes before and after cleavage with 30 and 60 mg/ml of DTT at 37 °C.

4.1.2.3. Aerodynamic characterization of agglomerates

Figure 22 shows the results of the cascade impactor studies done with liposomes agglomerated with DTBP, containing Ciprofloxacin to evaluate the aerodynamic properties of the agglomerates. The results suggest that the aerodynamic diameter of the agglomerates makes them highly respirable. Approximately 60% of the agglomerates had aerodynamic diameters in the respiratory range (between 1-5 μm). These diameters are clearly much lower than the geometrical sizes of these agglomerates (Prep I) measured by Fraunhofer diffraction (4-60 μm geometrical diameters). This data would be consistent with either fragmentation of the agglomerates in the nebulizer or low density of the porous agglomerates resulting in lowered aerodynamic diameters.

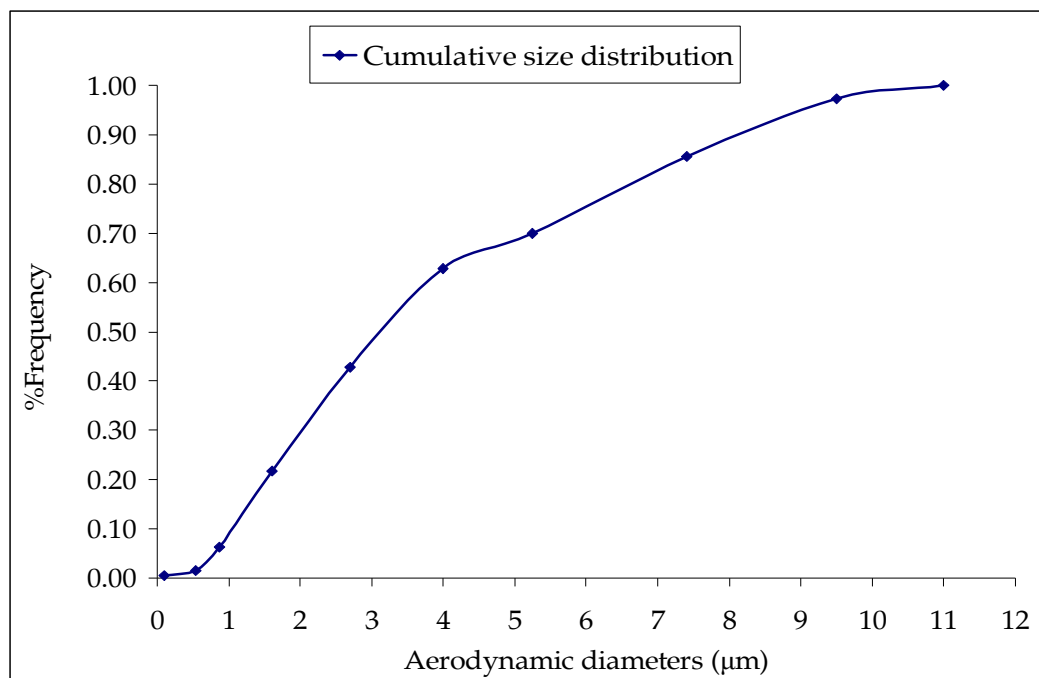


Figure 22. Aerodynamic diameters of DTBP agglomerates (Prep I) determined by cascade impaction.

Approximately 25% of the nebulized Ciprofloxacin (encapsulated within agglomerates) was collected and assayed in the impactor. The collection efficiency was low possibly due to wall losses in the impactor and possible losses while re-dissolving the material deposited on the plates, the elbow piece and the after-filter of the impactor prior to the assay. It is also suspected that the low efficiency may be contributed by the nebulizer, but could be improved in the future by optimizing the choice of the nebulizer.

4.1.2.4. Stability upon nebulization studies

The collection of the nebulisate was not very efficient. Only about 15% of the nebulized Ciprofloxacin (in both the cases of liposomes as well as agglomerates) was trapped in the saline. The remaining Ciprofloxacin was lost to the walls of the collection flask and some to the atmosphere, carried by the air stream exiting the flask. The material deposited on the walls was not included in the analysis since it might have dried and hence disrupted the bilayer of the liposomes, resulting in leakage. Leakage measured was only for the 15% of the material that was collected in the collection medium. While it is possible that some selection of the larger sizes did occur in the process, we tend to discount this since the air velocities in the flask are very low and impaction distances to both the liquid surface and the walls are about the same. It is therefore believed that the 15% collection is representative of the overall nebulized material.

It was expected that nebulization would cause a partial disruption of the particles. This was reflected by an increase in size of the liposomes upon nebulization as shown by the DLS result in figure 23.

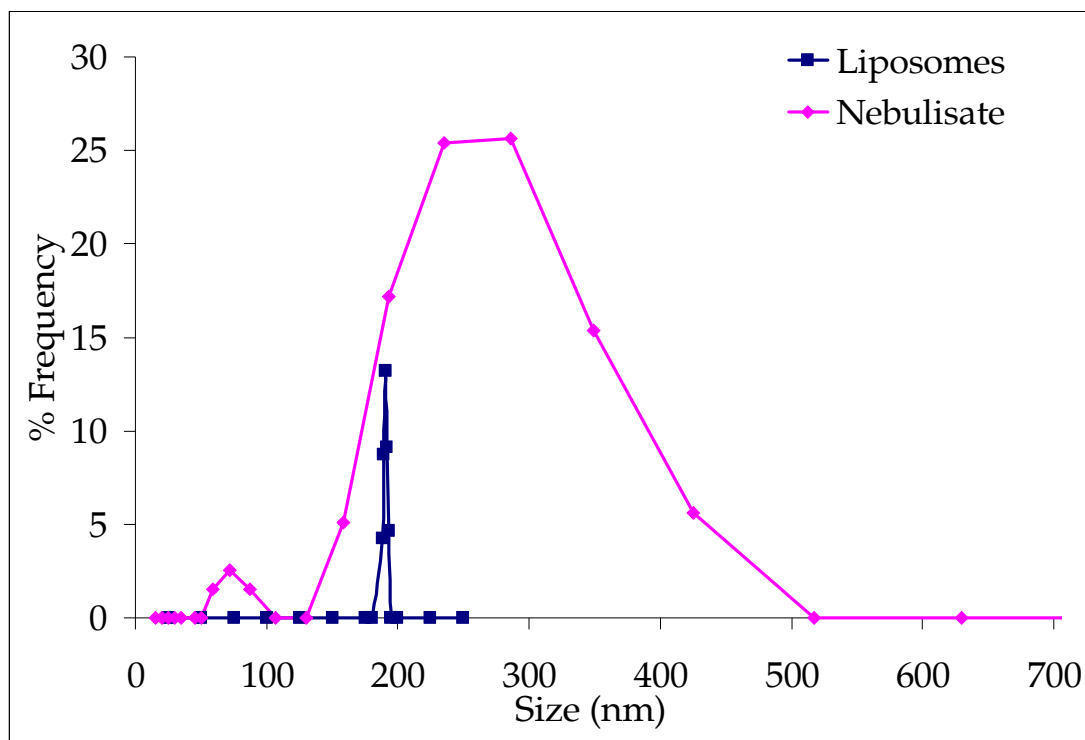


Figure 23. *Effect of nebulization on the size of liposomes*

One would expect similar disruption of the agglomerated particles. The size distribution of agglomerates (Prep I) collected in saline upon nebulization as analyzed by the Fraunhofer method, is shown in figure 24. It was observed that the nebulization caused very little disruption of the agglomerates. The size distribution of the nebulisate had a mode at 12.1 μm , whereas the agglomerates exhibited a mode at 21 μm before nebulization. This disruption is suggested not only by the shift of the peak of the agglomerates but also by the appearance of more parent liposomes in the collected samples of nebulisate.

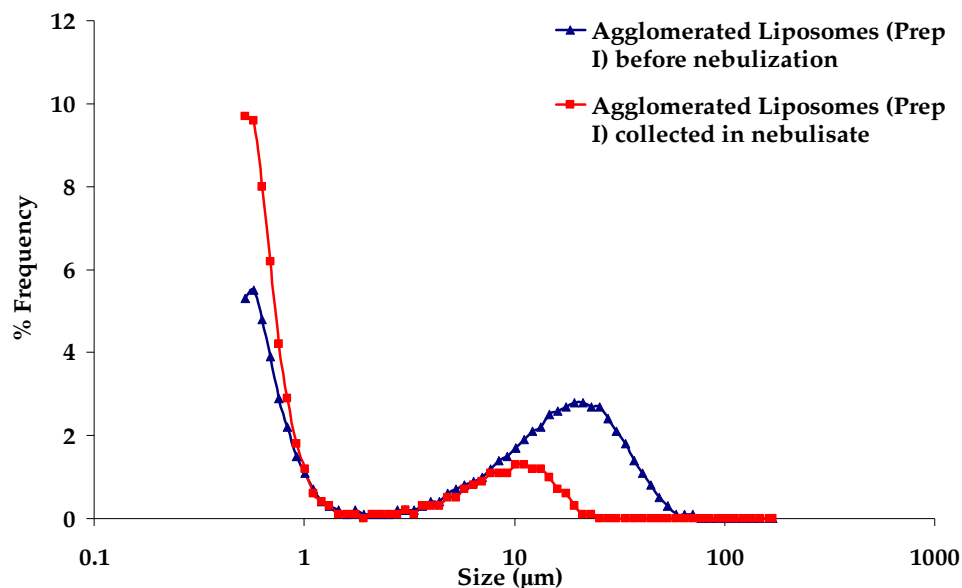


Figure 24. Effect of nebulization on the size of agglomerated liposomes.

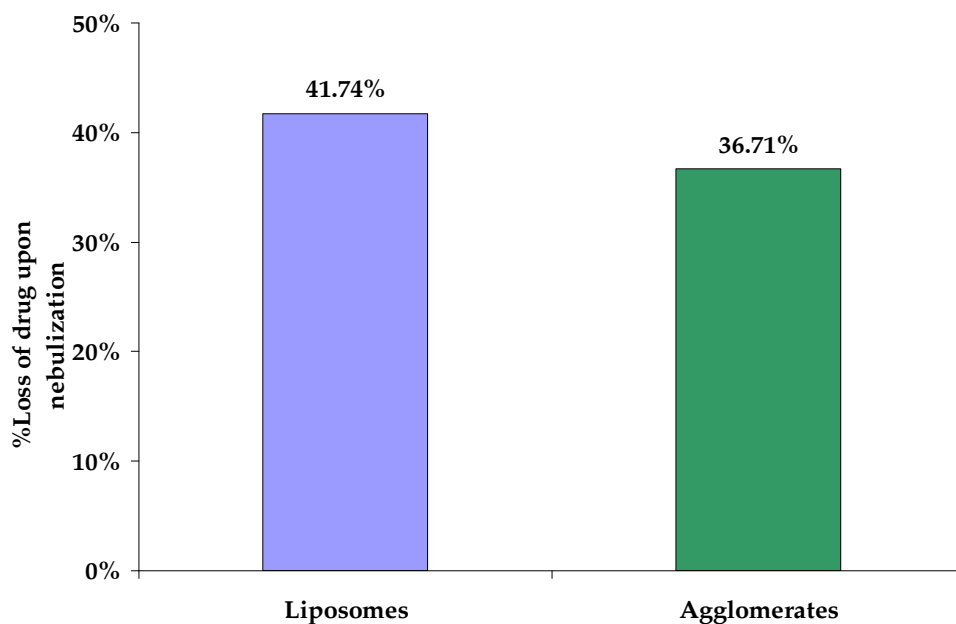


Figure 25. Loss of encapsulated Ciprofloxacin from liposomes and agglomerates after nebulization.

The nebulisate was assayed in order to measure the fraction of Ciprofloxacin remaining encapsulated after nebulization for both parent liposomes and the agglomerates. The results shown in figure 25 compare the loss

of the encapsulated Ciprofloxacin from the liposomes and the agglomerates. The results show a 41.74% loss of encapsulated Ciprofloxacin in the case of the liposomes, but on the other hand the agglomerated formulation showed a slightly lower loss of encapsulated drug. 36.71% of the encapsulated Ciprofloxacin was lost from the agglomerates.

The size distribution and loss of drug results suggest that the agglomerates were largely intact upon nebulization. It is possible that the nebulization breaks the agglomerate bonds but not the liposomes themselves. However, Wong et al [50] have shown that the force required to pull out a biotin-PEG-lipid (similar to NH₂-PEG-DSPE in this study) from a liposome is lower than the force needed to break a streptavidin-biotin bond (analogous to the cross-links in the study). Such pullout could result in leakage from the liposomes, such as observed in this study. The nebulisate contained more liposomes and smaller agglomerates than the pre-nebulized agglomerates supporting the fact that a pullout of a small number of liposomes from the agglomerates took place. It is therefore believed that the agglomerates remain largely intact during the nebulization process.

4.1.2.5. Release studies

Since each of the drug release experiments lasted for one or more days at 37 °C, a loss in the surfactant's activity was expected [51]. A possible degradation

of Ciprofloxacin was also expected due to the presence of proteolytic enzymes in the surfactant.

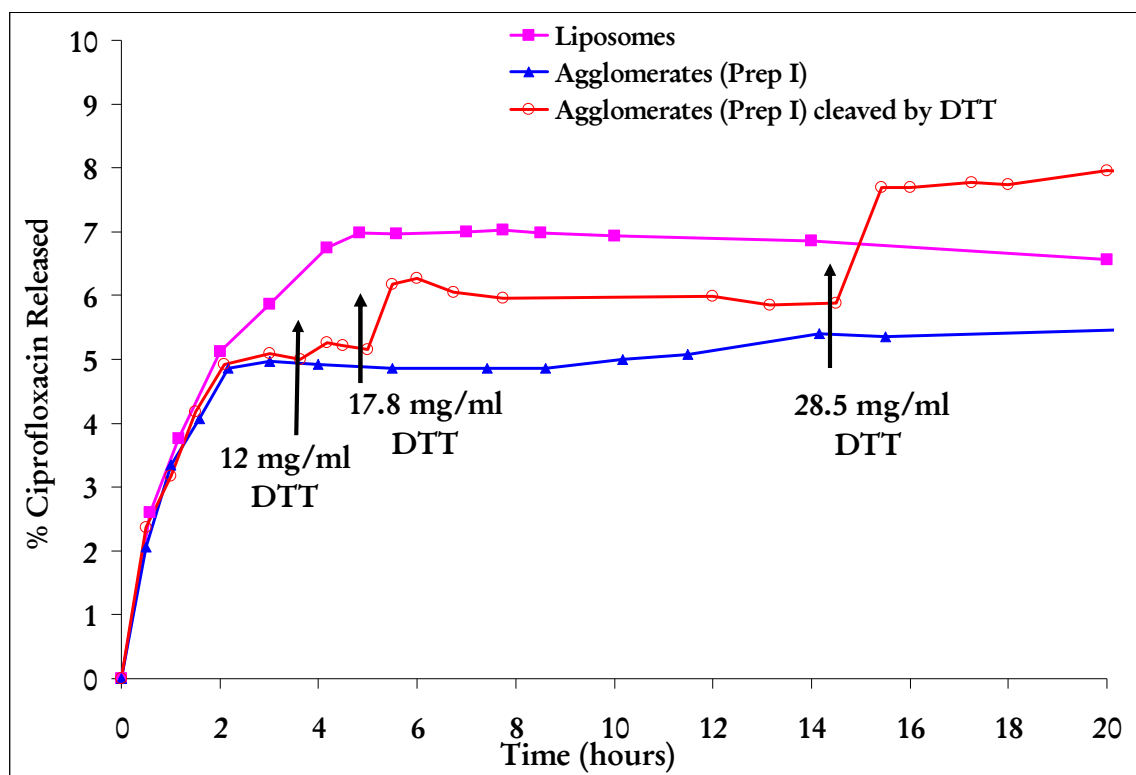


Figure 26. *In vitro* release of Ciprofloxacin from liposomes, and agglomerates (Prep I) with and without cleavage with DTT. Arrows indicate time points at which agglomerates were cleaved with DTT.

Figure 26 provides a comparison between the release profiles of Ciprofloxacin from parent liposomes, agglomerates (Prep I), and agglomerates cleaved with DTT. The agglomerates exhibited a similar initial burst as that of the parent liposomes, however, the release reached a lower plateau much earlier (~ 2 hours) as compared to almost 5 hours in the case of the liposomes. This indicates that the structure of the agglomerates possibly plays a role in protecting the liposomes in the inner core of the agglomerate from being exposed immediately to the surfactant. The arrows indicate the time points when the DTT

was added to the agglomerate and surfactant mixture. The introduction of the cleaving agent resulted in more release of Ciprofloxacin from the agglomerates, which reaches a higher plateau after sometime following the addition of DTT. The addition of higher amounts of the DTT resulted in a relatively higher release of Ciprofloxacin. This result suggests that the cross-links in the agglomerates are cleaved by DTT, thus exposing the interior of the agglomerate structure to the surfactant that consequently results in more release. This would be analogous to the reduction in size observed by Fraunhofer analysis (figure 21) upon cleavage. It was observed that after the last cleavage, the agglomerates released more drug than the parent liposomes. A possible explanation to this could be that the liposomes rearrange to form multi-lamellar vesicles (MLVs) in the presence of lung surfactant. Such a rearrangement would be hindered in the case of the agglomerated liposomes due to the cross-linkages.

4.1.3. *In vivo studies with Ciprofloxacin loaded liposomes*

4.1.3.1. Characterization of Ciprofloxacin loaded liposomes

The size of the liposomes, that were not agglomerated, was in the range of 160 to 400 nm with a mean of 330 nm. The size of liposomes that were agglomerated later with DTBP to form AVT1, was in the range of 150 – 300 nm with a mean of 260 nm.

In the case of the liposomes that were not agglomerated, the concentration of the encapsulated Ciprofloxacin was measured to be 26.4 mg/ml. This value corresponds to 64% of the initial amount of Ciprofloxacin used during loading. The concentration of encapsulated Ciprofloxacin of the liposomes used for making the AVT1 particles was measured to be 26.6 mg/ml, corresponding to 80% encapsulation of the total amount of Ciprofloxacin used in the loading procedure.

4.1.3.2. Agglomeration of liposomes with DTBP

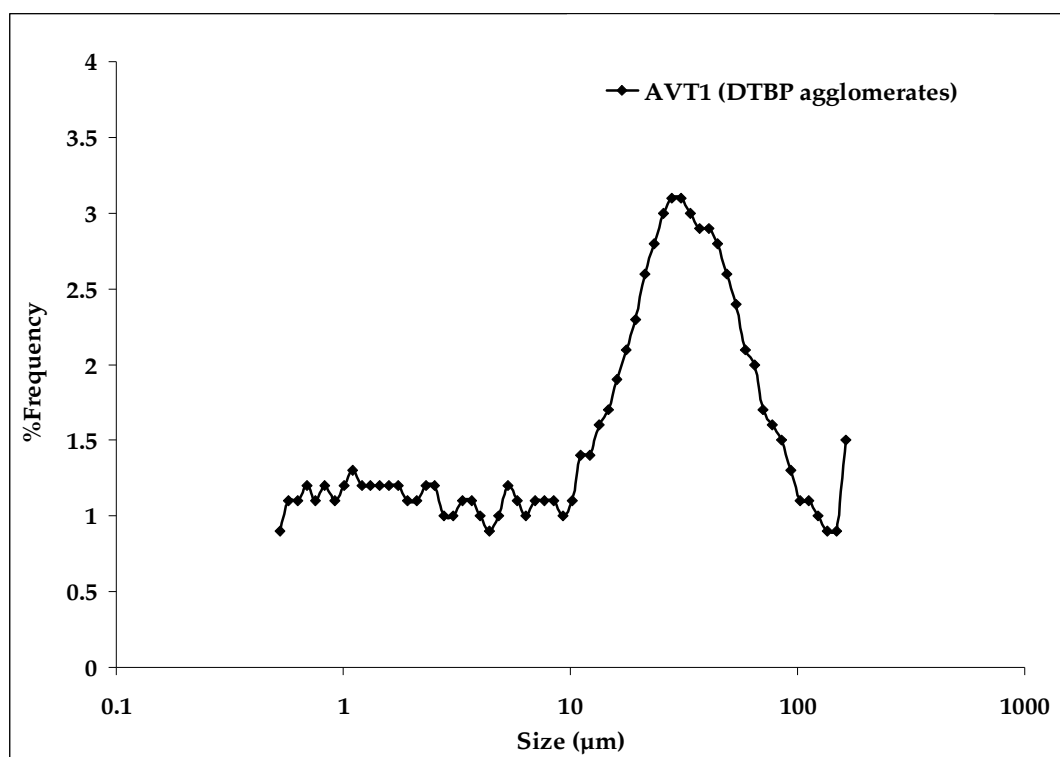


Figure 27. Size distribution of agglomerates (AVT1) used in animal studies.

Figure 27 shows the geometric size distribution of the agglomerates AVT1 by Fraunhofer diffraction analysis. Less than 10% of the particles were in the

submicron size range. The agglomerate population was broadly distributed from 1–140 μm with a mode at 31 μm . Upon performing a leakage study (by dialysis) after the agglomeration, the amount of Ciprofloxacin that leaked from the agglomerates was found to be less than 2%. The final encapsulated Ciprofloxacin concentration of AVT1 was 17.8 mg/ml.

4.1.3.3. Pharmacokinetic studies in rabbits

Figure 28 shows the blood levels of Ciprofloxacin after intratracheal instillation of the free Ciprofloxacin, liposome-encapsulated Ciprofloxacin, and AVT1 treatment. Each data point represents the mean and standard deviation of the group (3 rabbits per group). The difference of the means between groups was verified to be significant by variance analysis (Student's t-test). A *p*-value less than 0.05 was used to confirm significant differences at the 95% confidence level.

Table 3. Formulation of Ciprofloxacin instilled in the lungs of rabbits.

Formulation	Ciprofloxacin Dose (mg/kg)	Molarity of lipids (mM)	Drug:Lipid (molar)
<i>Liposome</i>	21.07 \pm 1.64	~120	0.66
<i>AVT1</i>	17.05 \pm 0.44	~50	1.07
<i>Free Ciprofloxacin</i>	15.4	NA	NA

The doses of the drug formulations instilled in the rabbits are tabulated in table 3. It should be noted that Ciprofloxacin has a very low solubility at neutral pH. Ciprofloxacin at a concentration of 21.9 mg/ml was instilled in the lungs in this study to compare with the concentrations used in experiments involving liposomes and the AVT particles. To keep Ciprofloxacin in solution at this concentration, the pH of the formulation was maintained at ~3.1. The rabbit

treated with the free Ciprofloxacin formulation showed signs of distress (heavy panting) after instillation. When the lungs were observed post mortem, there were signs of extensive injury highlighted by the darkening of the lung tissue. Hence, no more rabbits were used to evaluate free ciprofloxacin. The lung injury may be attributed to the high concentration of Ciprofloxacin that is in immediate contact with the tissue and the low pH of the formulation. To the best of our knowledge there are no studies reporting inflammation of the lungs or toxicity effects due to administration of Ciprofloxacin to the lungs. No such signs of damage were observed in the lungs of the rabbits that were used to evaluate the liposomes and AVT particles.

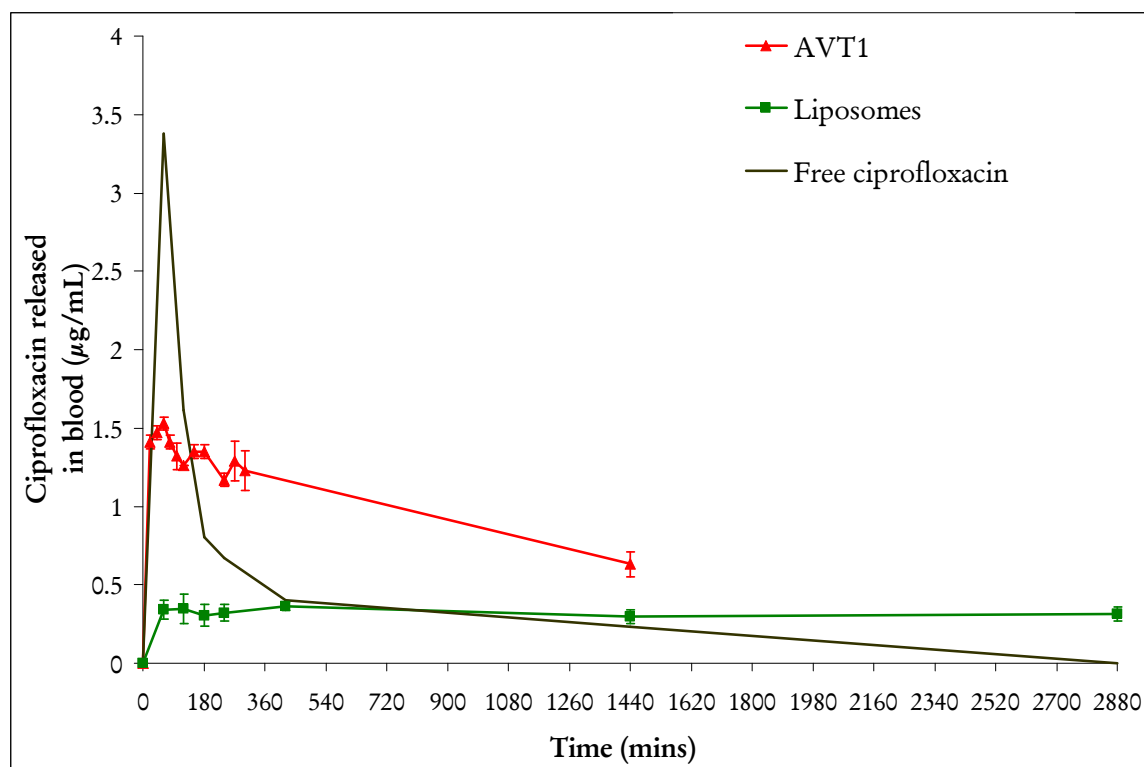


Figure 28. Pharmacokinetic data for the different formulation tested in rabbits. ($n=1$ for the free Ciprofloxacin study, and $n=3$ for the other studies. Study with liposomes and free Ciprofloxacin was done over 2 days. The AVT studies were done over 1 day).

A burst in release was observed in the case of the free Ciprofloxacin during the 1st hour, which then rapidly dropped to low values and eventually went to zero at the end of 48 hours. C_{\max} in blood was measured to be 3.38 $\mu\text{g/ml}$. This rapid release can be attributed to the fact that Ciprofloxacin is in direct contact with the tissue and is able to quickly diffuse out in the blood. An assay of the lungs of the rabbit at the end of 48 hours indicated no Ciprofloxacin remained in the lungs.

In the case of liposomes, and AVT1, though an initial burst in release of drug was observed, it was much lower than that for free Ciprofloxacin. However, the AVT1 particles and liposomes show that they are capable of extended drug release in the blood. C_{\max} for the liposomal formulation was $0.34 \pm 0.06 \mu\text{g/ml}$ and this level of drug in the blood was maintained through the 48 hour period. C_{\max} for AVT1 was observed to be $1.53 \pm 0.04 \mu\text{g/ml}$ with the level gradually falling to $0.63 \pm 0.08 \mu\text{g/ml}$ over 24 hours. Thus the entire curve for AVT1 was higher than that for liposomes, indicating a much higher systemic bioavailability. The lower initial release-burst for the liposomes and AVT1 particles is consistent with the fact that the Ciprofloxacin is encapsulated within the particles and is not in direct contact with the lung environment. As the drug leaks out of the particles, it is transported rapidly to the bloodstream, but at no point is the free drug concentration in the lung high enough to cause a large spike in the blood levels as observed in the free Ciprofloxacin case.

Table 4. AUC_{0-24} for pharmacokinetic data of figure 28.

Formulation	Dose (mg/kg)	AUC_{0-24} ($\mu\text{g/ml.hr}$)
Liposome-encapsulated Ciprofloxacin	21.07 ± 1.64	8.02 ± 2.3
AVT1	17.05 ± 0.44	19.8 ± 0.12

The areas under the concentration-time curves (AUC_{0-24}) for AVT 1, and liposomes for 24 hours were computed and are listed in table 4. The AUC's increase with the size of the particles, suggesting that the larger particles have an improved systemic bioavailability in comparison to the smaller particles.

4.1.4. *In silico study of pharmacokinetics of 1st generation AVT*

The input dose (known parameter) for the liposomes and AVT1 particles are tabulated in table 5. The internal volume of the liposomes (V_{Lips}), and AVT1 (V_{AVT}) that were instilled, were fixed at 2 ml. The surfactant volume of the rabbits was assumed to be 1.8 ml. This volume of the pulmonary fluid was estimated by comparing the known volume of the human pulmonary fluid (~35 mL) and correcting it with the body weight.

Table 5. Values of input dose used in the model.

Formulation	D (μg)
Liposome-encapsulated Ciprofloxacin	69000
AVT1	40500

The plot of the model fitted to data for liposomes after the convergence criteria were met is shown in figure 29. The parameters that the model estimates to fit the data points are given in table 6.

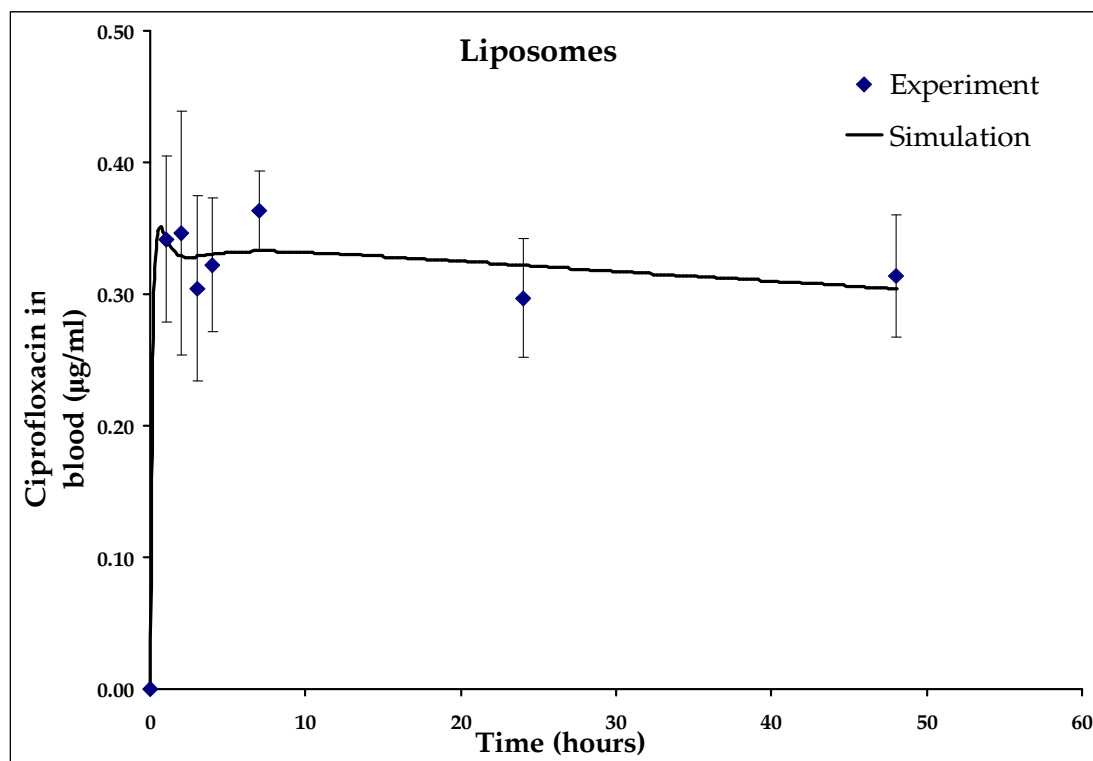


Figure 29. Model fit to data for pharmacokinetic studies done with liposomes.

Table 6. Unknown parameters estimated for pharmacokinetic study with liposomes

Parameter	Value (\pm sd)	95% confidence interval	
α (μ g)	549.54 (\pm 361.2)	352.03	652.53
k_{Lips} (hr^{-1})	0.0024 (\pm 0.003)	-0.006	0.01
k_{L0} (hr^{-1})	1.67 (\pm 1.33)	-2.01	5.35
k_L (hr^{-1})	0.012 (\pm 0.013)	-0.023	0.047

Upon instillation of the liposomes, the value of α indicated that 0.8% of the encapsulated drug leaked from the particles and appeared free in the lungs due to fragmentation of the particles. The first order release rate constant from the liposomes (k_{Lips}) was estimated to be very low. The elimination rate constant

of the drug from the lung (k_{L0}) was estimated by the model to be 2 orders of magnitude larger than the rate constant (k_L) that transfers drug from the lungs into the blood.

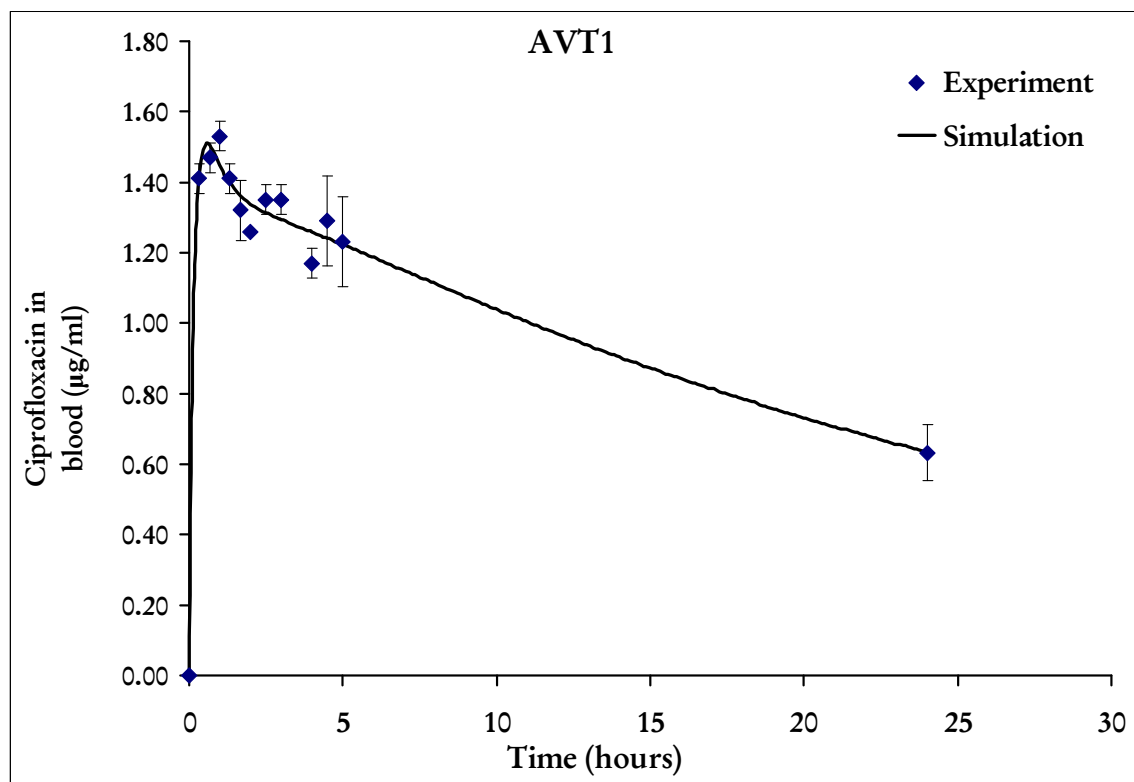


Figure 30. Model fit to data for pharmacokinetic studies done with AVT1.

The simulation fitted to the data for the AVT1 particles is shown in figure 30 with the unknown parameters estimated for the study are given in table 7. The value of ' α ' that was estimated represented 8% of the initial drug instilled in the lungs. The value of α is higher than that for the liposomal treatment suggesting that after the instillation, the AVT are fragmented to a higher extent than the liposomes resulting in a higher drug leakage into the lung compartment (with subsequent release into the blood compartment). The fragmentation in turn may be caused due to the significant motion of the lungs during breathing, applying

shear to the AVT particles. This is not the case when it comes to the liposomes as they are compact and resist to a greater extent the shearing action of the lungs during breathing.

Table 7. Unknown parameters estimated for pharmacokinetic study with AVT1.

Parameter	Value (\pm sd)	95% confidence interval	
α (μ g)	3133.12 (\pm 381.64)	2269.8	3996.44
k_{AVT} (hr^{-1})	0.035 (\pm 0.006)	0.023	0.048
k_{L0} (hr^{-1})	0.881 (\pm 0.204)	0.72	2.14
k_L (hr^{-1})	0.006 (\pm 0.001)	0.004	0.008

The estimates suggest that AVT1 have a better release rate than the liposomes ($k_{AVT} > k_{Lips}$). This is also supported by the higher levels of drug that is maintained in the blood. The marginally lower clearance rate constant of AVT1 in comparison to the liposomes (k_{L0}) suggests that the amount of drug that is cleared from the lungs is mostly free drug in the case of the AVT1 plus drug that may be associated with the fragments that may be formed due to the shearing nature of the lungs. In the case of the liposomes, the drug cleared is free drug plus drug encapsulated within the liposomes that may be cleared by the macrophages. The action of the macrophages is assumed to be lower in the case of the AVT1 due to their large size, with only the fragmented particles being taken up if they are within the size range for macrophage activity.

4.2. The 2nd generation of AVT (in vivo cleavable)

The commercially available cross-linker DTSSP was identified to be cleavable by cysteine (acceptable for in vivo use). In this section the results of the studies that were undertaken in vitro to show size reduction and drug release upon cleavage are reported. Additionally the in vivo studies that were undertaken to suggest modulated release capabilities of the agglomerates made with this linker are also discussed.

4.2.1. *In vitro studies with blank liposomes*

4.2.1.1. Characterization of liposomes

The size of the liposomes extruded through the 400 nm polycarbonate membrane, as measured by DLS was in the range of 180-340 nm with a mean diameter at 244 nm. These were consistent with the sizes achieved during the numerous undertakings for fabricating the liposomes.

4.2.1.2. Agglomeration of liposomes with DTSSP

Agglomerates of liposomes that were made with DTSSP were incubated with different amounts of cysteine at 37 °C in order to see if cleavage was possible. The sizes of the agglomerates were analyzed by the Fraunhofer diffraction method, before and after cleavage. The results of these studies are shown in figure 31. The agglomerates of liposomes (50 mM lipid) made with 20 fold molar excess of DTSSP had sizes between 3.5 – 95 µm with a mode at 19.4 µm.

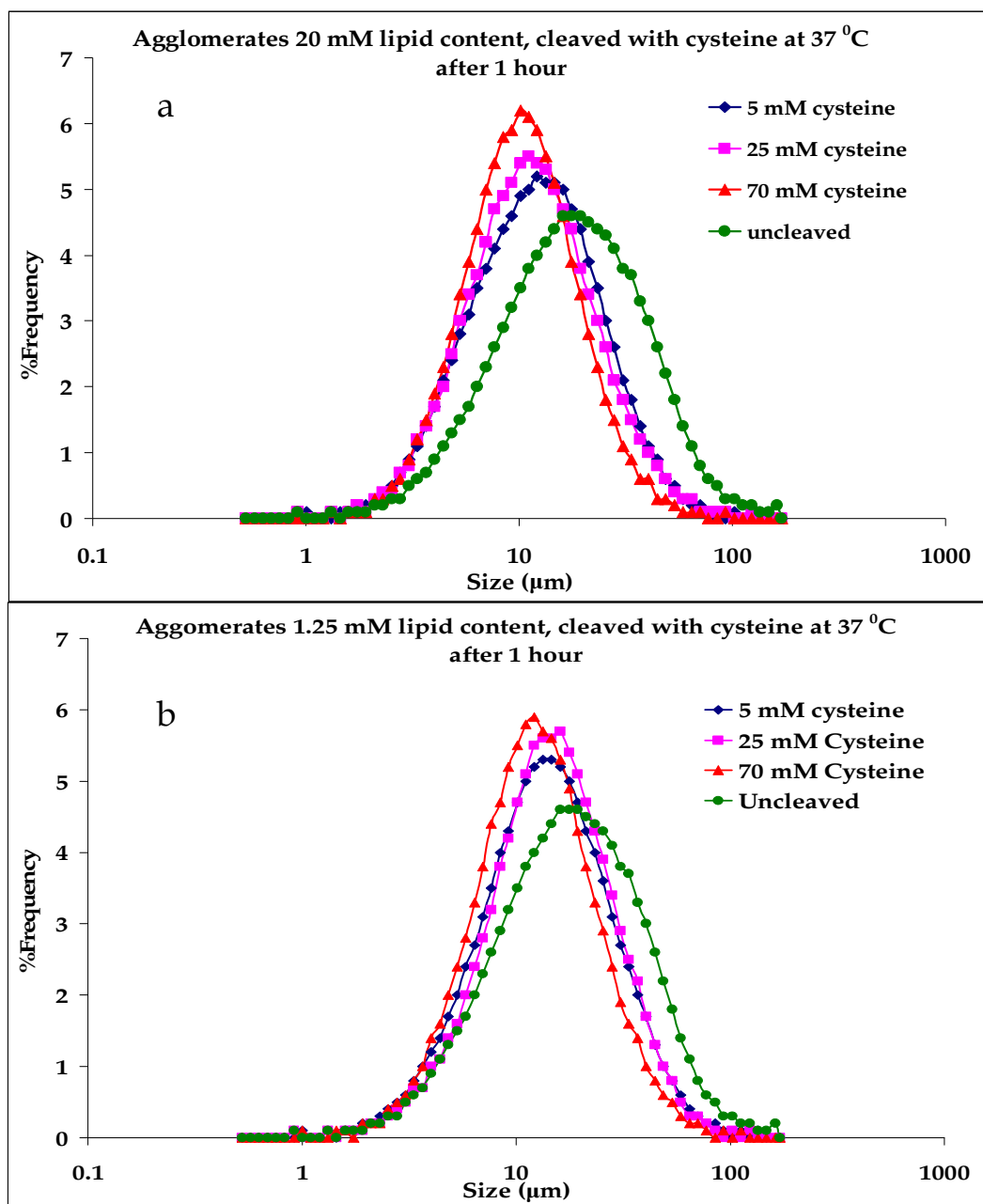


Figure 31. Fraunhofer diffraction analysis of liposomes agglomerated with DTSSP, and subsequent cleavage with cysteine at 37 °C. Agglomerates with (a) 20 mM lipid, and (b) 1.25 mM lipid.

These agglomerates were then cleaved with different amounts of cysteine at lipid molarities of 20 mM (figure 31a) and 1.25 mM (figure 31b). It was observed that the reduction in the size of the agglomerates was proportional to the amount of cysteine that was used. This is evident by a shift in the size

distributions to the smaller sizes with an increase in the fraction of particles in the 4-16 μm , and a fall in the fraction of agglomerates larger than 30 μm . However, the cleavage was not extensive, i.e. it did not result in the formation of parent liposomes. It was anticipated that this cleavage of the agglomerates would result in accelerated release of the drug.

4.2.2. *In vitro studies with carboxyfluorescein (CF) loaded liposomes*

4.2.2.1. Characterization of liposomes

The liposomes encapsulating 5 mM CF that were extruded through 400 nm polycarbonate membrane had a size distribution between 170-350 nm with a mean diameter of 241 nm. These sizes were consistent with those achieved with the extrusion process.

4.2.2.2. Agglomeration of liposomes with DTSSP

The liposomes encapsulating CF were agglomerated with DTSSP and were sized by Fraunhofer diffraction analysis. The size distributions are shown in figure 32. The agglomerates were distributed from 1-90 μm .

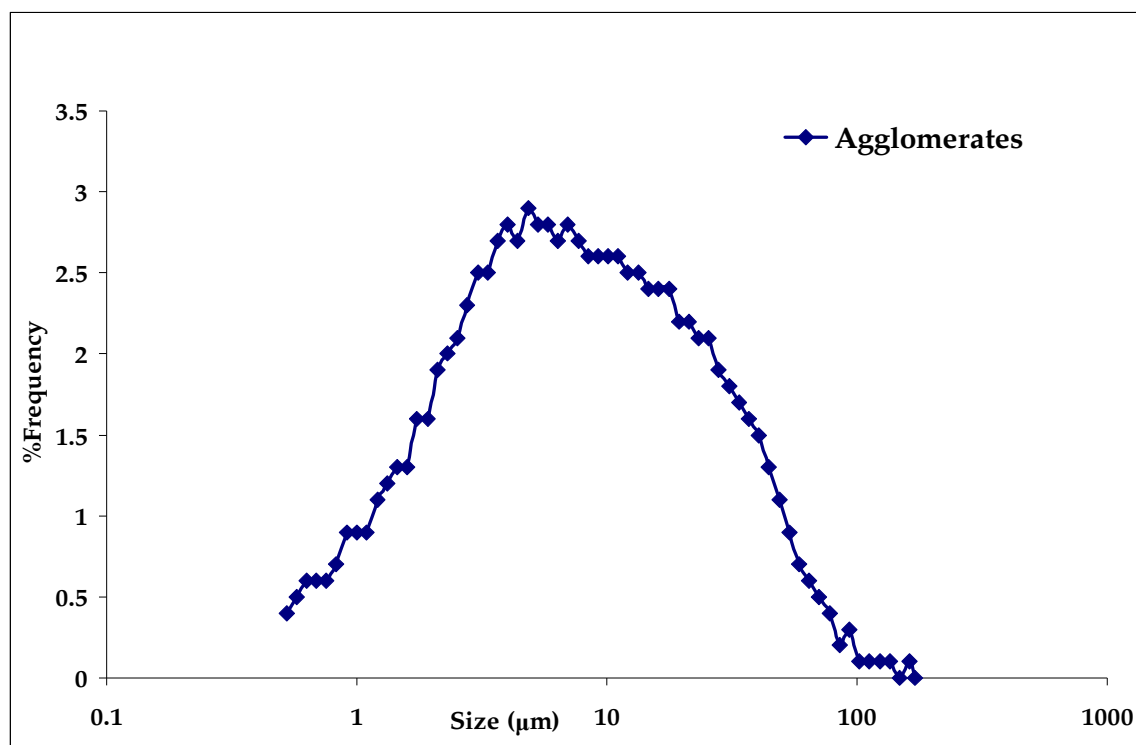


Figure 32. *Fraunhofer analysis of agglomerates of liposomes encapsulating CF.*

These agglomerates were used for visual analysis of the structure of the agglomerate by confocal microscopy.

4.2.2.3. Visual analysis of agglomerates by Confocal microscopy

A montage of the slices of the one of the agglomerates that was imaged is shown in figure 33. The Z-stack for the slices was set at 0.5 μm. The stack size of the image was 36.6 μm x 36.6 μm x 7.5 μm. The pixel resolution of each slice was 512 x 512. The size of the agglomerate seen here is between 3-8 μm. The slices through the agglomerate indicate the presence of compact domains (bright areas) and porous domains (dark areas within the agglomerate). This heterogeneity in the structure can be attributed to two things that may be happening during the reaction: (1) The initial fast reaction leads to the formation of smaller compact

agglomerates of the liposomes, (2) the activated ligands on the liposomes present at the outer boundary of these compact agglomerates then form cross-links with the un-activated ligands on other agglomerates to form the larger agglomerate.

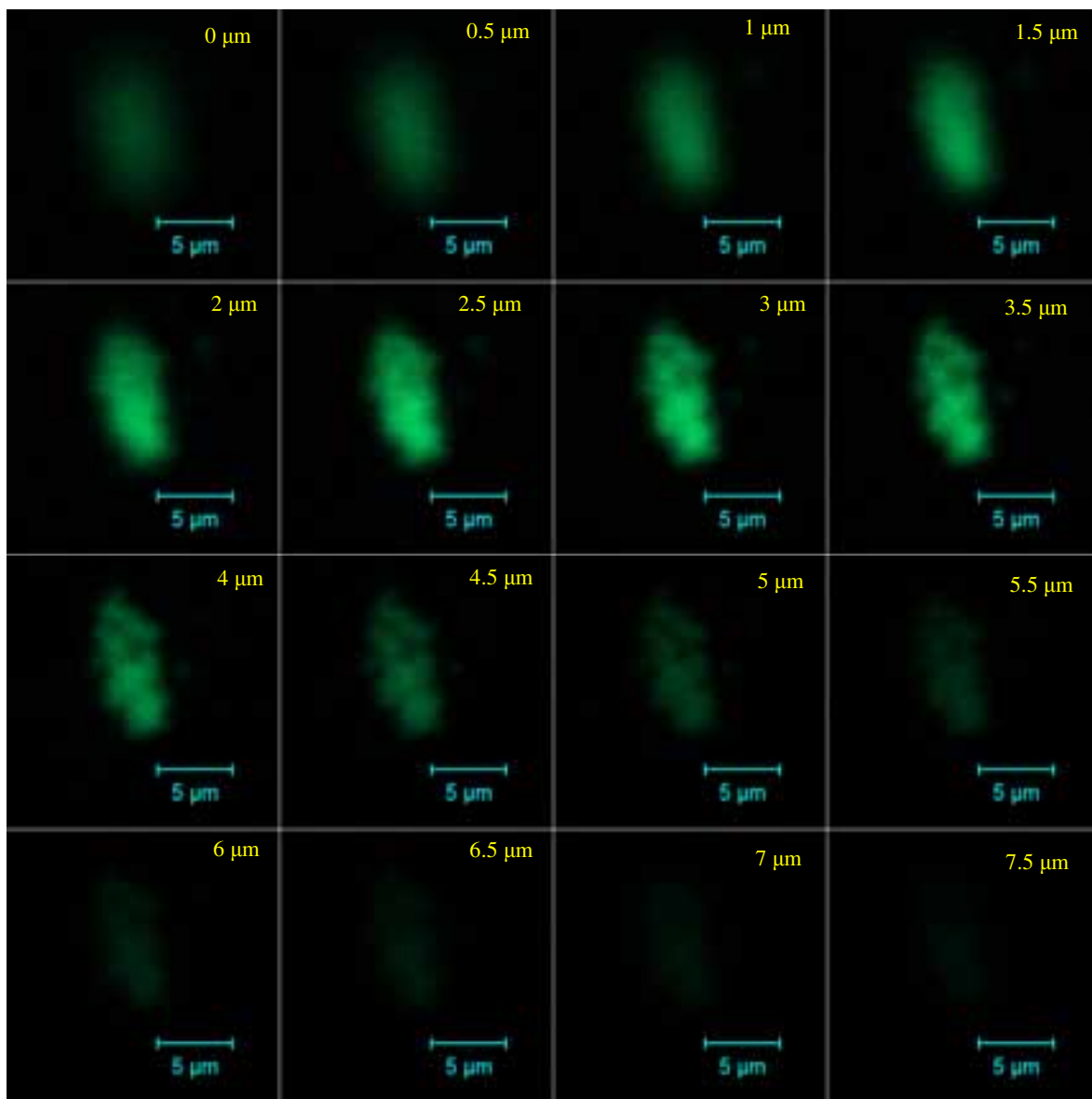


Figure 33. Slices of confocal image of an agglomerate encapsulating carboxyfluorescein. Data at top right corner of each image is the Z-stack height, with Z-stack slices taken every 0.5 μm .

The image slices that were obtained were then processed and analyzed with ImageJ (NIH) to determine the void area fraction of the agglomerate. Briefly, each slice was converted to an 8 – bit grayscale image. A binary threshold was then applied to the resulting image. Using the Wand tracing tool in ImageJ, the boundary of the resulting agglomerate structure was determined. The area fraction of this bounded image was then determined using the built-in macro ‘MeasureAreaFraction’. The void fraction of the agglomerate was determined to be 5-10% of the total area of the agglomerate.

4.2.3. *In vitro studies with Ciprofloxacin loaded liposomes*

4.2.3.1. Characterization of Ciprofloxacin loaded liposomes

The sizes of the Ciprofloxacin loaded liposomes as determined by DLS were in the range of 140 – 350 nm with a mean at 210 nm. This was consistent with the sizes obtained after extrusion through the 400 nm polycarbonate membrane. After removal of the unencapsulated Ciprofloxacin by dialysis the final concentration of Ciprofloxacin was found to be 21 mg/ml, which represented 80% of the initial drug used during the loading.

The agglomerates of these liposomes made with the cysteine cleavable linker DTSSP were used for both in vitro and in vivo studies.

4.2.3.2. Agglomeration of Ciprofloxacin loaded liposomes with DTSSP

The sizes of the agglomerates as determined by the Fraunhofer diffraction technique are shown in figure 34. The agglomerates had a size distribution between 2 – 100 μm with a mode at 5.5 μm . These agglomerates were used in vitro drug release experiments.

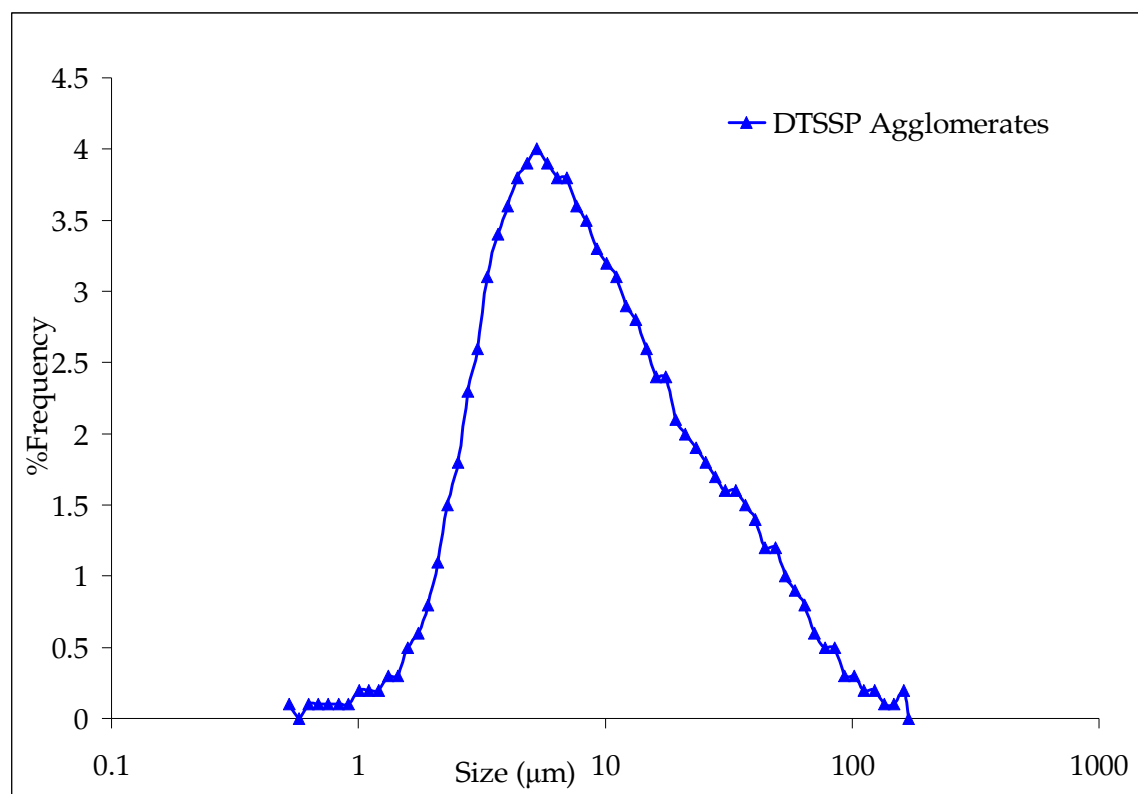


Figure 34. Size distribution of agglomerates of liposomes encapsulating Ciprofloxacin.

4.2.3.3. Visual analysis of agglomerates by negative stain electron microscopy

The agglomerates of DTSSP made in the previous section were visualized by negative stain electron microscopy. Figure 35 shows the negative stain electron microscope (EM) images of liposomes and AVT particles encapsulating

Ciprofloxacin. Figure 35a shows the EM image of the parent liposomes with diameters around 200 nm. Since the length of the PEG anchor (~7 nm) is very small compared to the size of the liposome, linked liposomes are in close proximity as shown in Figures 35b–d.

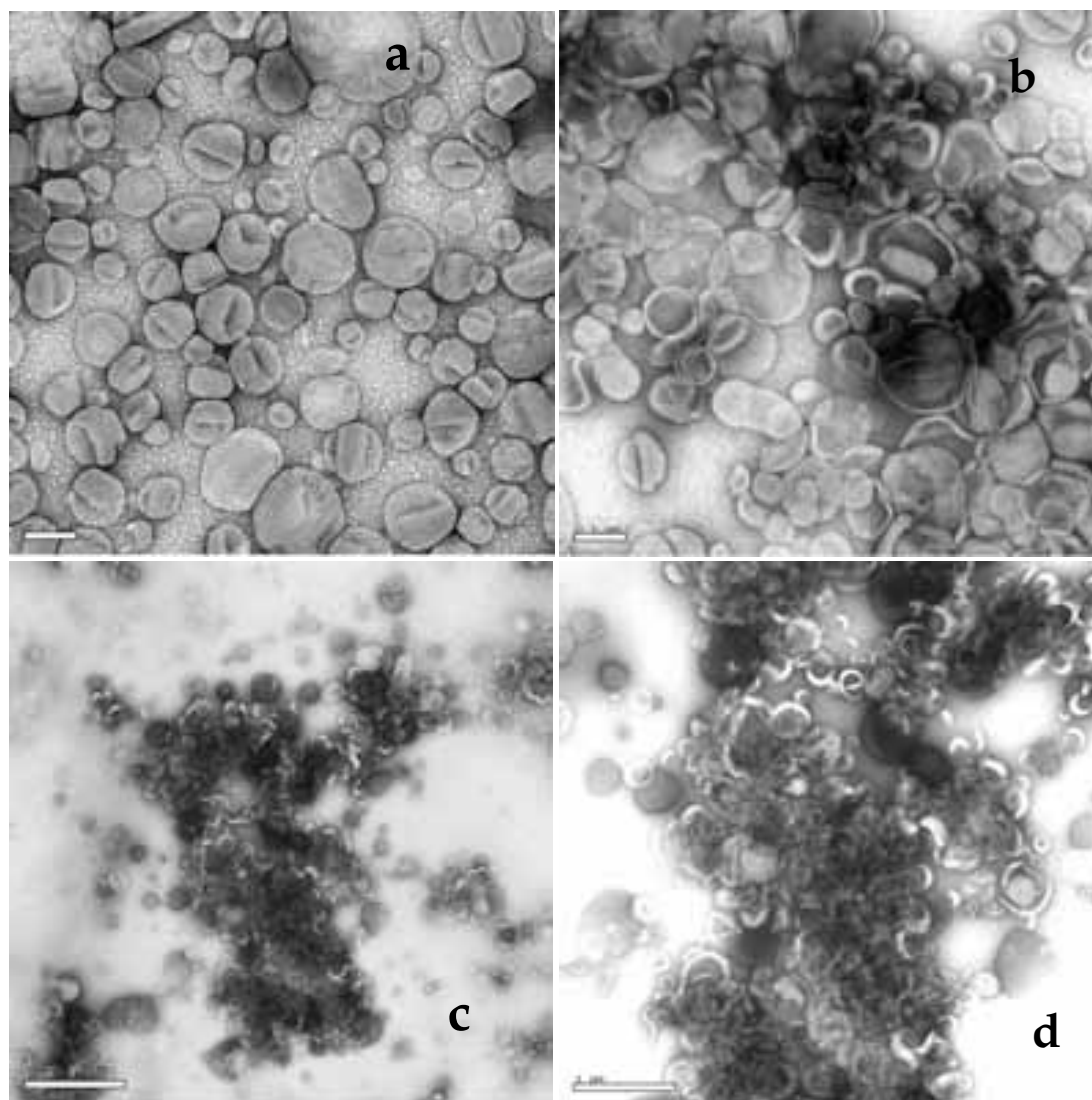


Figure 35. Negative stain electron microscope images (1% uranyl acetate) taken on a JEOL JEM 1230. (a) liposomes at 10 K magnification, scale bar 0.2 μm ; (b) agglomerate at 10 K magnification, scale bar 0.2 μm ; (c) agglomerate at 2 K magnification, scale bar 2 μm ; (d) agglomerate at 4 K magnification, scale bar 1 μm .

The agglomerates clearly consisted of clusters of cross-linked liposomes incorporating high amounts of the negative stain suggesting high accessibility of the aqueous phase to the interior of the agglomerate structure. A heterogeneous structure can be seen that includes highly porous as well as compact domains within the agglomerate. As the compact structures were nucleated rapidly, diffusion-limitations dominated during the agglomeration reaction, resulting in the formation of porous structures of the compact “nuclei”. Similar structures are expected for all the agglomerates formed, since the reaction conditions for each were very similar. One therefore expects that drug release properties of each of the agglomerates would also be very similar to each other.

4.2.3.4. Release studies

The results of the in vitro release experiments undertaken to show modulated release of the drug from the agglomerates after treatment with cysteine are shown in figure 36. To show that the modified release from the agglomerates was due to cysteine alone and not due to any other factors, a third study was done where a volume of plain buffer equivalent to that of cysteine (50 μ l) was introduced at similar time points. Upon the introduction of cysteine into the dialysis bag accelerated release of drug into the external phase was observed. The results suggested as expected that the increased release was due to cysteine addition and not due to other factors. The overall release from the cleaved agglomerates was higher than from the agglomerates that were not cleaved.

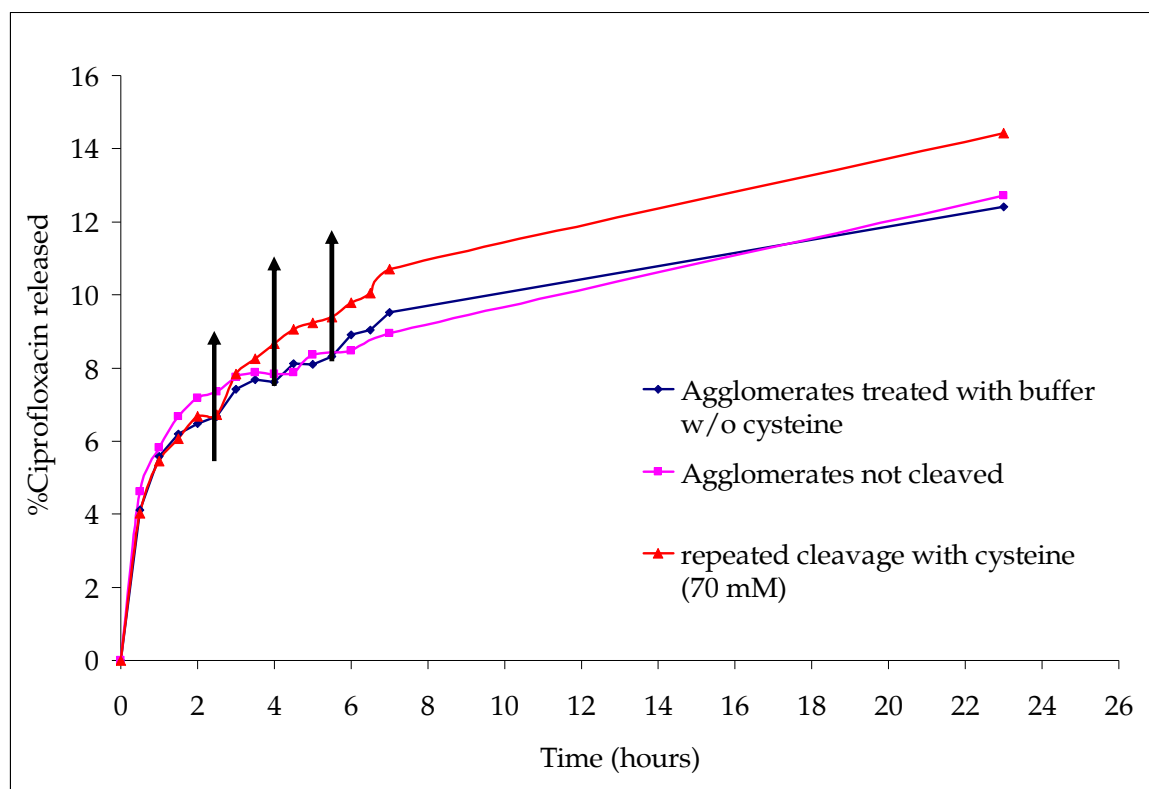


Figure 36. *In vitro* release profiles from uncleaved agglomerates, agglomerates that were repeatedly cleaved with cysteine, and agglomerates treated with plain buffer. (Arrows indicate time points at which 50 μ l of either buffer or cysteine containing buffer is introduced.)

This result suggests that the cross-links in the agglomerates are cleaved by cysteine, thus exposing the interior of the agglomerate structure to the surfactant that consequently results in more release. This would be analogous to the reduction in size of the DTSSP agglomerates observed by Fraunhofer analysis (figure 31) upon cleavage with cysteine.

4.2.4. *In vivo* cysteine triggered release studies

4.2.4.1. Characterization of liposomes

The size of the liposomes encapsulating Ciprofloxacin was in the range of 140 – 350 nm with a mean at 210 nm. The liposomes incorporating fluorescent tagged lipid (used in the lipid assay from the lungs) were in the range of 177 – 460 nm with a mean at 290 nm.

4.2.4.2. Agglomeration of liposomes with DTSSP

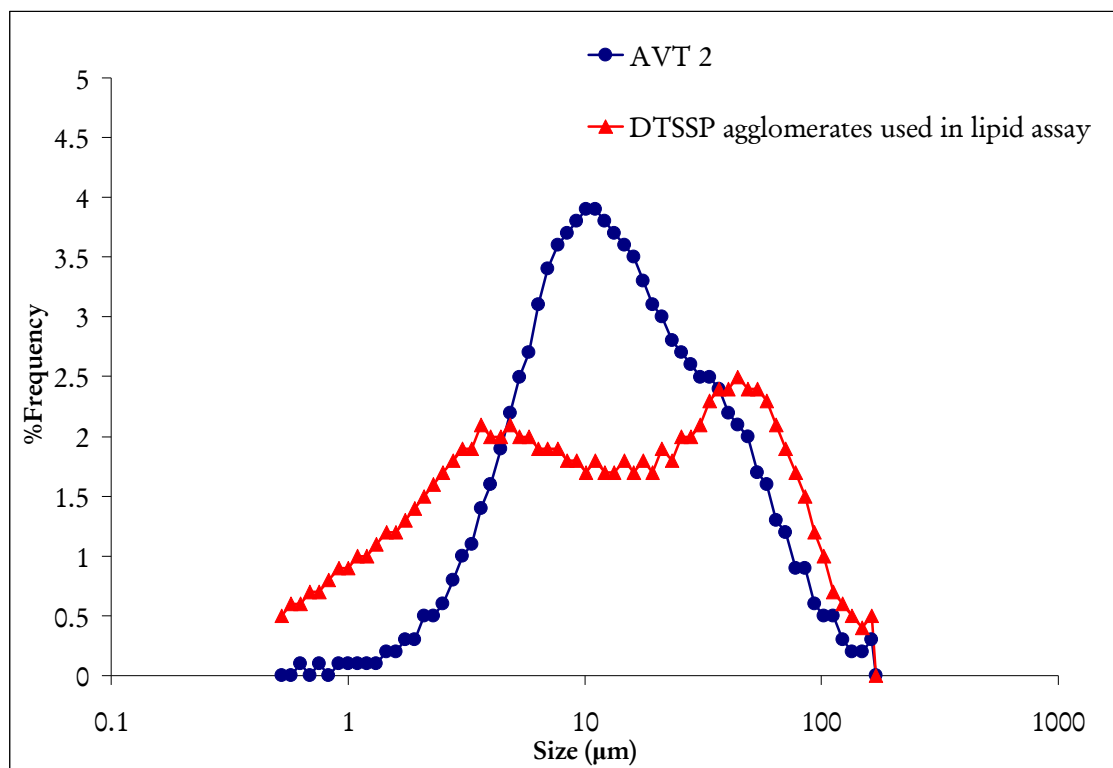


Figure 37. Particle size distribution, by Fraunhofer Diffraction, of the agglomerates used in the pharmacokinetic and lipid assay studies.

The particle size distributions, by Fraunhofer Diffraction, of AVT2 (DTSSP agglomerates of liposomes encapsulating Ciprofloxacin used *in vivo*) that were

used for the pharmacokinetic studies, and that of the agglomerates used for the lipid assay studies, are shown in figure 37. The agglomerate populations for AVT2 were distributed from 2 –120 μm with a mode at 11 μm .

The agglomerates of DTSSP that were used for the lipid assay studies showed a bimodal distribution from 1 – 125 μm , with one mode at 5 μm and the second one at 44 μm .

4.2.4.3. Pharmacokinetic studies in rabbits

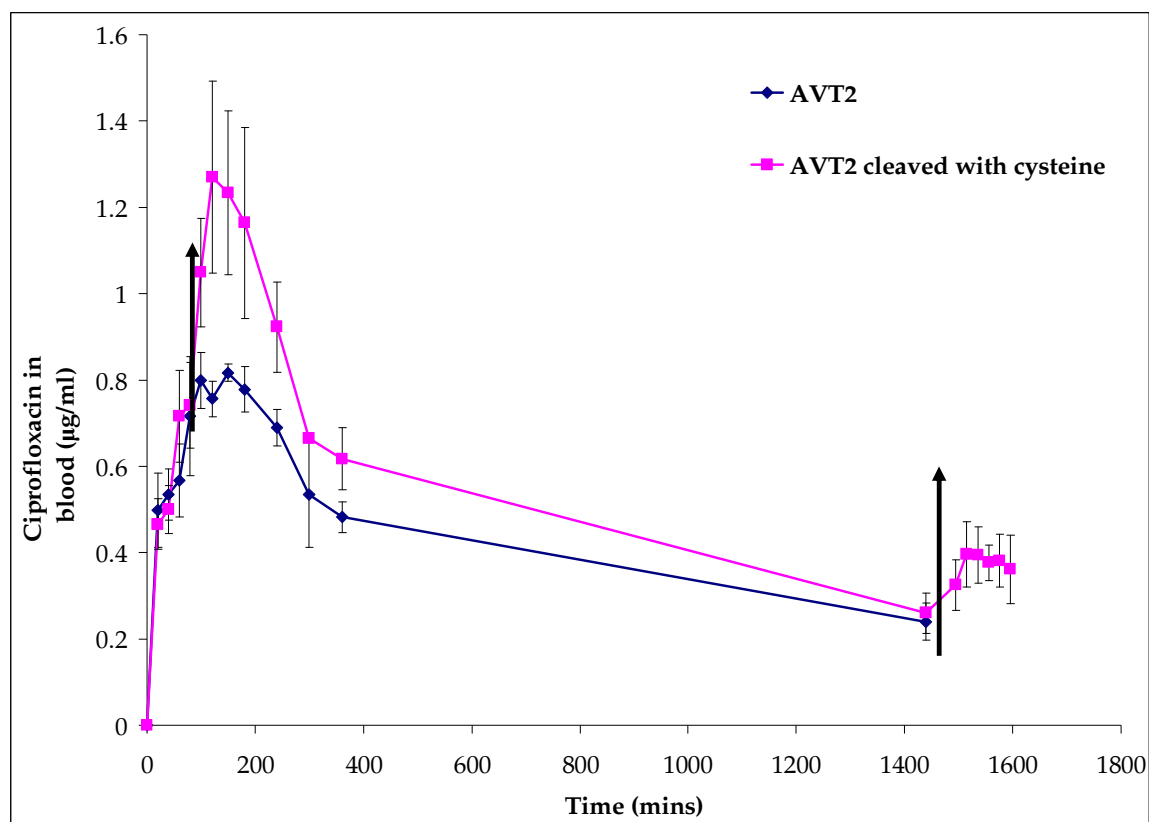


Figure 38. Pharmacokinetic data of AVT2 particles, with and without cysteine treatment. Arrows indicate time points when 1 ml cysteine (60 mg/ml) was instilled. $n=3$ animals.

Figure 38 shows the blood levels of Ciprofloxacin after intratracheal instillation of the AVT 2, and AVT 2 + cysteine treatment. Each data point represents the mean and standard deviation of the group (3 rabbits per group). The difference of the means between groups was verified to be significant by variance analysis (Student's t-test). A p -value less than 0.05 was used to confirm significant differences at the 95% confidence level. The dose of the AVT2 that was instilled in the rabbits for the two studies is shown in table 8.

Table 8. Dose of AVT2 instilled in the lungs of rabbits.

Formulation	Ciprofloxacin Dose (mg/kg)	Molarity of lipids (mM)	Drug:Lipid (molar)
<i>AVT 2</i>	18.31±0.62	~50	1.07

The AVT2 exhibited an initial burst in release, but the levels were lower compared to the study done with the free Ciprofloxacin (section 4.1.3.3). The AVT 2 particles exhibited a C_{\max} of 0.8 ± 0.07 $\mu\text{g/ml}$ followed by a gradual drop to 0.24 ± 0.04 $\mu\text{g/ml}$ in 24 hours.

After instillation of cysteine at 90 minutes into the lungs of the rabbits an elevation in release rate was observed. The C_{\max} attained due to cysteine instillation was 1.27 ± 0.22 $\mu\text{g/ml}$. The blood levels of drug in animals treated with AVT2 and then with cysteine are significantly different ($p < 0.05$) from those for the same formulation with no cysteine treatment. The systemic bioavailability of the AVT2 particles is clearly improved after cysteine instillation as indicated by the increase in the AUC.

A 40% increase in total release (as measured by the area under the curve, AUC) was caused by the cysteine instillation. After 24 hours a repeat cysteine instillation resulted in further triggered release. However, smaller drug amounts were released consistent with overall lower residual drug content in the particles at this extended time post administration. The triggered release due to cysteine addition may be attributed to the cleaving of the disulfide linkages on the DTSSP that links two liposomes. This breakage would result in the rupture of the structure of the microparticle resulting in accelerated drug release.

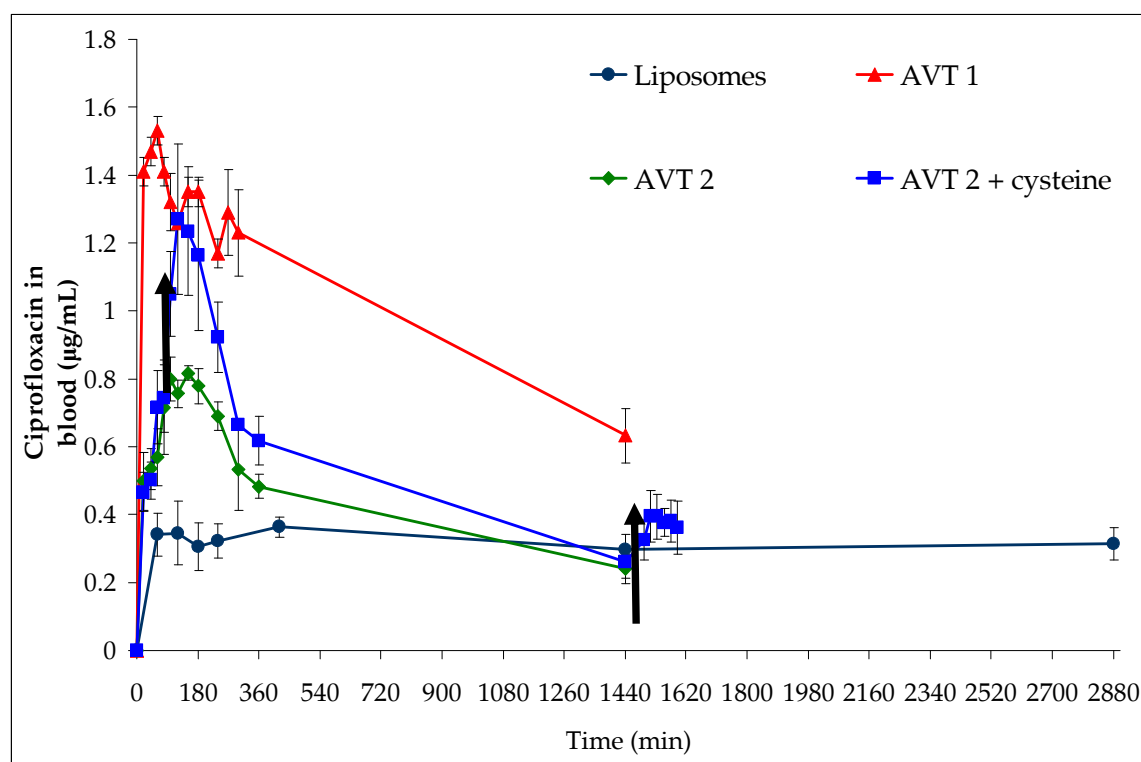


Figure 39. Comparison of the pharmacokinetics of liposomes, AVT1, AVT2, and AVT2 followed by cysteine. Study with liposomes was done over 2 days. The AVT studies were done over 1 day. $n=3$ animals.

A comparison of the pharmacokinetics of the AVT2 particles with the previous treatment of liposomes and AVT1 (section 4.1.3.3) is shown in figure 39. The differences in size and the nanostructure of the particles affect the release properties of the microparticle formed. On the basis of size AVT1 > AVT2 > Liposomes. A compact structure of the agglomerate would represent a high concentration of drug-bearing nanoparticles, which may not promote diffusive transport. On the other hand, a more porous, open structure would represent a lower concentration of drug-bearing particles, but a higher diffusive transport rate. Also, due to the dynamic nature of the lungs, large and loose agglomerates maybe more susceptible to rupture and consequent increase in drug release in comparison to smaller compact agglomerates. This would mean more drug being released into the systemic circulation. As seen in figure 39 AVT1 show higher release of drug into the blood as compared to AVT2.

Table 9. AUC_{0-24} for each of the formulations tested.

Formulation	Dose (mg/kg)	AUC_{0-24} ($\mu\text{g/ml.hr}$)
Liposome-encapsulated Ciprofloxacin	21.07 ± 1.64	8.02 ± 2.3
AVT 1	17.05 ± 0.44	19.8 ± 0.12
AVT 2	18.31 ± 0.62	10.45 ± 0.92
AVT 2 + cysteine	18.56 ± 0.54	14.51 ± 2.3

A comparison of the areas under the concentration-time curves (AUC_{0-24}) for AVT1, AVT2, AVT2 + cysteine, and liposomes, is shown in Table 9. The

AUC's increase with the size of the particles, suggesting that the larger particles have an improved systemic bioavailability in comparison to the smaller particles.

4.2.4.4. Lipid assay of instilled formulations in rat lungs

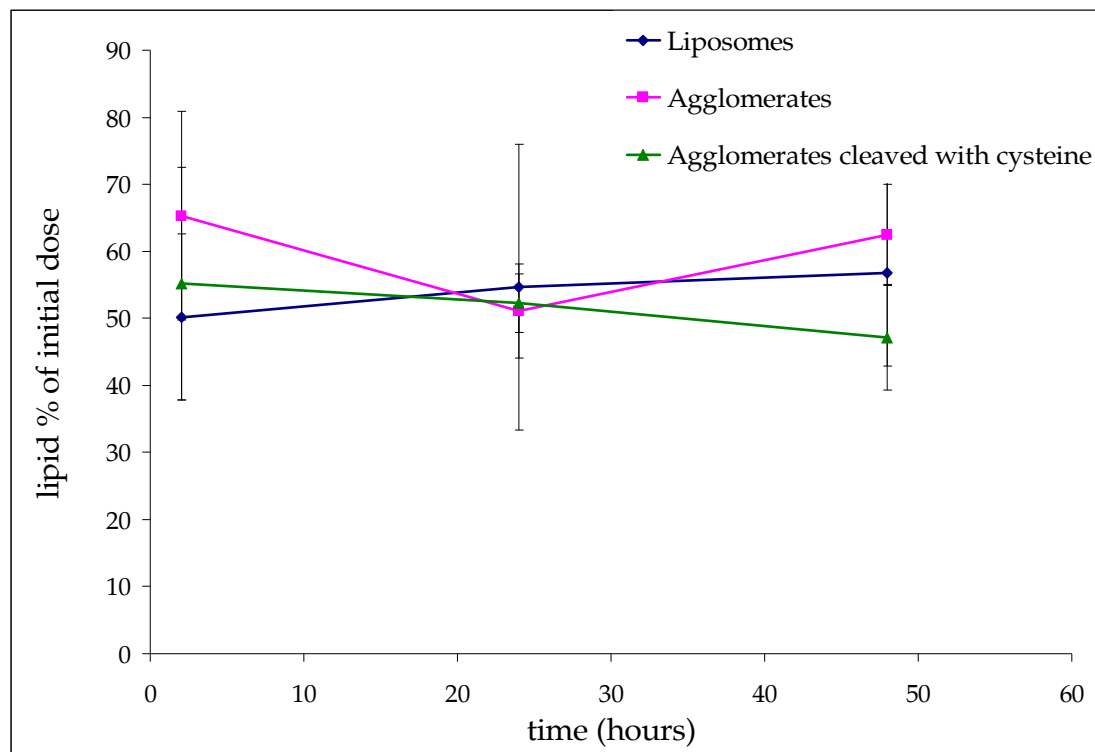


Figure 40. Percentage of original dosed lipid remaining in the lungs on the basis of fluorescence assay of the tagged lipid. $n = 3$ animals.

The measurement of lipid retained in the lungs indicated that there is no significant difference between liposomes and agglomerates (figure 40). Further, there is no systematic change in lipid levels during the 48 hour observation period; 50 – 60% of the initial amount of lipids dosed is observed in the lungs at all times. This is an offset of the experiment, due to losses during the processing of lungs tissue before the assay. This result is similar to those of Webb et al [52] who showed that after instillation of liposomes the amount of lipid observed in

the lungs during 24 hours post administration was between 76 – 106% of initial lipid dose suggesting that the lipids are not transported into the circulation. We therefore believe that the total lipid (as particles) is remaining in the lungs for the entire time of the experiment (48 hours), and that drug release from the particles into the lungs then results in the transport of free drug into the systemic circulation.

4.2.4.5. Histology of rat lungs to assess inflammation

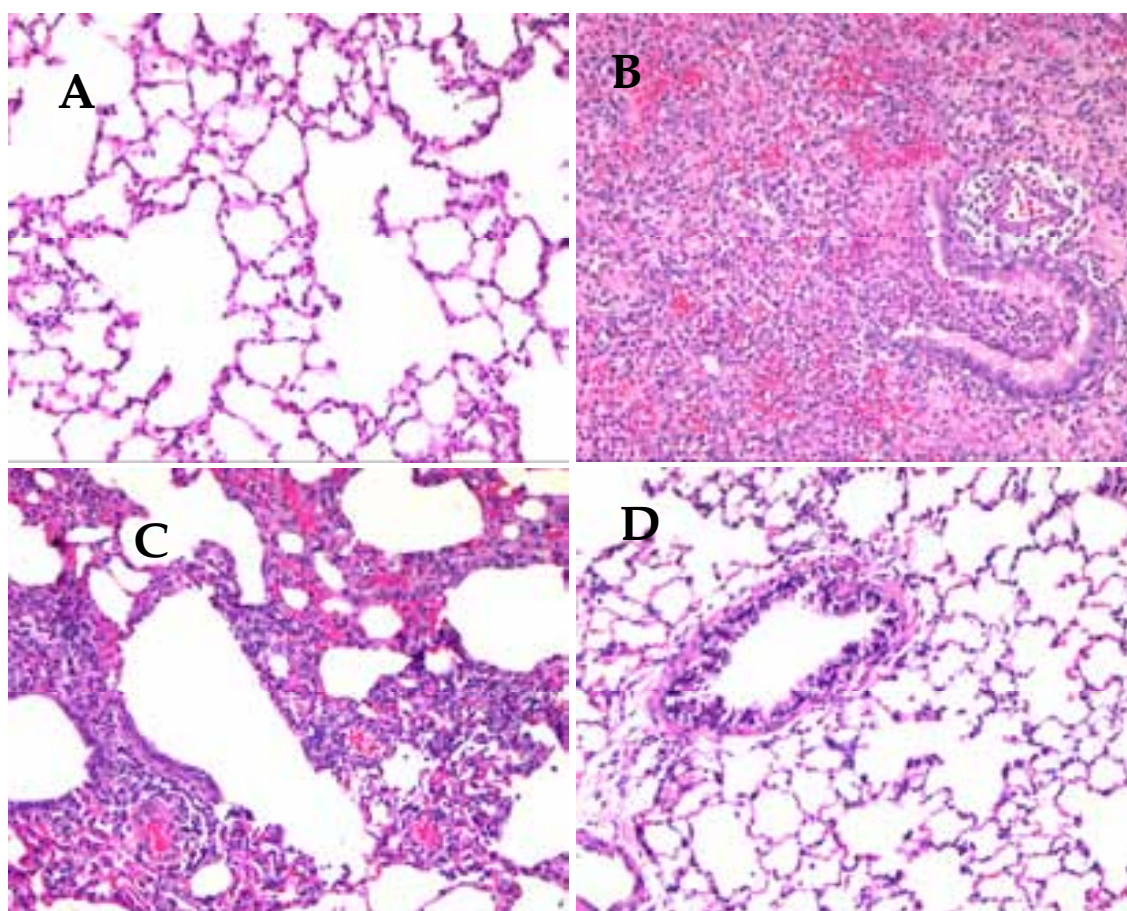


Figure 41. Histological analysis of hematoxylin-eosin stained lung tissue 24 hrs after treatment (original magnification 100X); (A) saline-treated animals; (B) ConA-treated rats; (C) liposome-treated animals; (D) AVT-treated animals. *n* = 2 animals

A qualitative analysis of inflammation after instillation of the formulations was done by histology. The HE stained sections of lung tissue were rank ordered by a practicing Pathologist and are shown in figure 41.

In saline-treated rats (figure 41A), the lung tissue was observed to be almost entirely normal. The ConA-treated (Concanavalin A) rats (figure 41B) demonstrated extensive pneumonic changes in their lungs. A bronchiole and adjacent alveoli showed mixed inflammatory cell infiltrates including neutrophils and lymphocytes, accompanied by alveolar hemorrhage. In the liposome-treated animals (figure 41C), patchy lymphocytic infiltrates were noted around a bronchiole, blood vessels, and in the interstitium in the left upper lobe of one of the rats receiving the liposomes. In AVT-treated animals (figure 41 D), the majority of the lung tissue in the rats had a normal appearance. This suggested that the AVT particles do not elicit a major inflammatory response, and are therefore safe to be used in therapy. The reason for this may be attributed in part to the large size of the AVT particles and also the fact that they are composed of phospholipids, which is a major component of the lung surfactant.

4.2.4.6. Cytokine assay from rat lungs as a measure of inflammation

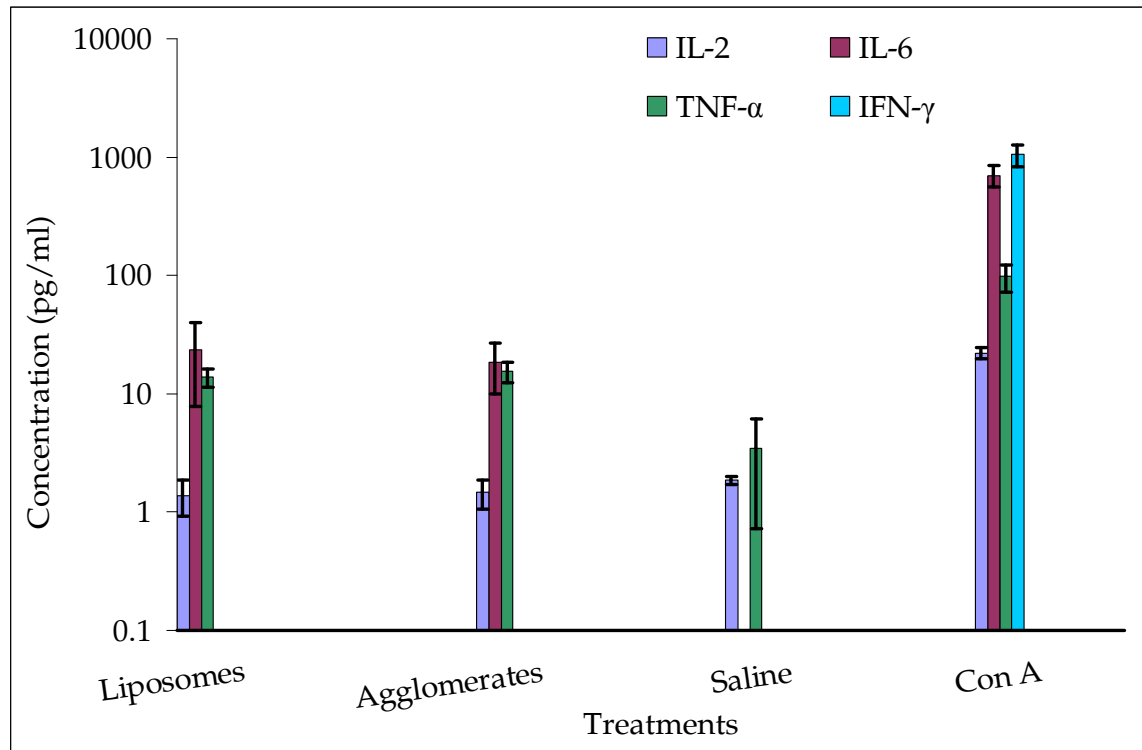


Figure 42. Levels of cytokines detected 48 hours after the different treatments ($n = 3$ animals)

The levels of cytokines that were assayed for the different treatments are as shown in figure 42. As expected for the ConA treatment the levels of the 4 cytokines that were assayed were higher than the levels of the respective cytokines for the other treatments. The IFN- γ levels were detected only for the ConA treatment. The IL-2 levels for the liposomal and AVT treatment were comparable to the saline treatment. The TNF- α levels of the liposomes and AVT particles were approximately 5 times the levels of the saline treatment. No IL-6 was detected in the saline treated animals. The levels of the respective cytokines were similar for the liposomal and AVT treatment. Some level of inflammation was expected due to the instillation of foreign material into the lungs; however

these levels are much lower than the ConA treatment, which suggest that these treatments do not elicit a huge inflammatory response and support the findings from the histological analysis.

4.2.5. *In silico study of Ciprofloxacin pharmacokinetics*

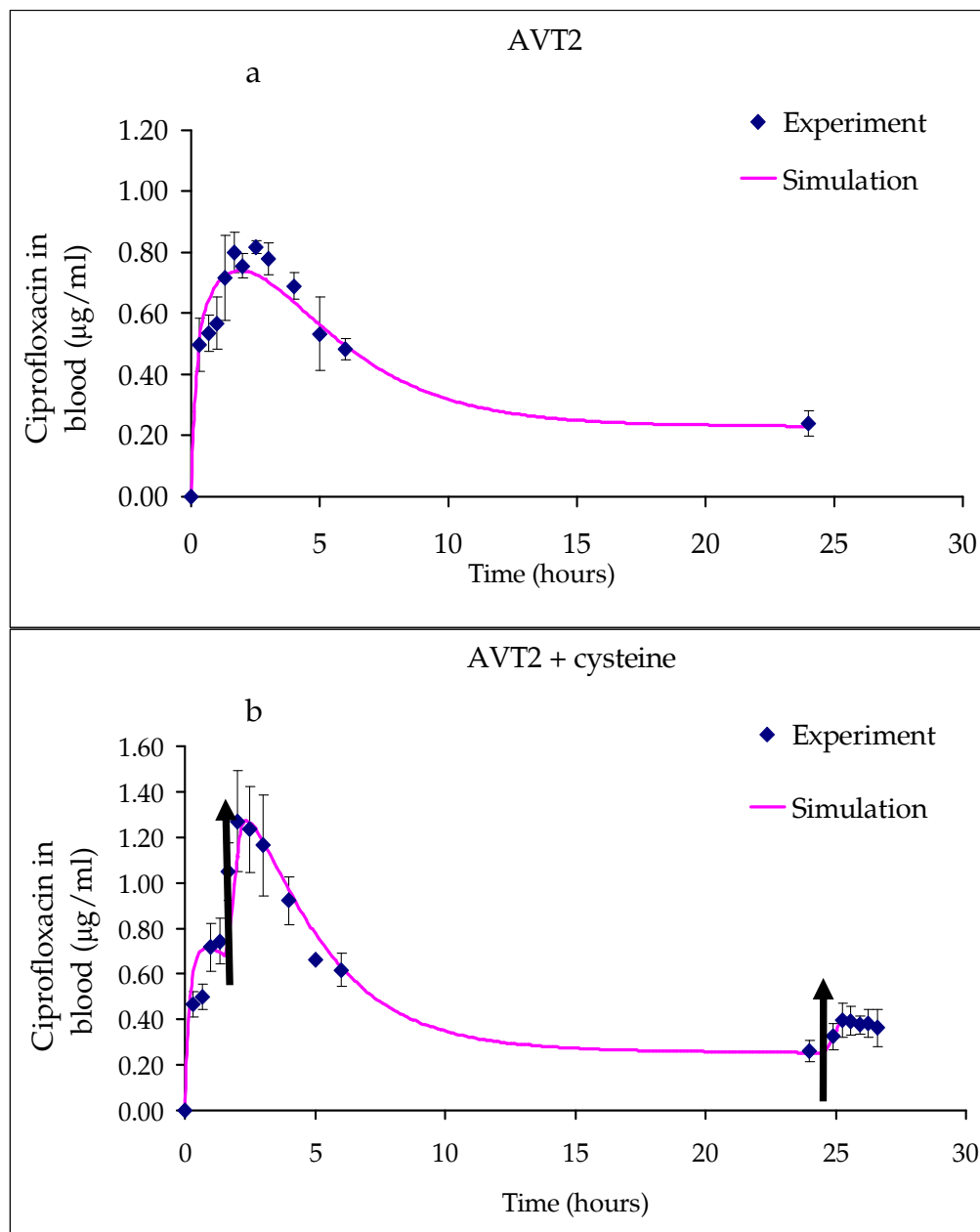


Figure 43. Model fit to experimental data for (a) AVT2, and (b) AVT2 + Cysteine.

The results of the model that was fitted by the SAAM II software to the experimental pharmacokinetic data (section 4.2.4.3) for the AVT2 particle treatment are shown in figure 43. The input dose 'D' (known parameter) for the AVT2 particles was 46783 μg . The unknown parameters that were estimated for the AVT2 treatment (figure 43a) are shown in table 10.

Table 10. *Unknown parameters estimated for pharmacokinetic study with AVT2.*

Parameter	Value ($\pm\text{sd}$)	95% confidence interval	
α (μg)	1116.27 (± 36.9)	1035.77	1196.76
k_{AVT} (hr^{-1})	0.0027 (± 0.002)	-0.001	0.006
k_{L0} (hr^{-1})	0.42 (± 0.16)	0.12	0.91
k_{L} (hr^{-1})	0.006 (± 0.000)	0.005	0.008

The value of α that was estimated represents 2.4% of the initial amount of drug dosed. A comparison of the k_{AVT} values of AVT2 with the liposomes (section 4.1.4) suggests that the diffusion rate of the drug is similar. The elimination rate constant (k_{L0}) is lower than the liposomes, suggesting that in addition to the free drug being cleared, the clearance due to macrophages is lower.

For the AVT2 followed by cysteine treatment the values of α , k_{AVT} , and k_{L} were fixed. Due to instillation of cysteine, a cleavage of the linkages between the liposomes was expected and hence a leakage of drug (represented by α'') was assumed due to the fragmentation in the structure of the microparticle. Also, because of the cleavage and fragmentation the elimination of the AVT2 would be

different due to the changes in sizes; hence k_{L0} was also estimated assuming that it would be different from the treatment with only AVT2. The values of these estimated parameters are shown in table 11.

Table 11. Unknown parameters estimated for pharmacokinetic study with AVT2 + cysteine.

Parameter	Value (\pm sd)	95% confidence interval	
α'' at 90 minutes (μ g)	2240.92 (\pm 530.5)	1103.12	3378.72
α'' at 24 hrs and 35 minutes (μ g)	469.1 (\pm 400.53)	-390.04	1328.21
k_{L0} (hr^{-1})	0.853 (\pm 0.231)	0.356	1.349

The value of α'' at 90 minutes was estimated to be 10% of the drug that remained in the lungs at 90 minutes. The value of α'' at 24 hours and 35 minutes was estimated to be 2.3% of the drug that remained in the lungs at that time point. The model estimated that the elimination of drug from the lungs (k_{L0}) was higher in the case of the treatment with agglomerates followed by cysteine. This suggested that the clearance of the drug (due to lymphatic or macrophage clearance) is increased after the cleavage.

Chapter 5

Conclusions and Future work

5.1. Conclusions

In the preliminary studies that were undertaken [38], the use of different cross-linkers was investigated in order to form agglomerates of nano-sized liposomes. Keeping in mind the modulation of release of drug from these microparticles after instillation in the lungs; DTBP, a thiol cleavable linker was extensively studied. Large microparticles were fabricated exhibiting diameters of 10's of microns. The sizes of the agglomerates could be controlled by the stoichiometry of the reaction (e.g. by changing either the lipid molarity of the parent liposomes or the amount of the linker), and the conditions of the reaction (e.g. pH). By following different agglomeration protocols agglomerates of different size distributions were achieved with geometrical diameters ranging from 2-140 μm .

The aerodynamic properties of there large agglomerated particles were determined by cascade impaction study, which is a recommended USP method that is used by industry to test the aerodynamic properties of drug particles that are used as an inhalation therapy. It was observed that the large agglomerates had aerodynamic diameters in the respiratory range (1-5 μm). The size

characterization upon nebulization showed that the agglomerates were largely intact and only a small fraction of them were disrupted. Additionally, the nebulized agglomerates retained most of the encapsulated drug. These results suggested that the agglomerates remained intact during the nebulization process.

The *in vitro* release experiments from the agglomerates of the 1st generation showed that by the introduction of a cleaving agent that breaks the linkages between the liposomes within an agglomerate modulation in the release of the drug could be achieved. However, the cleaving agent used was DTT, which is not a suitable candidate for use *in vivo*.

In order to bring about post-administration modulation of drug release *in vivo*, cross-linkers that can be cleaved *in vivo* were researched. DTSSP a commercially available linker was found to be cleavable by cysteine (acceptable for *in vivo* use). The *in vitro* experiments carried out with this linker suggested that the agglomerates of liposomes made with this linker are cleavable by cysteine. *In vitro* release experiments suggested that a modulation in release could be achieved by the cleavage of the cross-links with cysteine.

An analysis of the agglomerates by confocal microscopy and negative staining electron microscopy suggested a heterogeneous structure that included highly porous as well as compact domains within the agglomerate. As the compact structures were nucleated rapidly, diffusion-limitations dominated during the agglomeration reaction, resulting in the formation of porous structures of the compact “nuclei”. The void fraction within the agglomerates

was estimated to be between 5-10% of the entire agglomerate. This porous property of the agglomerate also supports the lower aerodynamic diameters (by cascade impaction) exhibited by the agglomerates with large geometric diameters.

The in vivo experiments showed that, when the AVT particles of DTSSP were cleaved by cysteine, a triggered release of Ciprofloxacin was achieved. Both the AVT particles and unagglomerated liposomes appear to remain in the lung for at least 48 hours after administration. The mechanism by which Ciprofloxacin is delivered to the blood therefore appears to be (1) a release of Ciprofloxacin from the particles into the lung fluid, followed by (2) transport of the free Ciprofloxacin into the bloodstream. Specifically, the transport of encapsulated Ciprofloxacin into the blood is not suggested by our results. In contrast, previous work by Wong et al. [53] showed that liposomal Ciprofloxacin was more effective than free Ciprofloxacin against intracellular pathogens such as *F. tularensis*, suggesting that liposomal drug was possibly transported intact into macrophages. However, the liposomal formulations used by Wong were substantially different from those used in this work, and it is possible that changes in the bilayer composition affect the route of clearance from the lung.

AVT particles also exhibited higher bioavailability than the liposomes, as indicated by the higher AUC for the AVT particles. This is somewhat counterintuitive, since one expects the higher surface area of the parent liposomes to result in higher release rates. However, this phenomenon has been

previously observed in vitro, and it is believed that the larger AVT particles, being subjected to larger shear forces in the lung, were disrupted more easily than the smaller liposomes. Thus, AVT particles are expected to have two mechanisms for drug release (1) diffusion of the drug out of the liposomes themselves and (2) bulk leakage due to bilayer disruption. This mechanism is consistent with the repeated observation that AVT particles have higher bioavailabilities than liposomes.

The two AVT formulations tested in vivo also had somewhat different bioavailabilities. While the reasons for this are yet unclear, they are probably related to the different size distributions of the two AVT particle formulations. The in vivo non-cleavable formulation - AVT1, had larger particles than the in vivo cleavable AVT2, and hence was prone to a larger extent of disruption and subsequent drug leakage, due to the shearing forces of the lung than the smaller AVT2. Thus, AVT1 had a higher release and bioavailability.

Cleavage of the links in AVT2 by the administration of exogenous cysteine caused an immediate increase in Ciprofloxacin release. Further, the release rate appears to remain at this elevated level, reflected by an increased blood concentration of Ciprofloxacin at subsequent times. The cumulative release, measured by the AUC, is also higher for the cleaved formulation, consistent with this overall increased release rate.

The toxicity studies that were done by histology and cytokine analysis indicate that the AVT particles did not elicit a major inflammatory response. This

was supported by lower infiltration of neutrophils and lymphocytes. The cytokine levels were low as well. These low levels of inflammation can be attributed to the phospholipid composition of the particles which is similar to that of the surfactant that lines the lungs.

This study is the first demonstration of in vivo modulated release of drug in the lungs. Though the formulations were instilled into the lungs of animals, the aerodynamic characteristics of the particles suggest that the platform that has been developed holds great promise for delivering drugs into the lungs of humans.

5.2. Future work

The technology in its present form is capable of being delivered by nebulizers. An optimal nebulizer for delivering these agglomerates with minimal structural damage needs to be evaluated. This technology can also be applied to MDIs and DPIs, but issues of drying the particles need to be kept in mind. Drying the liposomes would destroy the integrity of the bilayer, however, they can be protected with sugars [54-56] and then dried. Sugar protection is known to retain a layer of water in close proximity to the bilayer, thus stabilizing it.

Though inflammation studies were performed, the cellular uptake of the AVT particles needs to be investigated. It would be particularly interesting to see if macrophages are capable of engulfing these large agglomerates. Only a single time point was used for the evaluation of inflammation. However, the time

evolution of inflammation needs to be evaluated to see if the levels remain low at different time points.

Since, the platform could be used over a prolonged time period for treatment; chronic toxicity studies need to be undertaken. Owing to the fact that the acute toxicity studies showed minimal inflammation, lower levels of chronic toxicity are expected.

5.3. Clinical perspectives of the work

The AVT is a platform technology and can, therefore, be used to deliver therapeutic molecules to treat local lung diseases and also systemic diseases. In this work it was sought to see if triggered/modulated release of drug is possible from carriers that are administered to lungs. It was envisioned that repeated doses of the drug formulation could be replaced with a single dose. This is particularly helpful in delivering drugs that are not easily portable, and also where the concerns of excipient buildup in the lungs due to repeated dosing can be an issue. Current technologies do provide controlled release of drug, but if the need arises for more drug to be delivered an additional dose of the formulation would be required. This work showed that modulation can be achieved from the AVT particles by the introduction of a second agent that is easily portable and stable.

The present work with Ciprofloxacin suggests that the technology can be used both as a prophylactic as well as a treatment, with lower drug dosages.

Similarly, other anti-infective drugs for treating both local as well as systemic diseases can be used. This could prove to be useful in biologically hot environments like hospitals, where noscomial infections can be prevented. This technology can also prove helpful by providing protection in a military combat situation dealing with the use of biological agents, for example weaponized aerosol form of anthrax.

This work has important implications in developing particles that are sensitive to the product of a disease, and are thus capable of modulating drug release without the need for administration of additional agents. For example, if insulin release were to be triggered by the glucose level, it would enable a versatile, feedback control system for diabetics. Therefore, it was sought to fabricate glucose-sensitive AVT particles capable of being cleaved by elevated pulmonary glucose. A concanavalin A (ConA) based linkage was implemented between liposomes in the AVT particles. Liposomes with glycosyl groups at the distal ends of PEG tethers were rapidly agglomerated by ConA. Upon exposure of the agglomerates to free glucose, a reduction in size was observed due to cleavage of the links resulting from the preferential binding of ConA to free glucose. It was envisaged that this cleavage would result in triggered release of insulin from these AVT particles. Since pulmonary glucose levels are virtually zero in normal humans, but are elevated in diabetics the glucose-ConA system appeared to be a suitable candidate for auto-modulated release of insulin. The AVT particles made from this construct were tested in rats which showed

controlled and auto-modulated release of insulin [57]. Though this construct has limitations due to toxicity concerns of ConA, the underlying hypothesis that auto-modulation is possible was demonstrated. Currently, substitutes for ConA that are acceptable for use in vivo, like boronates, are being investigated.

To treat local lung diseases, the particle could target a specific site of the lungs by appropriate adjustment of the aerodynamic properties. Additionally, it could “sense” an onset of the problem and trigger the release of additional drug. For example, the first line of asthma therapy is based on inhaled corticosteroids and β_2 agonist catecholamines acting as bronchodilators. Once the particle carrying the bronchodilator deposits in the lungs, it would continuously release small amounts of its drug content, thus providing prophylaxis. However, once the particle “senses” (where the AVT particle can be made sensitive to elevated levels of cytokines, chemokines, etc.) an asthma attack, extra amounts of the bronchodilator and an anti-inflammatory drug (e.g. albuterol) could be released to control the condition.

It is envisioned that this technology can be used with a variety of drugs, providing significant control over a disease condition and also improve patient compliance.

Bibliography

1. O'Callaghan C, Nerbrink O, Vidgren M. The History of Inhaled Drug Therapy. Drug delivery to the Lung, Lung Biology in Health and Disease, vol. 162, Marcel Dekker, Inc. NY, 2002, pp 1-3.
2. Adjei AL, Gupta PK. Inhalation delivery of therapeutic peptides and proteins, Lung Biology in Health and Disease, vol. 107, Marcel Dekker Inc., New York, 1997.
3. Mckone T, Huey B, Downing E, Duffy L. Strategies to protect the health of deployed U.S. forces: Detecting, characterizing, and documenting exposures, editors; Division of Military Science and Technology and Board on Environmental Studies and Toxicology, National Research Council (Ed.), 2000.
4. Wigley FM, Londono JH, Wood JH. Insulin across respiratory mucosa by aerosol delivery, Diabetes 20 (1971), pp 552-556.
5. Patton JS, Bukar JG, Eldon MA. Clinical pharmacokinetics and pharmacodynamics of inhaled insulin, Clin. Pharma. 43 (2004), pp 781-801.
6. Edwards D, Hanes J, Caponetti G, Hrkach J, Ben-Jebria A, Eskew M, Mintzes J, Deaver D, Lotan N, Langer R. Large porous particles for pulmonary drug delivery, Science 276 , 1997, pp 1868-1871.

7. Bhavane R, Karathanasis E, Annapragada AV. Agglomerated vesicle technology: A new class of particles for controlled and modulated pulmonary drug delivery, *Jour. of Controlled Release* 93, 2003, pp 15– 28.
8. Karathanasis E, Ayyagari AL, Bhavane R, Bellamkonda RV, Annapragada AV. Preparation of 'in vivo' cleavable agglomerated liposomes suitable for modulated pulmonary drug delivery, *Jour. of Controlled Release* 103, 2005, pp 159-175.
9. Karathanasis E, Bhavane R, and Annapragada AV. Triggered Release of Inhaled Insulin from the Agglomerated Vesicles: Pharmacodynamic Studies in Rats. *Jour. of Controlled Release* 113 (2), 2006, pp 117-127.
10. Stocks J. Developmental physiology and methodology. *Am. Jour. Resp. Crit. Care Med.* 151, 1995, S15-S17.
11. Martin TR, Feldman HA, Fredberg JJ, Castile RG, Mead J, Wohl MEB. Relationship between maximal expiratory flows and lung volumes in growing humans, *Jour. Appl. Physiol.* 65, 1988, pp 822-828.
12. Gray H. *Anatomy of the human body*, 20th edition, Philadelphia: Lea & Febiger, 1918, New York: Bartleby.com, 2000.
13. Weibel ER. *Morphometry of the human lung*, New York, Academic Press 1963.
14. Thurlbeck WM. The internal surface area of nonemphysematous lungs, *Am. Rev. Respir. Dis.* 95, 1967, pp 765-770.

15. Stone KC, Mercer RR, Gehr P, Stockstill B, Crapo JD. Allometric relationships of cell numbers and size in the mammalian lung, *Am. Respir. Cell Mol. Biol.* 6, 1992, pp 235-243.
16. Patton JS. Mechanisms of macromolecule absorption by the lungs, *Advanced Drug Delivery Reviews* 19, 1996, pp 3-36.
17. Edwards DA, Dunbar C. Bioengineering of therapeutic aerosols, *Annual Reviews of Biomedical Engineering* 4, 2002, pp 93-107.
18. Annapragada A, Swanson P, Muzzio F. Biophysics of inhaled drug particles, *Inhalation delivery of therapeutic peptides and proteins*: Adjei AL, Gupta PK, editors, Marcel Dekker Inc., New York, 1997, pp 27-58.
19. Davis SS. Delivery of peptide and non-peptide drugs through the respiratory tract, *PSTT* 2, 1999, pp 450-456.
20. Zalipsky S. Synthesis of an end-group functionalized polyethylene glycol-lipid conjugate for preparation of polymer-grafted liposomes, *Bioconjugate chemistry* 4, 1993, pp 296-299.
21. Hermanson G. *Bioconjugate techniques*, Academic press, New York, 1996.
22. Brady R, Ball R. Fractal growth of copper electrodeposits, *Nature* 309, 1984, pp 225-229.
23. Feder F, Jossang T, Rosenqvist E. Scaling behavior and cluster fractal dimension determined by light scattering from aggregating proteins, *Physical Review Letters* 53, 1984, pp 1403-1406.

24. Meakin P. Computer simulation of growth and aggregation processes of
On Growth and Form: Fractal and Non-Fractal Patterns in Physics, Stanley
E and Ostrowsky N, editors, Nijhoff, Boston, 1986, pp 111-135.
25. Mandelbrot BB, Vespignani A, Kaufman H. Crosscut analysis of large
radial DLA: departures from self-similarity and lacunarity effects,
Europhysics Letters 32, 1995, pp 199-204.
26. Kisak ET, Kennedy MT, Trommeshauser D, Zasadzinski JA. Self-limiting
aggregation by controlled ligand-receptor stoichiometry, Langmuir 16,
2000, pp 2825-2831.
27. Zalipsky S, Qazen M, Walker II J, Mullah N, Quinn Y, Huang S. New
detachable poly(ethylene glycol) conjugates: Cysteine-cleavable
lipopolymers regenerating natural phospholipids, diacyl
phosphatidylethanolamine, Bioconjugate Chemistry 10, 1999, pp 703-707
28. Lasic D, Martin F. Stealth Liposomes, CRC Press Inc, 1995.
29. Lasic D, Papahadjopoulos D. Medical applications of liposomes, Elsevier,
1998.
30. Lasic D, Liposomes from physics to applications, Elsevier, 1993.
31. Bridges P, Taylor K. An investigation of some of the factors influencing
the jet nebulization of liposomes, International Journal of Pharmaceutics
204, 2000, pp 69-79.
32. Miyajima K. Role of saccharides for the freeze-thawing and freeze-drying
of liposome, Advanced drug delivery reviews 24, 1997, pp 151-159.

33. Mitra R, Pezron I, Li Y, Mitra A. Enhanced pulmonary delivery of insulin by lung lavage fluid and phospholipids, *International journal of pharmaceutics* 217, 2001, pp 25-31.
34. Madden TD, Harrigan PR, Tai LCL, Bally MB, Mayer LD, Redelmeier TE, Loughrey HC, Tilcock CPS, Reinish LW, and Cullis PR. The accumulation of drugs within large unilamellar vesicles exhibiting a proton gradient: a survey. *Chem. Phys. Lipids* 53, 1990, pp 37-46.
35. Hope MJ and Wong KF. Liposomal formulation of Ciprofloxacin, Shek PN, editors, *Liposomes in biomedical applications*. Harwood Academic Publishers, Germany, 1995, pp 121-134.
36. Lasic DD, Ceh B, Stuart MCA, Guo L, Frederik PM, and Barenholz Y. Transmembrane gradient driven phase transitions within vesicles: lessons for drug delivery, *Biochim. Biophys. Acta*, 1239, 1995, pp 145-156.
37. Oh YK, Nix DE, and Straubinger RM. Formulation and efficacy of liposome-encapsulated antibiotics for therapy of intracellular *Mycobacterium avium* infection. *Antimicrob. Agents Chemother.* 39, 1995, pp 2104-2111.
38. Bhavane R. Agglomerated particles for pulmonary drug delivery. MS Thesis, Cleveland State University, OH, 2002.
39. Herb C, Berger E, Chang K, Morrison I, and Grabowski E. Using quasi-elastic light scattering to study particle size distributions in

- submicrometer emulsion systems, in: Particle size distribution, Provder T, editor, ACS symposium series 332, 1985, pp 89-104.
40. Gulari E, Annapragada A, Jawad B. Determination of particle size distribution using light-scattering techniques, in: Particle size distribution, Provder T, editor, ACS symposium series 332, 1985, pp 133-143.
 41. Annapragada A, Adjei AL. An analysis of the Fraunhofer Diffraction method for particle size distribution analysis and its application to aerosolized sprays, *International Journal of Pharmaceutics* 127, 1996, pp 219-227.
 42. Finlay WH and Stapleton KW. Undersizing of droplets from a vented nebulizer caused by aerosol heating during transit through an Andersen impactor, *J. Aerosol Sci.*, vol. 30, no. 1, 1999, pp 105-109.
 43. Desai TR, Hancock REW, and Finlay WH. A facile method of delivery of liposomes by nebulization, *Jour. Of Controlled Release*, 84, 2002, pp 69-78.
 44. Colino CI, Turino AG, Navarro AS, and Lanao JM. A comparative study of Ofloxacin and Ciprofloxacin erythrocyte distribution, *Biopharm. Drug Dispos.* 19, 1998, pp 71– 77.
 45. Barret PHR, Bell BM, Cobelli C, Golde H, Schumitzki A, Vicini P, and Foster DM. SAAM II: Simulation, analysis, and modeling software for tracer and pharmacokinetic studies, *Metabolism* 47, 1998, pp 484-492.
 46. Heatherington AC, Vicini P, and Golde H. A pharmacokinetic/pharmacodynamic comparison of SAAM II and

- PC/WinNonlin modeling software, Journal of Pharmaceutical Sciences 87, 1998, pp 1255-1263.
47. Bell BM, Burke JV, and Schumitzky A. A relative weighting method for estimating parameters and variances in multiple data sets, Computational Statistics & Data Analysis 22, 1996, pp 119-135.
48. Matot I, Manevich Y, Al-Mehdi A, Song C, and Fisher A. Fluorescence imaging of lipid peroxidation in isolated rat lungs during nonhypoxic lung ischemia. Free Radical Biology & Medicine, vol. 34, no. 6, 2003, pp 785–790.
49. Sood S, Characterization of liposome manufacturing using extrusion, Master's thesis, 1999.
50. Wong JY, Kuhl TL, Israelachvili JN, Mullah N, and Zalipsky S. Direct measurement of a tethered ligand-receptor interaction potential, Science 275, 1997, pp 820-822.
51. Krill SL, Harn J, Hahn KR, and Gupta SL. Activity loss on room temperature storage of Survanta, a bovine lung extract based surfactant, International Journal of Pharmaceutics 132, 1996, pp 89-94.
52. Webb MS, Boman NL, Wiseman DJ, Saxon D, Sutton K, Wong KF, Logan P, and Hope MJ. Antibacterial Efficacy against an in vivo *Salmonella typhimurium* infection model and pharmacokinetics of a liposomal Ciprofloxacin formulation. Antimicrobial Agents and Chemotherapy, vol. 42, no. 1, 1998, pp 45–52.

53. Wong JP, Yang H, Blasetti KL, Schnell G, Conley J, and Schofield LN. Liposome delivery of Ciprofloxacin against intracellular *Francisella tularensis* infection, *Journal of Controlled Release* 92, 2003, pp 265–273.
54. Kim C, Chung H, Lee M, Choi L, and Kim M. Development of dried liposomes containing b-galactosidase for the digestion of lactose in milk, *International Journal of Pharmaceutics* 183, 1999, pp 185–193.
55. Hinch DK and Crowe JH. Trehalose increases freeze–thaw damage in liposomes containing chloroplast glycolipids, *Cryobiology* 36, 1998, pp 245–249.
56. Quintilio W, Sato RA, Sant’Anna OA, Esteves MI, Sesso A, de Araujo PS, and Bueno da Costa MH. Large unilamellar vesicles as trehalose-stabilized vehicles for vaccines: storage time and in vivo studies, *Journal of Controlled Release* 67, 2000, pp 409–413.
57. Karathanasis E. Triggered and autoregulated pulmonary delivery of insulin, PhD thesis, University of Houston, TX, 2005.